MODELING OF GLASS MAKING PROCESSES FOR IMPROVED EFFICIENCY

(SUBTITLED: HIGH TEMPERATURE GLASS MELT PROPERTY DATABASE FOR MODELING)

FINAL TECHNICAL/SCIENTIFIC REPORT

Thomas P. Seward III
Principal Investigator

1. OVERVIEW

1.1 Executive Summary

The overall goal of this project was to develop a high-temperature melt properties database with sufficient reliability to allow mathematical modeling of glass melting and forming processes for improved product quality, improved efficiency and lessened environmental impact. It was initiated by the United States glass industry through the NSF Industry/University Center for Glass Research (CGR) at Alfred University [1]. Because of their important commercial value, six different types/families of glass were studied: container, float, fiberglass (E- and wool-types), low-expansion borosilicate, and color TV panel glasses. CGR member companies supplied production-quality glass from all six families upon which we measured, as a function of temperature in the molten state, density, surface tension, viscosity, electrical resistivity, infrared transmittance (to determine high temperature radiative conductivity), non-Newtonian flow behavior, and oxygen partial pressure. With CGR cost sharing, we also studied gas solubility and diffusivity in each of these glasses.

Because knowledge of the compositional dependencies of melt viscosity and electrical resistivity are extremely important for glass melting furnace design and operation, these properties were studied more fully. Composition variations were statistically designed for all six types/families of glass. About 140 different glasses were then melted on a laboratory scale and their viscosity and electrical resistivity measured as a function of temperature.

The measurements were completed in February 2003 and are reported on here. The next steps will be 1) to statistically analyze the compositional dependencies of viscosity and electrical resistivity and develop composition-property response surfaces, 2) submit all the data to CGR member companies to evaluate the usefulness in their models, and 3) publish the results in technical journals and most likely in book form.

1.2 Project Name: Modeling of Glass Making Processes for Improved Efficiency (Subtitled: High Temperature Glass Melt Property Database for Modeling)

1.3 Performing Organization:
NSF Industry-University Center for Glass Research
NYS College of Ceramics at Alfred University
2 Pine Street
Alfred, NY 14802

1.4 Principal Investigators:
Thomas P. Seward III (July 1997-present)
(607) 871-2432 (ph)
(607) 871-2383 (FAX)
seward@alfred.edu

William C. LaCourse (September 1996-July 1997)
(607) 871-2466 (ph)
(607) 871-2392 (FAX)
lacourse@alfred.edu

1.5 Other Participating Researchers:

Dr. Alexis G. Clare (Alfred University)
Dr. David A. Earl (Alfred University)
Mr. Douglas M. Korwin (to May, 2000 - Center for Glass Research, AU)
Dr. William C. LaCourse (Alfred University)
Dr. Dolun Oksoy (Alfred University)
Dr. James E. Shelby (Alfred University)
Dr. Arun K. Varshneya (Alfred University)
Ms. Terese Vascott (from May, 2000 - Center for Glass Research, AU)
Dr. Oleg A. Prokhorenko (Laboratory of Glass Properties, St. Petersburg, Russia)
Dr. Pavel Hrma (Pacific Northwest Laboratory, Redland, WA)

1.6 Sub-contracts:
CELS at Corning Incorporated, NY
Laboratory of Glass Properties (formerly Thermex), St. Petersburg, Russia
Pacific Northwest National Laboratories, Richland, WA
Integrex Testing Systems, Granville, OH

1.7 Project Participants: The New York State College of Ceramics (NYSCC)
The NSF Industry-University Center for Glass Research

The New York State College of Ceramics at Alfred University was the official project recipient and administered the contract through its Office of Sponsored Programs, Dr. Vasantha Amarakoon, Acting Director, (607) 871-2486.

The CGR provided oversight for the project and, as cost sharing, funded eight (8) additional research projects in direct support of this DOE/OIT grant as described in Sections 2.1, 3.4 and 5.3 below.

In addition to direct CGR cost sharing, individual CGR member companies provided technical assistance and sample quantities (25 – 50 Lbs.) of the six commercial glasses employed in the study.

1.8 DOE Project Team: DOE-OIT Glass Team Leader – Elliott Levine
DOE Program Manager –Elliott Levine
DOE Project Manager – Matae H. McCray
Grant Administrator – Marshall Garr
Industry Contact – Industrial Liaison Board of the NSF Industry/University Center for Glass Research at Alfred University

1.9 Date Project Initiated: September 15, 1996

1.10 Completion Date: December 31, 2002 (database reported here)
December 31, 2003 (estimate for validation of models by CGR member companies)

1.11 Introduction and Background

Glass manufacturing is a capital-intensive industry. In 1996, the cost of a new float glass facility was estimated to be about $150 million. The corresponding figures for fiberglass, container glass and color TV tube bulbs were $80, $100 and $300 million, respectively [2]. Furnace rebuilding costs run into millions of dollars. It is imperative that any proposed changes in furnace design have near 100% assurance of success. Lost production resulting from a poor furnace design can ultimately cost far more than the construction. Radical changes in design are almost always considered “high risk.” On the positive side, design changes that improve production yields or result in even a 5% decrease in fuel consumption per ton of glass melted would have important economic and environmental benefits for the industry. Consequently modeling of the glass-melting process to predict performance has become a necessity for any new furnace design.

In July 1996, the U.S. Department of Energy (DOE) and the NSF Industry/University Center for Glass Research (CGR) conducted a workshop at Alfred University on “Modeling in the Glass Industry.” Two of the primary needs identified for virtually all modeling of the glass melting process are 1) reliable data on high-temperature melt properties and 2) improved sensors for in-line measurement of process variables. Also deemed important is an “improved understanding” of the fundamental principles of combustion and the fluid flow models themselves.

1.12 Melt Properties Important for Furnace Modeling

Table 1 lists the key properties for glass furnace modeling identified at the Workshop. They are important for quantifying glass flow, energy transfer, electrical heating and gas exchange in bubbles. Mathematical models are sensitive to these properties to varying degrees and the accuracy to which these properties are known varies considerably. Table 2 places the properties of Table 1 on a matrix of model sensitivity versus measurement accuracy. Clearly, some of the most sensitive properties are considered to be the least accurately measured. The concentrations of dissolved gases in the melt, their solubilities (Henry's law constants) and their diffusivites top the list; equilibrium constants for gas-producing reactions within the melt are a close second.

Following the Workshop, faculty members at Alfred University and the industrial representatives to the CGR agreed to address the need for improved data on glass melt properties and a proposal was submitted to the DOE for grant support to help develop such a melt properties database. Because reliable gas solubility and diffusivity data is such a pressing need, the Center agreed to fund faculty researchers for additional research in this area independent of this proposal. In fact, the CGR has long recognized this need and has a history of funding projects in this area. This DOE grant (DE-FG07-96EE41262) was awarded in the fall of 1996 and three CGR-funded projects related to gas solubility were started at that same time. In effect, the investigations discussed in this report represent a DOE - Alfred University - CGR cost sharing effort. [Properties in Table 1 related to glass batch and furnace refractories were not part of the present study, however the CGR is currently funding some projects in these areas as well.]

1.13 Objectives of Study

In keeping with the introduction above, the main objective of the proposed work was the development of a comprehensive and reliable data base for glass forming melts that will allow full use of numerical simulation models by a broad cross-section of the glass industry for the purpose of achieving energy savings, improving product quality, increasing productivity, and meeting present and future environmental regulations. To insure that the data will be useful for this application, an industrial advisory group from the CGR was closely involved in every aspect of this project.

CGR member companies supplied commercial (production) glasses from six families - container, float, fiberglass (E- and wool-types), low expansion borosilicate and TV panel glasses. The analyzed compositions are shown in Table 3. The properties selected for investigation, the chosen measurement techniques, and proposed temperature (or property ranges) are shown in Table 4.

Since glass melt properties are sensitive to varying degrees to the composition of the glass and the temperature of the measurement, as well as other variables, for each property a sensitivity matrix should be created. This may be better possible as a result of the present study. To this end, for each family of glasses, a composition range to be studied was agreed upon by a team of CGR industrial representatives, as were the temperature ranges over which property measurements should be made. For each family of glasses, a set of 24 compositions for investigation was statistically designed. Approximately 15 glasses from each set (~90 total) were melted during the first years of this project (Phase I), the balance toward the end (Phase II).

While the project goal was primarily to develop a reliable database and to determine the sensitivity of each property to composition variations, it was recognized at the outset that measurement techniques needed to be developed in several key areas. So the development of suitable techniques became a third objective. The final objectives are for CGR member companies to utilize the data in their proprietary process modeling programs and evaluate their usefulness.

One can reclassify the properties of Table 4 according to their dependencies on different variable factors. Table 5 divides the properties into three classes: I) Those dependent primarily on the bulk glass composition (usually the major components) and temperature; II) those additionally dependent upon minor chemical components of the glass, such as coloring ions, and upon their redox state; and III) those with more complex composition dependencies. Viscosity, density, heat capacity and electric conductivity generally fall in class I. The effect of ferrous/ferric ion equilibrium on radiative thermal conductivity is a good example for class II. As an example for III, gas solubility depends upon the identity of the gas specie being studied, the melt composition, temperature and, for gases that dissolve chemically in the melt (reactive species), the partial pressures of other reactive gases (such as H_2O and O_2) present in and surrounding the melt. Surface tension shows similar dependencies.

1.14 Glass Compositions Studied

During the summer of 1997, several CGR member companies provided bulk quantities (25 to 50 pounds) of glass in each of the six key composition areas. These glasses were chemically analyzed and provided long term "standards" for the project (Table 3). A focus group of industry technical representatives provided information about the key composition variables and ranges they wished to see investigated. This information provided the basis for experimental design of the composition variations to be further investigated.

1.15 Statistically Designed Composition Study

Principal Investigator: Dr. Dolun Oksoy (AU)

Our factorial designs are based on Plackett-Burman Design and are coded as pbxxyy; where pb stands for Plackett-Burman, xx stands for number of factors, and yy stands for number of runs (compositions). The six experimental composition sets were designed as follows: container glass (CO) - pb1124; E-glass (E) - pb1024; float (FL) - pb1224; low-expansion borosilicate (LO) - pb724; color TV panel glass (TV) - pb1724; and wool-type fiberglass (WO) - pb1024. These sets are shown in Table 6.

1.16 Glass Melting and Analysis

Although the initial proposal called for the melting (from batch raw materials) of all the glass compositions required by this study, once the statistical design was completed it became obvious that we had neither the time, manpower nor facilities to successfully undertake that task. We also realized that for the data to be meaningful, we would need to verify by chemical analysis how closely in composition the melted glasses matched their designed values.

Following competitive bidding, the CELS (Corning Engineering Laboratory Services) group at Corning Incorporated (Corning, NY) was given a subcontract to melt and chemically analyze the laboratory-scale melts of E-glass, low-expansion borosilicate glass and color TV panel glass. Approximately two-pound quantities of more than 70 different glasses were prepared and analyzed by CELS. Students at Alfred University prepared laboratory scale melts of the remaining glasses (less than two pounds quantities each). With the exception of some fiberglass wool compositions, these glasses were chemically analyzed, either by CELS or Owens-Corning's Integrex Testing Services group (Granville, OH). The available chemical analyses are shown in Table 7.

2. PROPERTIES MEASURED ONLY ON THE SIX COMMERCIAL BASE GLASSES

2.1 Gas Solubility

Dr. James Shelby (Alfred University) was funded under this grant to study solubility and diffusivity of the gases He, Ne, Ar and N_2. Dr. Shelby, Dr. Herbert Giesche (Alfred University), and Drs. Oleg Mazurin and Oleg Prokhorenko (St. Petersburg Russia) were funded directly by the Center for Glass Research to carry out further gas solubility and diffusivity projects in support of this program. This work began in July 1997 (Mazurin, Prokhorenko and Shelby) and September 1997 (Giesche). (See descriptions that follow.)

2.1.2 Background

The gases He, Ne, Ar and N_2 dissolve physically in glass melts, that is, the gas molecules occupy interstices in the glass structure. The larger the atom or molecule, the less its solubility. (Under certain conditions nitrogen can be chemically dissolved in the glass, as in “nitrided” glasses, but except under extremely reducing conditions, nitrogen does not react with oxide glasses, so for our purposes is considered inert.) Reactive gases like H_2, O_2, H_2O, and CO_2 behave differently. They dissolve both physically and chemically. They can dissolve as molecules, they can form bonded species within the melt or they can react with the melt to change the oxidation state of other ions. For example, H_2O dissolves primarily by reacting with Si-O-Si bonds in the network to generate pairs of Si-OH bonded species. Oxygen can react with multivalent metal ions, entering the glass structure by oxidizing these elements. In commercial melts, CO_2 and SO_2 may be present as species chemically bound to the network, for example at sites of non-bridging oxygens, being released only slowly, making measurements of their equilibrium concentrations extremely difficult. A recent book by Shelby discusses these complications more fully [3].

2.1.3 He, Ne, Ar, N_2 and H_2O

Principal Investigator: Dr. James E. Shelby; Research Scientist: Melissa G. Mesko; Graduate Assistants: Brian Kenyon, Kirk Newton, Douglas Rapp and Chris Tournour; Undergraduate Assistants: Penny A. Schader, Rachel Alley (summer of 1997)

[Note: some of the funding for these students was provided by the Center for Glass Research as part of their separately funded gas solubility studies and some through an NSF grant for undergraduate women and minority students.]

Gas solubility measurements are extremely time consuming, and published data are "suspect" since the reported data can vary by almost 1 order of magnitude. Because gas solubility and diffusivity data are so critical to effective modeling of the glass melting process and because much of the data in the literature are inconsistent, beginning in January 1997, the CGR provided cost-sharing funds for three additional projects on the same topic. Over the course of the next three years another five CGR projects were initiated in this area. The extra funds not only accelerated progress, but also provided the capability for employing more than one technique to obtain the data.

The techniques used for measurement of He, Ne, Ar and N_2 solubilities are straightforward: saturate the melt at the desired temperature and pressure, then drive off the dissolved molecules under vacuum, measuring the quantity of gas released. The techniques are described in Reference 3. Unavoidably however, as the molecular size increases, the solubility and the accuracy of its measurement both decrease. Water solubility measurements are also rather straightforward, when suitable care is taken.

Helium solubility was measured for all six base glasses. Data for the three of the six is shown in Figure 1. Because of lack of commercial interest by the CGR member companies, investigations of

neon solubility were abandoned after the solubilities were measured for the low-expansion base glass. Argon solubility was measured over the full range of temperatures for the low-expansion borosilicate, at 1200°C and 1300°C for the wool glass, and at 1300°C for float, container and TV glasses, but technical difficulties with the instrumentation interrupted the work. Nitrogen solubility was so low in all the glasses that measurement was impossible due background "noise" from atmospheric nitrogen, i.e., it was below the detectability limit of the instrument. Data from the inert gas solubility studies are reported in References 4a to 4e.

H_2O (water) solubility for all six base glasses and several related compositions are reported in References 5a to 5h.

2.1.4 CO_2 and SO_2

CO_2 and SO_2 solubility determinations are considerably more difficult, hence justifying the greater time and funding allotted to them in this project. Shelby has recently reviewed the literature related to CO_2 in glass melts [6] and concluded that for silicate melts, CO_2 solubility increases with increasing NBO (non-bridging oxygen) concentration and is influenced by the nature of the modifier cation species which cause the NBOs to form. At this point in the project, CO_2 solubility measurements have been completed for all six commercial base glasses over the approximate range of 1000°C to 1400°C (the specific temperature range is different for each composition). Shelby's team developed and uses a fluxing technique to more efficiently outgas CO_2 from the melt samples. Shelby has pointed out that the extremely low solubilities of carbon dioxide (from 0.2×10^{16} to 2.0×10^{16} molecules/gram-atmosphere) in the relatively acidic commercial glass compositions studied made these measurements extremely difficult and their accuracies less than what might be desired. (By comparison, solubilities in the more basic melts commonly reported in the literature range from approximately 10^{18} to 10^{22}, on the same scale.) Evaluation of the CO_2 data is still under way.

The situation for sulfur is even more complicated. Sulfur can exist in glass melts as elemental sulfur, sulfides (S^{2-}), sulfur dioxide (SO_2), sulfite (SO_3^{2-}), and sulfate (SO_4^{2-}). Factors affecting the solubility of sulfur in glass melts include composition of the melt, partial pressure of the vapors of sulfur compounds present in the atmosphere, partial pressure of oxygen, partial pressure of water (H_2O), and temperature. Prokhorenko and co-workers, in St. Petersburg, were funded by the CGR from mid-1997 to study solubility and diffusivity in this complicated system. Very low rates of exchange of dissolved SO_2 gas with the atmosphere challenge the normal techniques for equilibration. Prokhorenko concluded that transport of the sulfur species between melt and atmosphere is controlled not only by the diffusion process, but also by reactions at the interface. In fact, sulfate layers tend to form at the melt-vapor interface. Prokhorenko's team tried several techniques to overcome this difficulty and has developed at least one to the point whereby reliable saturation and desorption are achieved. They also have developed special diffusion couples for measuring the diffusion coefficients. Mathematical models of the SO_2/SO_3 transport processes at free surfaces and into rising bubbles are being developed.

Unfortunately for modelers, the solubility data for CO_2 and SO_2 are not simply functions of the specified glass composition and temperature.

Note on time requirements for gas solubility measurements: Complete characterization of gas solubility requires weeks per glass composition and gas type. Thus, we would not have been able to characterize all 125 or more compositions with the funding provided by the DOE or within the time frame available.

2.1.5 Another Investigation

Dr. Herbert Giesche (AU) was funded during 1997-98 to investigate the feasibility of alternative methods of measuring gas solubility in glass using a volumetric gas absorption unit. These studies did not yield useful results and were abandoned after the initial period.

2.1.6 Gas Diffusivity

Water diffusivity measurements for all six base glasses by Shelby's team are complete. See References 5a to 5h. Data were also obtained for seventeen ternary soda-lime-silica and seven alkali-alkaline earth-silica glasses. Graduate student Douglas Rapp has recorded these results in a masters thesis [5f].

Further, water (H_2O) solubility and diffusivity were measured at 1200°C for 17 compositions in the ternary soda-lime-silica system and 7 other alkali-alkaline earth-silica compositions. This information will supplement our understanding of the behavior of the float and container glasses.

SO_2 (sulfur dioxide) - The Russian investigators concluded that transport of the sulfur species between melt and atmosphere is controlled not only by the diffusion process, but also by reactions at the interface. Special diffusion couples were developed for measuring diffusion coefficients. Measurements are complete. Mathematical models of the desorption process at free surfaces were developed.

2.2 Surface tension, density and thermal expansion

Principal Investigator: Dr. Alexis G. Clare (AU); Co-investigator: Dr. Linda E. Jones (AU); Graduate assistants: Ahmet Kucuk and Douglas R. Wing

[These investigations were partly funded by the CGR and partly by the DOE grant.]

These three properties were treated together, since the same apparatus, and often the same set of measurements, are used to determine each. Sessile and pendant drop techniques were used. The sessile drop technique for measuring density and surface tension of liquids (a stationary drop on a horizontal, non-wetting substrate) was developed in the 19th century by Bashforth and Adams [7]. More recently, the technique has been significantly improved by use of computerized curve fitting and image analysis [8]. The experimental set-up used by Clare and co-workers is shown in Figure 2a, and described in Reference 9. An improved version of the set-up, used for the most recent measurements by Wing, is shown in Figure 2b and described in Reference 10. The main cause of experimental error, volatilization of the drop during measurement causing mass loss and composition changes, was addressed and minimized by designing a device to hold the glass in a cool zone of the furnace until the furnace was stabilized and then inserting the glass into the hot zone and allowing the glass to equilibrate at temperature on the substrate before measurement commences. (The equilibration time is short because the drops are only 1 cm in diameter.) The method ensures the glass is at the high temperature for a minimum time.

Reference 9 discusses measurements on soda-lime-silica glasses and verifies difficulties with the drop techniques to include changing mass and changing surface tension during the experiment due to volatilization of glass components. These effects were investigated further [11, 14]. For sessile drop measurements, the drop of molten glass rests on a non-wetting polished graphite substrate. With surface tension measurements in oxidizing atmospheres, which would attack the graphite, the experimental procedure was modified to use pendant drops (suspended drop from a platinum alloy ring). The effects of relative humidity (water vapor present in the measuring furnace) and other atmospheres (reducing and oxidizing) were investigated [12, 13, 14], as were the effects of iron

redox (Fe^{2+}/Fe^{3+}) [13, 14]. Surface tension measurements for four of the six commercial base glasses of this project have been reported elsewhere [11] and show that the surface tension of commercial float glass is affected by the oxygen and water content of the atmosphere. For the soda-lime-silica glass at 1400°C, surface tension in wet vs. dry air decreases by about 5 % for as little as 4% water concentration.

The algorithms used to calculate the surface tension assumed a non-wetting situation, which limited the atmosphere to inert so that graphite could be used as a substrate. This was solved by adapting the experiments to be able to measure pendant drops, which do not require non-wetting situations.

The chief limitations of the experiment are that data may only be collected up to a temperature of 1500°C, the limit of the current furnace, or to where volatility of the glass becomes too severe.

Results of density and surface tension measurements performed on four of the five commercial glass provided by our industrial members (Section 1.14, above) were presented to the CGR membership at their Semiannual Research Meeting in Santa Barbara, CA, in January, 1998. The density and surface tension behaviors of all six commercial base glasses are shown here as functions of temperature in Figures 3a and 3b. Thermal expansion behavior can be determined from the density data in a straightforward manner.

2.2.1 A caution for process modeling applications of the data:

For process modeling, several different "surface tensions" must be considered, depending upon which glass surface is involved. First, there is the top surface of the glass, in contact with the furnace atmosphere. This surface tension, $g_{(melt\text{-}atmosphere)}$, is important for modeling fluid motion and corrosive activity at the glass-refractory-atmosphere metal line and for modeling fining and foaming behavior at the point where a rising bubble is constrained as it approaches and deforms the glass surface above it. This surface tension is dependent on the reactive components in the atmosphere above the melt; for examples, typically 71% N_2, 14% H_2O, 12% CO_2 and 3% O_2 (by volume) in an air-gas fired furnace, 64% H_2O, 31% CO_2, 4% N_2, and 1% O_2 in an oxy-gas fired furnace, and 79% N_2, 21% O_2 and ~1% Ar in an electrically heated furnace. Further, if the glass contains highly volatile components, the surface composition may differ from the bulk, so surface tension measurements based on the bulk composition may not apply. Second, there is the surface tension, $g_{(melt\text{-}bubble)}$, which controls the growth and shrinkage of bubbles. Here the compositions of the bubble gases are important, for example CO_2, O_2, and SO_X, since they affect the surface tension. These gases are generally not in equilibrium with the atmosphere above the melt. Finally, there are the surface tensions, $g_{(nucleation)}$, involved in calculating the critical super saturation for nucleating gas bubbles within the melt, or at the melt-refractory interface. Here, the atmosphere of concern consists primarily of the supersaturated gas specie(s) in the melt.

2.3 Radiative Conductivity of Melts

Principal Investigator: Dr. Oleg A. Prokhorenko; Senior Scientist: Dr. Marina V. Chistokolova; Technical Advisor: Dr. Oleg Mazurin (all, St. Petersburg, Russia)

2.3.1 Background

It is well known that in the range of about 500°C to 1000°C, both thermal acoustic vibrations (phonons) and radiated light energy (photons) contribute significantly to thermal conductivity. Above about 1000°C, radiative (photon) conductivity is the dominant component of heat transfer. The most effective and dependable way to determine this component is by measuring the absorption spectra of the glass melt in the wavelength region between 0.6 and 3.8 mm. Having done this, the

key factors controlling radiative heat transfer (radiative conductivity and mean free path length) can be calculated using the Rosseland approximation, valid when the mean free path for radiation is less than the dimensions of the glass. In the case of optically thin glass layers, more advanced mathematical approaches as, for example, MRCA recently developed at the LGP (Laboratory of Glass Properties – see below), should be used.

Researchers led by Dr. Oleg Mazurin at the Laboratory for Glass Properties at the I.V. Grebenschikov Institute for Silicate Chemistry (St. Petersburg, Russia) and operating as the Thermex Company, with support from the NSF Industry/University Center for Glass Research from 1994-98, developed a method for measuring absorption spectra of glass melts at high temperatures [15]. The method gives repeatable results of considerable accuracy. Results of such measurements on a series of float glasses of different iron content were reported in 1997 [16]. We elected to use this technique for our studies and sub-contracted the work to the St. Petersburg group (led by Dr. Oleg Prokhorenko since 1998). In 2002 Oleg Prokhorenko established a new business – LGP LLC - and his group left the Institute. Oleg Mazurin joined LGP LLC in 2001 as the Chief Scientist.

2.3.2 Procedure and Results

The St. Petersburg group's SF-2-LGP and SF-3-LGP fully automatic spectrophotometers were used. During the course of the investigation a system for fast heating and cooling, which consists of a heat-resistant tube and a moveable high temperature furnace to provide rates of cooling up to 50K/min, was developed. The methodology employed utilizes those special spectrophotometers and high-temperature sample cells containing sapphire windows. It is important to account for the effects of the presence of the windows and to ensure bubbles do not form nor any devitrification of the glass occurs within the optical path of the instrument. A four-step procedure is involved, consisting of 1) measurement of the absorption spectrum at room temperature, 2) measurement of changes of absorption coefficients (as a function of wavelength) caused by heating from room temperature to a temperature T_{11} corresponding to a viscosity of 10^{11} Poise, done twice, once with no windows in the cell and once with windows wet by the glass, 3) measuring the changes related to heating to temperatures T_X lying within the range $T_{11} < T_X < 1200°C$ (this can be done for nine or more heating cycles between the two temperatures), and 4) investigating irreversible changes in absorption that take place between 1100°C and 1450°C (due to bubbles, redox changes, devitrification, etc.) to determine heating-cooling cycles that will avoid those changes. E-glass measurements were especially sensitive to irreversible changes due to its higher bubble formation and devitrification tendencies. Additional techniques involving a slow-scan digital camera (developed with PPG Industries funding) were beneficial in such cases and were reported at the 6th International Conference on Fusion and Processing of Glass, held in Ulm, Germany, May 2000 [17].

To determine radiative conductivity for thin layers, where the Rosseland approximation is not valid, a modified approximation and corresponding computer software (MRCA) has been developed by the St. Petersburg workers.

The high temperature spectral transmittance and calculated properties for each of the six commercial glasses are shown in Figures 4 a-f.

2.4 Non-Newtonian Flow Behavior of Melts

Principal Investigator: Dr Arun K. Varshneya (AU); Graduate Assistant: Joshua Jacobs

The graduate assistant joined the program in the fall of 1997. Progress that semester was primarily

related to modifying the hydraulic Instron™ universal testing machine, determining needed supplies, and other facets of these experiments including quality assurance and library research. To become familiar with the cylinder compression method for the non-Newtonian flow studies, samples of soda-lime-silica glass were run in a parallel plate viscometer. The information gained enabled specification of the Instron modifications needed to allow it to perform the functions of a parallel plate viscometer.

All six base glasses were studied on the modified Instron machine at viscosities of 10^{10} Pa·s and seven different strain rates. The deviations from Newtonian behavior were characterized. Figure 5 illustrates the observed behavior.

2.5. Oxygen Partial pressure (Redox)

Principal Investigator: Dr. Thomas P. Seward (AU); Research Scientist: Terese Vascott; Student assistant: Ryan Kuehn

Because some melt properties can be sensitive to the redox state of the glass (for example, high temperature radiative conductivity can depend on the ionization state of multi-valent ions such as iron in the glass), it is important to know the partial pressure of oxygen within the glass melt. This is not determined during routine chemical analysis. We made such measurements at Alfred using a commercial Rapidox™ oxygen partial pressure measurement system made by Heraeus Electro-Nite Company. This system uses a disposable probe that is inserted into a crucible rotating within a furnace. The design of the equipment and principles of the measurements are given in Reference 18. As a reference for the current project and future work, the oxygen partial pressures of all the commercial base glasses were measured, as shown in Figure 6. The low-expansion borosilicate glass was measured using a high-temperature Mo/Mo_2 reference sensor probe; the other glasses were measured using the standard Ni/NiO reference probe.

3. PROPERTIES MEASURED ON THE FULL ARRAY OF EXPERIMENTAL GLASSES

3.1. Viscosity

Background: Glasses are generally melted in large furnaces at temperatures considerably above 1200°C where the melt viscosity is on the order of 100 Poise (10 Pa·s); they are formed into useful objects (e.g., sheet, tubing, containers, CRT bulbs, etc.) at lower temperatures, corresponding to viscosities near 10,000 Poise (1,000 Pa·s). Glass is tempered at viscosities near 10^{10} Poise (10^9 Pa·s) and annealed at viscosities near 10^{13} Poise (10^{12} Pa·s). Accurate knowledge of viscosity as a function of temperature over this range and more is essential for process design and operation. Because the viscosity of interest spans such a wide range, 10^1 to 10^{14} Poise (10^0 to 10^{13} Pa·s), no single technique is capable of measuring over this range. Hence, we employed three techniques:

3.1.1. Rotating spindle viscosity measurements (10^1 - 10^4 Poise)

Preliminary investigations:

Principal Investigator: Dr. William C. LaCourse (AU); Graduate Assistant: Nathan Canfield

The concentric cylinder technique, using the equipment available, was believed capable of measurements in the 1 Pa·s to 10,000 Pa·s range at temperatures to approximately 1500°C. During 1997 tests were first performed on a NIST standard glass. The results were within acceptable limits over the low viscosity range, but in the high viscosity range (>10,000 Pa·s) differences were unacceptable. This would limit the viscosity range over which we could provide data by the

concentric cylinder technique, but the acceptable range covers what we had anticipated being able to do. Reproducibility was checked and results were well within the anticipated limits. Measurements on 4 of the commercial glass compositions (supplied by industry) were completed.

Based on results the first year, it appeared that at it would require about 4 days to measure each composition, including time for cleaning the crucible. Thus we were on schedule for completion of up to approximately 80 compositions by the end of the original contract period.

Intermediate Investigations:

Principal Investigator: Dr. Alexis G. Clare (AU); Graduate assistants: Saritha Rajamma and Juergen Walker

Upon graduation of Dr. LaCourse's graduate student in 1998, other student investigators took over the equipment. The next few years were fraught with multiple equipment failures. Although significant progress was made on measuring viscosity of the soda-lime-silica container glass compositions, it became clear that at our then current rate of progress, we would fall far short of our measurement goals by contract end. We sought alternative solutions. The one chosen, to contract the work to PNNL (Pacific Northwest National Laboratory) is reported below.

Upon further evaluation of the rotating cylinder/spindle viscosity data generated at Alfred, it became apparent that the deviations from standard occurred not only at the highest viscosities (as describe in the section above), but developed in a progressive manner over the temperature range of interest, being valid only at the lowest viscosities. Hence, all of that data has been abandoned, at least until we learn how to correct it systematically.

Final Investigations:

Principal Investigator: Dr. Pavel Hrma (PNNL); Student assistants C.A. See, O.P. Lam, and K.B.H. Minster

As a result of equipment difficulties at Alfred, many of these high temperature rotating spindle viscosity measurements were conducted at PNNL using G-PLUS funding (Schott Glass Technologies, 2002) and some supplemental DOE funding from this grant. This investigation and the data generated are reported elsewhere [19]. But, because the PNNL data will be incorporated into our statistical model, we also report their procedures here.

Excerpting almost verbatim from Reference 19:

> Viscometer - The viscosity of glasses was measured using two rotating spindle viscometers. One viscometer was a manual Brookfield Digital Viscometer Model LVTD and the other a programmable Brookfield Digital Viscometer DV-III+ Rheometer. Each viscometer was set up above a vertical tube Deltech furnace and was equipped with a Pt-Rh spindle—a cylindrical disc 14 mm in diameter and 2 mm thick located 8 mm from the end of the rod. The temperature-recording thermocouple was located under the crucible. The setup is schematically shown in Figure 7.
>
> Method- The measurement was conducted according to the PNNL test procedure (Standard Viscosity Measurement Procedure for Vitrified Nuclear Waste, GDL-VIS). However, the procedure was modified for the commercial glasses that melt at higher temperatures than the waste glasses (generally, waste glasses are processed at ~1150°C).

Each sample of the glass was prepared by crushing the glass into pieces 5 to 25 mm in size. The glass volume of 50±5 mL was measured using liquid (ethanol) displacement. Dry glass was added to a 5-cm diameter platinum crucible and melted in a melting furnace. The crucible with molten glass was transferred to the viscometer furnace. The position of the crucible on the alumina pedestal and the spindle in the crucible were carefully centered. The spindle was lowered into the melt so its lower end was 2 mm from the bottom of the crucible.

The glass was melted at an estimated lowest temperature, T_{min}, at which the viscosity was measurable by the viscometers (~300 Pa·s for the manual viscometer and ~700 Pa·s for the programmable viscometer). For glasses tested in this study, T_{min} could be as low as 1000°C and as high as 1400°C. The T_{min} was initially estimated using viscosity models for waste glasses. After a sufficient database of commercial glass was accumulated, first-order models were developed for the commercial glass composition region and used for more accurate predictions.

For a majority of glasses, four measurements were taken at 100°C intervals, starting at 1200°C and ending at 1500°C. If the maximum operating temperature for the furnace would exceed 1550°C, the temperature interval, the number of temperature set points, or both, were decreased accordingly. For example, if $T_{min} \approx$ 1400°C, three measurements were taken in 50°C intervals.

The glass was heated to each set point and allowed to stabilize, i.e., to reach thermal equilibrium, for 25 min. As the spindle rotates at a constant speed, the torque value is registered by the viscometer. For the optimum strain of the spring, the spindle speed was manually adjusted on the manual viscometer; for the programmable viscometer, the Theta Viscometer Controller adjusts the speed automatically.

When the melt stabilized in the manual viscometer, the temperature, torque, and speed were recorded three times over 5 minutes (the initial, intermediate, and final readings). The final reading (an averaged value if the readout was oscillating) was used to calculate the viscosity. The torque value oscillated nearly sinusoidally as a result of the apparatus construction and measurement setup. The oscillation frequency and amplitude changed with glass viscosity. Generally, the amplitude increased as the viscosity increased.

The programmable viscometer was set to record the temperature, time, torque, and spindle speed at 30-s intervals throughout the run. The average of ~20 readings at each set temperature was used to calculate viscosity. This large number of readings was used because the program recorded random values of the oscillating torque rather than the purposefully recorded maximum and minimum values for the manual viscometer. The torque readout statistics for three randomly selected measurements is shown in Table B1, Appendix B, of Reference 19. The corresponding standard deviations for viscosity are 0.11, 4.19, and 0.78 Pa·s, representing 0.5, 5.6, and 0.5% of the viscosity value.

The accuracy of the viscosity measurement has been established in previous studies. Samples of glasses were sent to Corning Engineering Laboratory Services (CELS) for viscosity overcheck testing. The CELS and PNNL data showed good agreement.

Calibration - The viscometers were calibrated using National Institute for Standards and Technology (NIST) 710a soda-lime-silica glass, for which

$$\log(\eta) = A + \frac{B}{T - T_0} \qquad (1)$$

where η is the viscosity, T is the temperature, and A, B, and T_0 are coefficients that have the following values: T_0 = 240.8°C, A = –1.7290 (for η in dPa·s), and B = 4560.0 K.

The calibration data were used to calculate the spindle factor, F, defined as

$$F = \eta \frac{\omega}{\tau} \qquad (2)$$

where τ is the torque, and ω is the spindle speed.

The temperature range for calibration on the manual viscometer varied from 1200°C to 1500°C. The measurement began at 1200°C. For each subsequent measurement, the temperature was increased by 100°C. The highest temperature was 1500°C. Then the temperature was decreased to 1200°C by 100°C intervals, following the procedure developed for waste glasses that are prone to crystallization. The measurement during decreasing temperature was unnecessary for commercial glasses and was no longer followed for the programmable viscometer. On the programmable viscometer, the temperature range varied from 1200°C to 1500°C for the first calibration and from 1100°C to 1500°C for following calibrations (the programmable viscometer operated at a wider viscosity range).

The viscometer was calibrated monthly at regular intervals (by the number of measurements rather than time) and when [new crucibles or spindles] were implemented.[(i)]

When the viscometer was calibrated in response to an equipment adjustment, the new spindle factor was used for the glasses following the calibration. During the intervals when the spindle factor changed without replacing a part of the equipment, we [PNNL workers] reasoned that the crucible and spindle sustained progressive deformation with each additional test. Therefore, the spindle factor was determined by the equation

$$F = F_0 + \Delta F \frac{n}{n_t} \qquad (3)$$

where F_0 is the spindle factor from the preceding calibration, ΔF is the spindle factor change (from the preceding to subsequent calibration), n_t is the number of glasses tested between the calibrations, and n is the count of glasses tested since the preceding calibration.

The viscosity of glasses was calculated using Equation (2) rearranged as

$$\eta = F \frac{\tau}{\omega} \qquad (4)$$

This concludes the excerpt from PNNL report.

3.1.2. Parallel plate viscosity measurements (~ 10^5 - 10^9 Poise)

Principal Investigator: Dr. Arun K. Varshneya (AU); Post-doctoral Researcher: Alex Fluegel; student assistants Cory Bishop and Jessica Torrey.

(i) Manual viscometer furnace was repaired starting 8/7/02 and ending 8/12/02, and the programmable viscometer crucible and spindle were changed on 11/1/02.

A schematic representation of the parallel-plate viscometer used is shown in Figure 8. A disk of glass, roughly 6-8 mm diameter by 3-5 mm thick, is sandwiched between two parallel plates inside a well-insulated furnace as shown. Direct contact with the plate material is avoided by employing thin Pt foil or alumina substrates. The upper pedestal is loaded, and the rate of sagging is recorded as a function of time. The equipment and method are described more fully in Reference 20. The data from this study are plotted in Figures 9 and 10.

3.1.3. Beam bending viscosity measurements (~ 10^{10} - 10^{13} Poise)

Principal Investigator: James E. Shelby (AU); Research Scientists: Melissa G. Mesko and Holly Shulman

This transformation range viscosity was measured using the beam-bending method originally developed by Hagy [21] and later modified by the principal investigator [22]. Figure 11 is a schematic illustration of the apparatus. The modified method allows use of a much smaller bar than required by the original method.

The beam-bending method relies on the measurement of the rate of deflection due to viscous flow of the mid-point of a bar loaded in a 3-point configuration. Viscosity is calculated from the deflection rate and other information about the sample and apparatus, including the span width, the thickness and width of the bar, the density of the glass, and the load applied to the mid-point of the bar.

As reported by Shelby [23a], the beam-bending viscometer was calibrated by using NIST viscosity standards 710, 711 and 717. Several measurements were made using these glasses. The viscosity was measured at ~5 K intervals and plotted against temperature, as indicated by a thermocouple placed within 2 mm of the top of the sample. The temperatures corresponding to 10^{12}, 10^{11} and 10^{10} Poise were determined from a curve fit through the data. The experimental temperature corresponding to each of these viscosities was then plotted against the "correct" temperature for that viscosity according to the NIST data sheets. A combined plot of experimental versus NIST temperature for several sets of measurements using all three standards was fit with a straight line which was then used to correct all experimental data for the samples.

The temperatures corresponding to 10^{12}, 10^{11} and 10^{10} Poise were determined from the experimental data for all available glasses and are listed in Table 8.

3.2. Electrical Resistivity

Principal Investigators: Drs. Thomas P. Seward Arun K. Varshneya (AU); Research Scientists: Terese Vascott and D.M. Korwin; Post Doctoral Researcher: Ramesh Karuppannan; Undergraduate Research Assistants: Heather K. Neil and Jeffrey M. Jones

A two-point probe method as shown in Figure 12 was used to measure electrical conductivity of the glass melts. The system used for these measurements had to be rebuilt and calibrated at the start of the investigations, primarily because a new Lindberg Blue M furnace with 1,550°C capability was brought into service. Calibration and verification of the sample cell was performed using potassium chloride solutions at room temperature and an NIST standard glass SRM1414 at the glass melt temperatures. Measurements were made on all six commercial base glasses and all of the 144 experimental glass compositions. The resistivity behaviors for all six families of glass are shown in Figures 13 and 14.

In 2001-02, Dr. David Earl and a graduate research assistant, Rebecca Neill, completed the statistical analysis of the available electrical resistivity data for the full set of TV panel glasses. The data was fitted to Arrhenius plots with only 3 out of 360 data points found to be statistical outliers. This analysis phase stopped in May 2002 when Rebecca's funding ran out, but the results were encouraging for the full statistical analysis to be undertaken as described in Section 5.7.

3.3. Glass Physical Properties

Principal Investigator: James E. Shelby (AU); Research Scientists Melissa G. Mesko and Holly Shulman; Undergraduate research assistants: Sara Scheffler, Kelly Murphy and Cleo Shelby

In 2001, Dr. James Shelby and several of his co-workers undertook to measure important glass physical properties on all the available glasses from this study, using supplemental funding from the CGR and the PI's discretionary research funds. These properties include density, refractive index, coefficient of thermal expansion, dilatometric softening point, glass transition temperature, dissolved water concentration and electrical conductivity at 200°C and 300°C. At this point, the properties have been measured on all but about twenty-five of the experimental glasses. Although this work is outside the scope of the present grant and is reported elsewhere [23], it is mentioned here to show another way in which the database begun with this grant will continue to expand.

4. ABANDONED PROPERTY MEASUREMENTS

4.1 Elastic-Viscoelastic Properties of Melts

Principal Investigator: Dr Arun K. Varshneya (AU); Graduate Assistant: Joshua Jacobs

The graduate assistant joined the program in the fall of 1997. Progress that semester was primarily related to modifying the Instron™ universal testing machine for the non-Newtonian viscosity measurements (see Section 2.4) and the ultrasonic elastic-viscoelastic equipment needed for this part of the study.

For the elastic and viscoelastic measurements, four ultrasonic transducers were obtained and a digital oscilloscope and pulser-receiver located. The scope and pulser-receiver had to be shared with another project. Because of the high temperatures and the oxide compositions involved in this study, the silica rods previously used (for chalcogenide glass studies) will no longer suffice as conductors of the ultrasonic waves into the melt. Preliminary design began for molybdenum rods, which will not corrode at the high temperatures used in the present research.

Unfortunately this study had to be abandoned, primarily because of experimental difficulties and because, when the student J. Jacobs graduated, insufficient funds remained to launch the required level of investigation.

4.2 High Temperature Heat Capacity

Principal Investigator: Dr Arun K. Varshneya (AU); Graduate Assistant:

As was pointed out in the proposal, in recent years high temperature DSC (differential scanning calorimeter) units capable of heat capacity measurements to 1400°C, as needed for this project, have become available. During 1997 the specifications for suitable unit were defined and bids solicited from three suppliers. The final choice was a Haake Model 6500, which was delivered at year-end. It was installed during the first quarter of 1998. We initially thought this delay would not be a particular problem, because these measurements are relatively simple and the work could be

completed in a short period of time. Unfortunately, preliminary measurements showed the instrument to be unstable and give irreproducible results above about 1000°C.

We pursued the problem with the equipment manufacturer who admitted that it was not designed to measure materials like glass, which soften and wet the sample chambers at high temperatures. After several attempts to work around this problem, the investigation was abandoned.

It is the opinion of the PI that the heat capacity calculated on the basis of the molecular content of the glass would be more accurate than any experimental determination currently possible.

4.3 Other Surface Tension Measurement Techniques

Principal Investigator: Dr. William C. LaCourse (AU); Graduate Assistant: Haochuan Jiang

Two other methods for surface tension measurement of molten glass were considered early in the project to extend the temperature range of the measurements and to provide independent determinations to verify the applicability of the techniques. These were the “maximum bubble pressure” and the “fiber elongation” methods. Equipment was available and measurements were being made on another project using the maximum bubble pressure method. However, since the pendant and sessile drop studies reported above were going well, this was not pursued. The fiber elongation technique could extend the surface tension measurements to higher viscosities, but it is a very tedious method and a student to perform the work was not available, so it was not pursued either.

4.4 Thermal Diffusivity of Glass Melts

Principal Investigator: Douglas M. Korwin (AU)

We proposed to measure the thermal diffusivity of selected glass melts by a modified Angstrom method [24]. Investigators at Alfred and elsewhere had successfully used this method to measure thermal diffusivity of glass melts in the range of 600 to 1500°C.

Before this award was granted, the PI identified for these investigations, Dr. Innocent Joseph, left Alfred University for employment elsewhere. Douglas Korwin succeeded him as the identified PI. During 1997 the equipment needed for this program was purchased, assembled, de-bugged, preliminary measurements performed and work begun on software for process control and data acquisition. However, Korwin completed the requirements for his PhD degree (working in an entirely different project area), graduated and left the University’s employ in Spring 2001. CGR member companies felt that the radiative conductivity measurements reported in Section 2.3 would suffice for their modeling needs, so the thermal diffusivity studies were discontinued.

5. STATUS AND FUTURE WORK

5.1 Condensed Statement of the Proposed Work (From original proposal)

“We proposed a two stage project that would involve the United States glass industry and the Center for Glass Research (CGR) at the New York State College of Ceramics at Alfred University. The major part of the project would involve the development of a comprehensive and reliable composition-property database for commercial glass forming melts that will allow full use of existing modeling programs by a broad cross section of the glass industry. During the final stage of the project the modeling programs will be tested by participating glass manufacturers using data developed during the initial part of the project. We believe that using the information developed

during this project, the glass industry will be able to refine their processes to achieve improved energy efficiency, better product quality and lower emissions from glass tank furnaces.

“The main objective of the proposed work is the development of a comprehensive and reliable data base for glass forming melts that will allow full use of numerical simulation models by a broad cross-section of the glass industry for the purpose of achieving energy savings, improving product quality, increasing productivity, and meeting present and future environmental regulations.

“The final stage of the project will involve testing of modeling programs by the industry participants using the data developed during the early part. Again, to insure that the data will be useful for this application, an industrial advisory group will be closely involved in every aspect of this project.”

5.2 Intended Market and Commercialization Plans

The intended market for the project results is the member companies of the CGR; particularly those researchers involved in furnace design and automated process control. Plans for "commercialization" of the results of the project were detailed in our original proposal. Several CGR member companies have agreed to use the database prepared in the project in order to test and improve their mathematical models. Once this is accomplished the data will be made available to all U.S. glass manufactures, probably via publication of a book, which, in addition to the raw data, will provide details of the measurement techniques and an analysis of the composition dependencies of the melt properties.

The expected outcome(s) of the project include improved modeling capabilities, which will lead to improved furnace efficiency and glass quality.

5.3 Review Funding and Cost Sharing

The CGR provided cost sharing funds in three ways: First, by providing “summer” salaries to those faculty members supervising the research during 1997 (CGR funding of faculty investigators ceased in 1998, as stipulated in the grant application); second, permitting significant fractions of time to be spent on this program by the CGR director and the assistant director for technology, probably in excess of 15% each; and third, through funding of eight separate gas solubility/diffusion studies:

Those projects are:

1) Carbon Dioxide Solubility in Soda-Line-Silicate Melts (Shelby, 97-99)
2) Solubility and Diffusion of Sulfur Compounds in Glass Melts at Temperatures of 1200-1450°C (Prokhorenko, 97-01)
3) Solubility of Gases in Glass Melts (Giesche, 97-98)
4) Water Solubility and Diffusion in Commercial Glasses (Shelby and Mesko, 98-00)
5) Transformation Range Viscosity of DOE Glasses (Shelby and Mesko, Summer 99)
6) Gas Solubility in Commercial Glasses and Melts (Shelby and Mesko, 99-01)
7) Water Solubility and Diffusion in Commercial Glasses II (Shelby and Mesko, 99-01)
8) Transformation Range Viscosity and Other Properties of DOE Database Glasses (Shelby and Mesko, 99-01)

5.4 Quality Assurance Program and Record-Keeping

Quality Assurance Officer: Douglas M. Korwin (1996-2000) and Terese Vascott (2000 to present) (each, Center for Glass Research Assistant Director for Technology)

A quality assurance program (QAP) was instituted for this project and was administered by the Center for Glass Research at Alfred University (CGR). The format of this QAP is patterned after a highly successful QAP employed at the New York State College of Ceramics at Alfred University during the execution of a contract with the West Valley Demonstration Project. The objective of the CGR quality assurance program is to produce reliable and verifiable data in a traceable manner.

NIST Standard Reference materials are used for calibration/verification whenever available.

All glass samples are labeled and stored in the Center's laboratory in Binns-Merrill Hall at Alfred University where careful identification and control procedures have been established.

Records of all data are maintained by the Center. The CGR Assistant Director for Technology receives data from the appropriate PIs and enters it into a computer database. She then posts summaries of this information, usually in graphical form, and in some cases descriptions of the measurement procedures themselves, onto our password protected Web site for accessibility by CGR members and participating faculty.

5.5 Progress versus Objectives

ID Number	Task / Milestone Description	Planned Completion	Actual Completion	Comments
Phase I	Designate systems to be measured, purchase and set up equipment, implement quality assurance program, calibrate equipment, train personnel, evaluate experimental procedures, implement industry suggestions, prepare glass samples, start data collection, write semiannual research reports.	12/97	12/98	Chemical analysis of all glass samples was added to the project task list. With the exception of melting/preparing some remaining glass samples and completing chemical analysis of three glass families, this phase is essentially complete.
Phase II	Complete data collection for all but visco-elastic properties, gas solubility and thermal diffusivity, analyze data, complete glass sample preparation, start data transfer to the industry, evaluate data, implement industry suggestions, maintain quality assurance program, write annual and semiannual research reports.	12/98	Ongoing	Thermal diffusivity was abandoned. Data collection is almost complete. Data analysis started. Data transfer to industry started through the CGR members Web site.

ID Number	Task / Milestone Description	Planned Completion	Actual Completion	Comments
Phase III	Complete data collection, complete data analysis, transfer data to industry, evaluate data, implement industry suggestions, collect data for any special compositions that are necessary, write annual and semiannual research reports	12/99	Ongoing	No-cost extension granted until 12/31/02. Additional funding was received from the DOE to allow completion of the glass melting at Alfred and the viscosity measurements at PNNL. When DOE funds are exhausted, most remaining measurements were performed using alternative funding sources by 2/28/03. Data analysis and transfer to industry will occur over the next 1 to 1.5 years.

Note: The explanation we offered the DOE for the additional time requested to complete this project was that the original proposal underestimated 1) the amount of time it would take to complete the work using student labor, 2) the difficulties that would be encountered melting/making the required quality and quantities of glass and 3) the difficulties that would be encountered with the calibration, standardization and maintenance of several key pieces of measurement equipment.

5.6 Plans and Expected Outcomes

While the data for our database have now been taken and compiled, two major tasks remain: 1) Statistically modeling the composition-property response surfaces for the viscosity and electrical resistivity data and 2) evaluation of the results by some CGR member companies.

5.7 Statistical Modeling

Principal Investigator: Dr. Dolun Oksoy (AU); Assisted by CGR Director, Dr. Thomas P. Seward; CGR Assistant Director for Technology, Terese Vascott, and Dr. Arun K. Varshneya.

We believe we have sufficiently high accuracy data to predict the viscosity and resistivity behavior of glass melts as functions of composition and temperature over the full range of compositions investigated. For viscosity, the data obtained for each glass by the three different techniques (three different viscosity ranges) will be combined into a single file. Each set of data will then be fitted to a Fulcher-type equation. The A, B and T_0 constants of the Fulcher equation will be obtained by non-linear regression. The viscosity and resistivity data for each glass type will then be analyzed by three different regression methods: linear, robust regression and neural network methods.

This work was in process as this report was being prepared. We anticipate having the results available for dissemination to the interested member companies by mid-2003.

5.8 Data Evaluation and Dissemination

Several CGR member companies have agreed to use the database generated by the project in order to test its applicability and improve their mathematical models. This activity should begin in mid-2003. It is planned that at the completion of this effort (1 to 1-1/2 years hence), the data will be made available to all glass manufactures, probably via publication of a book. In addition to the raw data, we will provide details of the measurement techniques, the analysis of the composition dependencies of the melt properties, their sensitivities to small composition variations, and an evaluation of the data's usefulness for process modeling.

Thus an ultimate outcome of the project will be improved modeling capabilities that will lead to improved furnace efficiency and glass quality. Another outcome has already been the education of graduate and undergraduate students, with practical experience, for employment in the glass industry.

6. SUMMARY

We proposed a two-stage project that would involve the United States glass industry and the Center for Glass Research (CGR) at the New York State College of Ceramics at Alfred University. The major part of the project, funded by this grant, involved the development of a comprehensive and reliable composition-property database for commercial glass forming melts that will allow full use of existing modeling programs by a broad cross section of the glass industry. It is anticipated that during the succeeding stage of the project, modeling programs will be tested by participating glass manufacturers using information and data developed during this project. We believe that by using this information and data, the glass industry will be able to refine their processes to achieve improved energy efficiency, better product quality, and lower emissions from glass tank furnaces.

7. REFERENCES

1. T.P. Seward, "The NSF Industry-University Center for Glass Research: An Overview," *59th Conference on Glass Problems*, C.H. Drummond, Ed., The American Ceramic Society, Westerville, OH, 1999

2. a) Proceedings of the DOE-CGR Workshop "Modeling in the Glass Industry" (1996)

   b) P. Sewell, "Industrial Perspective of Modeling in a Modern Float Glass Plant," The GlassResearcher **6** [2] 1-3 (1997), published by the NSF Industry-University Center for Glass Research, Alfred University, Alfred, NY.

3. J.E. Shelby, *Handbook of Gas Diffusion in Solids and Melts*, ASM International, Materials Park, OH (1996)

4. a) J.E. Shelby, "Solubility and Diffusion of Inert Gases in Silicate Melts," 18th International Congress on Glass, San Francisco, CA, July 1998

   b) M.G. Mesko, K. Newton and J.E. Shelby, "Helium Solubility in Sodium Silicate Glasses and Melts," Phys. Chem. Glasses **41** (3) 111-16 (2000) (CGR-funded)

c) M.G. Mesko, B.E. Kenyon and J.E. Shelby, "Helium Solubility in Commercial Borosilicate Glasses and Melts," Glastech. Ber. Glass Sci. Technol. **73(C2)** 33-42 (2000) (DOE- and CGR-funded)

d) M.G. Mesko and J.E. Shelby, "Helium Solubility in Ternary Soda-Lime-Silica Glasses and Melts," Phys. Chem. Glasses **43** (6) 283-90 (2002) (CGR-funded)

e) J.E. Shelby, C.C. Tournour and M.G. Mesko, "Inert Gas Solubility in Glasses and Melts of Commercial Compositions," accepted for presentation and publication, 7th International Conference on Fusion and Processing of Glass, Rochester, NY, July 2003

5. a) M.G. Mesko and J.E. Shelby, "Water Solubility and Diffusion in Melts of Commercial Silicate Glasses," Glastech. Ber. Glass Sci. Technol. **73(C2)** 13-22 (2000) (DOE-funded)

   b) M.G. Mesko and J.E. Shelby, "Solubility and Diffusion of Water in Melts of a TV Panel Glass," Phys. Chem. Glasses **42** (1) 17-22 (2001) (DOE-funded)

   c) M.G. Mesko and J.E. Shelby, "Water Solubility and Diffusion in Alkali Silicate Melts," Phys. Chem. Glasses **42** (3) 173-78 (2001) (CGR-funded)

   d) M.G. Mesko and J.E. Shelby, "Water Solubility and Diffusion on Melts of E and Wool Glasses," Phys. Chem. Glasses **42** (6) 383-90 (2001) (DOE-funded)

   e) M.G. Mesko, P.A. Schader and J.E. Shelby, "Water Solubility and Diffusion in Sodium Silicate Melts," Phys. Chem. Glasses **43** (6) 283-90 (2002) (CGR- and NSF-funded)

   f) D.B. Rapp, "Water Solubility and Diffusion in Glassforming Melts," Masters Thesis, Alfred University, Alfred, NY, June 2001.

   g) D.A. Rapp and J.E. Shelby, "Water Diffusion and Solubility in Soda-Lime-Silica Melts," submitted to Phys. Chem. Glasses (CGR-funded)

   h) J.S. Shelby, P.B. McGinnis, M.G. Mesko, "Water Diffusion and Solubility in Glasses and Melts of Float, Container, and Other Commercial Compositions," accepted for presentation and publication, 7th International Conference on Fusion and Processing of Glass, Rochester, NY, July 2003

6. J.E. Shelby, "Carbon Dioxide Solubility in Silicate Melts," Advances *in Fusion and Processing of Glass II (Ceramic Transactions 82),* A.G. Clare and L.E. Jones, Eds., The American Ceramic Society, Westerville, OH (1998) pp. 51-56 (CGR-funded)

7. F. Bashforth and J.C. Adams, *An Attempt to Test the Theories of Capillary Action*, Cambridge University Press, Cambridge, U.K. (1883)

8. Y. Rotenberg, L. Burokova and A.W. Neumann, "Determination of Surface Tension and Contact Angle from the Shapes of Axisymmetrical Fluid Interfaces." J. Coll. Inter. Sci. **93** [1] 169-83 (1983)

9. A. Kucuk, A.G. Clare and L.E. Jones, "Density and Surface Tension of Glass Melts as a Function of Composition at 1400°C," Advances *in Fusion and Processing of Glass II (Ceramic Transactions 82),* A.G. Clare and L.E. Jones, Eds., The American Ceramic Society, Westerville, OH (1998)

10. D.R. Wing, "Factors Influencing the Density and Surface Tension of Soda-Lime-Silica Melts Containing Multi-valent Ions," Ph.D. Thesis, Alfred University, Alfred, NY (April 2003; draft version, March 2003)

11. A. Kucuk, A.G. Clare and L.E. Jones, "Influence of various atmospheres on the surface properties of silicate melts," Glastech. Ber. Glass Sci. Technol. **73** [5] 123-129 (2000)

12. A. Kucuk, A.G. Clare and L.E. Jones, "Differences between the surface and bulk of glass melts I. Compositional differences and influence of volatalization on composition and other physical properties," J. Non-Crystalline Sol. **261**, 28-38 (2000)

13. A. Kucuk, A.G. Clare and L.E. Jones, "Differences between the surface and bulk of glass melts. Part 2. Influence of redox ratio on the surface properties of silicate melts," Phys. Chem. Glasses **41** [2] 75-80 (2000)

14. A. Kucuk, "Structure and the Physicochemical Properties of Glasses and Glass Melts," Ph.D. Thesis, Alfred University, Alfred, NY (February 1999)

15. a) O.A. Prokhorenko and O.V. Mazurin, "Problems of Spectrophotometry of Glass-Forming Melts. I. The current state of the Problem of Reliable Data Acquisition," Glass Physics and Chemistry **25** (2) 159-162 (1999)

    b) O.A. Prokhorenko, O.V. Mazurin, M.V. Chistokolova, S.V. Tarakanov, Yu.E. Reznik and I.N. Anfimova, "Problems of Spectrophotometry of Glass-Forming Melts. II. The Method of Measurement of Absorption Spectra of Glasses and Melts within Red and Near Infrared Spectral Regions in the Temperature Range from 20 to 1600°C," Glass Physics and Chemistry **26** (2) 187-198 (2000)

    c) O. Mazurin and O. Prokhorenko, "Thermal Conductivity of Glass Forming Melts: Technology Shifts Glass Measurements from Glass Function to Melt Properties," the GlassResearcher **10** (2) 36-38 (2001)

16. O.A. Prokhorenko and O.V. Mazurin, "High-temperature Radiative Conductivity of Commercial Iron-containing Glasses," *Advances in Fusion and Processing of Glass II (Ceramic Transactions 82),* A.G. Clare and L.E. Jones, Eds., The American Ceramic Society, Westerville, OH (1998)

17. O.A. Prokhorenko, "Absorption spectra and radiative thermal conductivity of E-glass at temperatures up to 1500°C," 6th International Conference - Advances in Fusion and Processing of Glass. Abstracts, German Society of Glass Technology, Frankfurt (2000); paper to be published.

18. a) P.J. McCarthy, "Rapidox Sensor Technology for Glass Melt Redox Measurement," the GlassResearcher Vol. 8, No. 2, 8-9 (1999)

    b) J. Plessers, A.J. Faber, T. Tonthat and P. Laimbock, Proceedings of the 58th Conference on Glass Problems, Urbana, Illinois, October 1997.

19. C.A. See, O.P. Lam. K.B.C. Minister and P.R. Hrma, "Viscosity of Commercial Glasses – Data Package," prepared for the U.S. Department of Energy under Contract DE-AC06-76RL01830, Pacific Northwest National Laboratories, March 2003.

20. A.K. Varshneya, N.H. Burlingame and W.H. Schultze, "Parallel Plate Viscometry to Study Deformation-Induced Viscosity Changes in Glass," in the Proceedings of the 2nd International Conference on Advances in the Fusion and Processing of Glass, October 22-25, 1990, Dusseldorf, Glasstech. Ber. **LXII K** (1990), 447-459.

21. H.E. Hagy, "Experimental Evaluation of Beam-Bending Method of Determining Glass Viscosities in the Range of 10^8 to 10^{15} Poises," J. Am. Ceram. Soc. **46**, 93 (1963)

22. J.E. Shelby, "Properties and Structure of B_2O_3-GeO_2 Glasses," J. Appl. Phys. **45** (12) 5272-7 (1974)

23. a) J.E. Shelby, M.G. Mesko and H. Shulman, "Transformation Range Viscosity and Other Properties of DOE Database Glasses – Final Report," NSF Industry/University Center for Glass Research, Alfred University, August 2002.

    b) J.E. Shelby, M.G. Mesko and H. Shulman, "Properties of Soda-Lime-Silica Glasses," accepted for presentation and publication, 7th International Conference on Fusion and Processing of Glass, Rochester, NY, July 2003

24. A.F. Van Zee and C.L. Babcock, "A Method for the Measurement of Thermal Diffusivity of Molten Glass," J. Am. Ceram. Soc. **34** [8] 144-250 (1951).

End of report

8. LIST OF TABLES

9. LIST OF FIGURES

4 – Radiative Conductivity versus Wavelength (at several temperatures, six base glasses)

5 – Non-Newtonian viscosity behavior (six base glasses)

6 – Partial Oxygen Pressure versus Temperature (six base glasses)

7 – PNNL Viscosity Measurement Apparatus

8 – Parallel-plate Viscosity Measurement Apparatus

9 – Log Viscosity versus Temperature (parallel-plate, six base glasses)

10 – Log Viscosity versus Temperature (parallel-plate, six families of glass)

11 – Beam-bending Viscosity Measurement Apparatus

12 – Electrical Resistivity Measurement Apparatus

13 – Electrical Resistivity versus Temperature (six base glasses)

14 - Electrical Resistivity versus Temperature (six families of glass)

TABLE 1 - PROPERTIES REQUIRED FOR FURNACE MODELING *

GLASS FLOW	Viscosity	ν
	Density	ρ
	Volume expansion coefficient	β
	Surface tension	$\gamma_{(melt\text{-}atmosphere)}$
ENERGY TRANSFER	Effective thermal conductivity	$k_{eff} \approx (16n^2\sigma T^3)/3\ \alpha_r$ **
	Absorption coefficient	α_λ, α_r
	Heat capacity	C_p
	Surface tension	$\gamma_{(melt\text{-}atmosphere)}$
GAS EXCHANGE WITH BUBBLES		
	Concentration of species "i" in glass	c_i
	Solubility	$S_i = c_{sat,i}/Pi$
	Diffusivity of species "i"	D_i
	Equilibrium constants for gas producing reactions	K_i
ELECTRICAL	Resistivity	ρ_{elec}
BATCH MATERIALS	Enthalpy (to melt)	ΔH_{batch}
	Thermal conductivity	k_{batch}
	Emissivity	ε_{batch}
REFRACTORIES	Thermal conductivity	$k_{refractory}$
	Emissivity	$\varepsilon_{refractory}$

* Adapted in part from a presentation by William W. Johnson, Corning Inc., at "Modeling in the Glass Industry" Workshop. CGR members added surface tension and refractory-related properties to the table after the Workshop.

** n = refractive index, σ = Stephan's constant, T = absolute temperature (K)

TABLE 2 - MODEL SENSITIVITY VS. PROPERTY MEASUREMENT ACCURACY

Model Sensitivity to Property	Accuracy of Present Day Measurements +/- 10 %	+/- 25%	+/- 50 to 100%
Very Sensitive		Gas reaction equilibrium constants	Gas concentrations in glass Gas solubilities Gas diffusivities
Sensitive	Viscosity Specific Heat Density Electrical resistivity Enthalpy required to melt batch Batch thermal conductivity	Thermal expansion Radiative absorption coefficient Effective thermal conductivity Emissivity of batch Thermal conductivity of refractory Emissivity of refractory	Radiative absorption coefficient (when low)
Insensitive	None	None	None

Glass Compositions as Analyzed

Base Glass ID	SiO_2	Al_2O_3	B_2O_3	MgO	CaO	SrO	BaO	Li_2O	Na_2O	K_2O	TiO_2
container	74.38	1.28		0.20	10.51	0.01	0.10		13.30	0.29	0.008
float	72.92	0.13		3.84	8.74				13.74	0.03	0.017
TV panel	61.53	2.06			0.05	9.19	9.23	0.010	7.64	7.55	0.430
E-glass	56.60	14.80	7.04	4.33	18.20				0.63		0.580
LE borosilicate		2.19	12.60	0.008	0.023			0.010	4.09	0.055	
wool		3.31	4.90	3.46	8.27				16.00	0.83	

Base Glass ID	CeO_2	ZrO_2	PbO	ZnO	Fe_2O_3	Sb_2O_3	F	FeO	SO_3	Total
container					0.036			0.008	0.21	100.33
float					0.109			0.042		99.57
TV panel	0.280	1.390	0.000	0.51	0.037	0.30		0.004		100.21
E-glass					0.350		0.220	0.100		102.85
LE borosilicate	0.005				0.026			0.016		19.02
wool					0.31			0.085	0.17	37.34

Table 3 – Commercial Base Glass Compositions (Analyzed Compositions)

TABLE 4 - PROPERTIES AND MEASUREMENT TECHNIQUES

PROPERTY	TECHNIQUE	MAX. TEMPERATURE or PROPERTY RANGE
Viscosity	Rotating Spindle Parallel Plate Beam Bending	10^1 to 10^4 Poise 10^5 to 10^9 Poise 10^{10} to 10^{13} Poise
Non-Newtonian Viscosity	Parallel Plate	Approx. 10^9 Poise
Density (Thermal Expansion)	Sessile/Pendant Drop with Image Analysis	1450°C
Surface Tension	Sessile/Pendant Drop with Image Analysis	1450°C
Heat Capacity	Differential Scanning Calorimetry	1500°C
Gas Solubility and Diffusivity	Saturation and Outgasing with specialized techniques	1500°C
Electrical Conductivity	Two Point Probe	1500°C
Radiative Conductivity	Optical Absorption	1500°C
Thermal Diffusivity	Modified Angstrom	1500°C

TABLE 5 - CLASSIFICATION OF PROPERTY DEPENDENCIES

PROPERTIES	DEPENDENCIES
I. Viscosity Density Heat capacity Electric conductivity	Glass composition (except trace components) Temperature
II. Radiative heat conductivity	Glass composition (including trace components) Redox state (partial O_2 pressure) Temperature
III. Gas solubility Surface tension	Glass composition (including dissolved gases) Redox state Atmosphere composition Temperature

Theoretical Glass Compositions

Oksoy ID	SiO_2	Al_2O_3	MgO	CaO	Li_2O	Na_2O	K_2O	Fe_2O_3	Cr_2O_3	TiO_2	SO_3	Total
1	0.810	0.01	0	0.07	0	0.11	0	0	0	0	0	1.0000
2	0.729	0.01	0	0.12	0	0.11	0.02	0	0.003	0.005	0.003	1.0000
3	0.700	0.01	0	0.12	0.01	0.15	0	0.004	0.003	0	0.003	1.0000
4	0.728	0.01	0.03	0.07	0	0.15	0	0.004	0.003	0.005	0	1.0000
5	0.707	0.01	0.03	0.07	0.01	0.15	0.02	0	0	0	0.003	1.0000
6	0.691	0.01	0.03	0.12	0.01	0.11	0.02	0.004	0	0.005	0	1.0000
7	0.718	0.03	0	0.07	0	0.15	0.02	0.004	0	0.005	0.003	1.0000
8	0.753	0.03	0	0.07	0.01	0.11	0.02	0.004	0.003	0	0	1.0000
9	0.685	0.03	0	0.12	0.01	0.15	0	0	0	0.005	0	1.0000
10	0.739	0.03	0.03	0.07	0.01	0.11	0	0	0.003	0.005	0.003	1.0000
11	0.647	0.03	0.03	0.12	0	0.15	0.02	0	0.003	0	0	1.0000
12	0.703	0.03	0.03	0.12	0	0.11	0	0.004	0	0	0.003	1.0000
13	0.732	0.01	0	0.07	0.01	0.15	0.02	0	0.003	0.005	0	1.0000
14	0.788	0.01	0	0.07	0.01	0.11	0	0.004	0	0.005	0.003	1.0000
15	0.696	0.01	0	0.12	0	0.15	0.02	0.004	0	0	0	1.0000
16	0.750	0.01	0.03	0.07	0	0.11	0.02	0.004	0.003	0	0.003	1.0000
17	0.682	0.01	0.03	0.12	0	0.15	0	0	0	0.005	0.003	1.0000
18	0.717	0.01	0.03	0.12	0.01	0.11	0	0	0.003	0	0	1.0000
19	0.744	0.03	0	0.07	0	0.15	0	0	0.003	0	0.003	1.0000
20	0.728	0.03	0	0.12	0	0.11	0	0.004	0.003	0.005	0	1.0000
21	0.707	0.03	0	0.12	0.01	0.11	0.02	0	0	0	0.003	1.0000
22	0.735	0.03	0.03	0.07	0	0.11	0.02	0	0	0.005	0	1.0000
23	0.706	0.03	0.03	0.07	0.01	0.15	0	0.004	0	0	0	1.0000
24	0.625	0.03	0.03	0.12	0.01	0.15	0.02	0.004	0.003	0.005	0.003	1.0000

Table 6a - Theoretical Container-type Glass Compositions – CO-pb1124

Theoretical Glass Composition

Oksoy ID	SiO_2	B_2O_3	Al_2O_3	MgO	CaO	Na_2O	K_2O	Fe_2O_3	TiO_2	F	Total
1	0.7150	0	0.12	0.005	0.16	0	0	0	0	0	1.0000
2	0.6540	0	0.12	0.045	0.16	0	0.005	0	0.01	0.006	1.0000
3	0.5570	0	0.12	0.045	0.24	0.02	0	0.008	0.01	0	1.0000
4	0.6310	0	0.16	0.005	0.16	0.02	0	0.008	0.01	0.006	1.0000
5	0.5700	0	0.16	0.005	0.24	0.02	0.005	0	0	0	1.0000
6	0.5360	0	0.16	0.045	0.24	0	0.005	0.008	0	0.006	1.0000
7	0.5860	0.09	0.12	0.005	0.16	0.02	0.005	0.008	0	0.006	1.0000
8	0.5220	0.09	0.12	0.005	0.24	0	0.005	0.008	0.01	0	1.0000
9	0.4790	0.09	0.12	0.045	0.24	0.02	0	0	0	0.006	1.0000
10	0.4890	0.09	0.16	0.005	0.24	0	0	0	0.01	0.006	1.0000
11	0.5100	0.09	0.16	0.045	0.16	0.02	0.005	0	0.01	0	1.0000
12	0.5370	0.09	0.16	0.045	0.16	0	0	0.008	0	0	1.0000
13	0.5940	0	0.12	0.005	0.24	0.02	0.005	0	0.01	0.006	1.0000
14	0.6210	0	0.12	0.005	0.24	0	0	0.008	0	0.006	1.0000
15	0.6420	0	0.12	0.045	0.16	0.02	0.005	0.008	0	0	1.0000
16	0.6520	0	0.16	0.005	0.16	0	0.005	0.008	0.01	0	1.0000
17	0.6090	0	0.16	0.045	0.16	0.02	0	0	0	0.006	1.0000
18	0.5450	0	0.16	0.045	0.24	0	0	0	0.01	0	1.0000
19	0.5950	0.09	0.12	0.005	0.16	0.02	0	0	0.01	0	1.0000
20	0.5610	0.09	0.12	0.045	0.16	0	0	0.008	0.01	0.006	1.0000
21	0.5000	0.09	0.12	0.045	0.24	0	0.005	0	0	0	1.0000
22	0.5740	0.09	0.16	0.005	0.16	0	0.005	0	0	0.006	1.0000
23	0.4770	0.09	0.16	0.005	0.24	0.02	0	0.008	0	0	1.0000
24	0.4160	0.09	0.16	0.045	0.24	0.02	0.005	0.008	0.01	0.006	1.0000

Table 6b - Theoretical E-type Fiberglass Compositions – E-pb1024

Theoretical Glass Compositions

Oksoy ID	SiO_2	Al_2O_3	MgO	CaO	MnO_2	Na_2O	K_2O	Fe_2O_3	Cr_2O_3	Co3O4	TiO_2	SO_3	Se	Total
1	0.7467	0.0200	0.0300	0.0700	0.0025	0.1200	0.0050	0.0010	0.0004	0.00000	0.0005	0.0000	0.00003	0.9961
2	0.7187	0.0010	0.0300	0.0700	0.0000	0.1500	0.0050	0.0150	0.0000	0.00000	0.0100	0.0000	0.00030	0.9997
3	0.7235	0.0010	0.0300	0.0700	0.0025	0.1500	0.0200	0.0010	0.0000	0.00015	0.0005	0.0000	0.00000	0.9985
4	0.6940	0.0010	0.0300	0.0900	0.0000	0.1500	0.0200	0.0010	0.0004	0.00000	0.0100	0.0000	0.00000	0.9964
5	0.6957	0.0010	0.0400	0.0900	0.0000	0.1500	0.0200	0.0010	0.0000	0.00015	0.0005	0.0000	0.00003	0.9982
6	0.6745	0.0200	0.0400	0.0900	0.0000	0.1500	0.0200	0.0010	0.0040	0.00000	0.0005	0.0000	0.00000	1.0000
7	0.6942	0.0200	0.0400	0.0900	0.0000	0.1200	0.0200	0.0150	0.0000	0.00000	0.0005	0.0000	0.00030	0.9997
8	0.6770	0.0200	0.0400	0.0900	0.0025	0.1500	0.0050	0.0150	0.0000	0.00000	0.0005	0.0000	0.00000	1.0000
9	0.7025	0.0200	0.0400	0.0700	0.0025	0.1200	0.0200	0.0150	0.0000	0.00000	0.0100	0.0000	0.00000	1.0000
10	0.6760	0.0200	0.0300	0.0900	0.0025	0.1500	0.0050	0.0150	0.0000	0.00015	0.0100	0.0000	0.00000	0.9985
11	0.6860	0.0010	0.0400	0.0700	0.0025	0.1500	0.0200	0.0150	0.0004	0.00015	0.0100	0.0000	0.00000	0.9949
12	0.7007	0.0200	0.0300	0.0900	0.0025	0.1200	0.0200	0.0010	0.0004	0.00015	0.0100	0.0000	0.00003	0.9946
13	0.7132	0.0010	0.0400	0.0900	0.0000	0.1200	0.0050	0.0150	0.0040	0.00150	0.0100	0.0000	0.00030	0.9982
14	0.7052	0.0200	0.0400	0.0700	0.0025	0.1500	0.0050	0.0010	0.0004	0.00015	0.0005	0.0000	0.00003	0.9946
15	0.6807	0.0200	0.0300	0.0700	0.0000	0.1500	0.0200	0.0150	0.0040	0.00000	0.0100	0.0000	0.00030	0.9997
16	0.7192	0.0010	0.0300	0.0900	0.0025	0.1200	0.0200	0.0150	0.0000	0.00015	0.0005	0.0000	0.00003	0.9982
17	0.7265	0.0010	0.0400	0.0900	0.0025	0.1200	0.0050	0.0010	0.0004	0.00000	0.0100	0.0000	0.00000	0.9964
18	0.7022	0.0200	0.0400	0.0700	0.0000	0.1500	0.0050	0.0010	0.0000	0.00015	0.0100	0.0000	0.00003	0.9982
19	0.7190	0.0200	0.0300	0.0700	0.0000	0.1200	0.0200	0.0150	0.0004	0.00015	0.0005	0.0000	0.00000	0.9949
20	0.7017	0.0010	0.0300	0.0900	0.0025	0.1500	0.0050	0.0150	0.0040	0.00000	0.0005	0.0000	0.00030	0.9997
21	0.7352	0.0010	0.0400	0.0700	0.0025	0.1200	0.0200	0.0010	0.0000	0.00000	0.0100	0.0000	0.00030	0.9997
22	0.7225	0.0200	0.0300	0.0900	0.0000	0.1200	0.0050	0.0010	0.0000	0.00150	0.0100	0.0000	0.00000	0.9985
23	0.7430	0.0010	0.0400	0.0700	0.0000	0.1200	0.0050	0.0150	0.0004	0.00015	0.0005	0.0000	0.00000	0.9949
24	0.7725	0.0010	0.0300	0.0700	0.0000	0.1200	0.0050	0.0010	0.0000	0.00000	0.0005	0.0000	0.00000	1.0000

Table 6c - Theoretical Float-type Glass Compositions – FL-pb1224

Theoretical Glass Compositions

Oksoy ID	SiO_2	B_2O_3	Al_2O_3	CaO	Na_2O	K_2O	BaO	Total
1	0.84	0.10	0.02	0	0.04	0	0	1.0000
2	0.80	0.10	0.02	0.02	0.04	0	0.02	1.0000
3	0.75	0.10	0.02	0.02	0.08	0.03	0	1.0000
4	0.76	0.10	0.07	0	0.04	0.03	0	1.0000
5	0.70	0.10	0.07	0	0.08	0.03	0.02	1.0000
6	0.71	0.10	0.07	0.02	0.08	0	0.02	1.0000
7	0.74	0.15	0.02	0	0.04	0.03	0.02	1.0000
8	0.73	0.15	0.02	0	0.08	0	0.02	1.0000
9	0.70	0.15	0.02	0.02	0.08	0.03	0	1.0000
10	0.70	0.15	0.07	0	0.08	0	0	1.0000
11	0.67	0.15	0.07	0.02	0.04	0.03	0.02	1.0000
12	0.72	0.15	0.07	0.02	0.04	0	0	1.0000
13	0.75	0.10	0.02	0	0.08	0.03	0.02	1.0000
14	0.80	0.10	0.02	0	0.08	0	0	1.0000
15	0.77	0.10	0.02	0.02	0.04	0.03	0.02	1.0000
16	0.77	0.10	0.07	0	0.04	0	0.02	1.0000
17	0.74	0.10	0.07	0.02	0.04	0.03	0	1.0000
18	0.73	0.10	0.07	0.02	0.08	0	0	1.0000
19	0.76	0.15	0.02	0	0.04	0.03	0	1.0000
20	0.77	0.15	0.02	0.02	0.04	0	0	1.0000
21	0.71	0.15	0.02	0.02	0.08	0	0.02	1.0000
22	0.72	0.15	0.07	0	0.04	0	0.02	1.0000
23	0.67	0.15	0.07	0	0.08	0.03	0	1.0000
24	0.63	0.15	0.07	0.02	0.08	0.03	0.02	1.0000

Figure 6d - Theoretical Low-expansion Borosilicate-type Glass Compositions
LO-pb724

Theoretical Glass Compositions

Oksoy ID	SiO_2	Al_2O_3	MgO	CaO	SrO	BaO	Li_2O	Na_2O	K_2O	TiO_2	CeO_2	ZrO_2	PbO	ZnO	As_2O_3	Sb_2O_3	F		Total
1	0.650	0.013	0	0	0.01	0.13	0	0.09	0.06	0.001	0.007	0.03	0	0	0.003	0.006	0		1.0000
2	0.706	0.035	0	0	0.01	0.02	0.005	0.06	0.09	0.001	0	0.03	0.03	0	0	0.006	0.007		1.0000
3	0.711	0.035	0.015	0	0.01	0.02	0	0.09	0.06	0.005	0	0	0.03	0.015	0	0.002	0.007		1.0000
4	0.707	0.035	0.015	0.035	0.01	0.02	0	0.06	0.09	0.001	0.007	0	0	0.015	0.003	0.002	0		1.0000
5	0.631	0.035	0.015	0.035	0.10	0.02	0	0.06	0.06	0.005	0	0.03	0	0	0.003	0.006	0		1.0000
6	0.514	0.035	0.015	0.035	0.10	0.13	0	0.06	0.06	0.001	0.007	0	0.03	0	0	0.006	0.007		1.0000
7	0.527	0.013	0.015	0.035	0.10	0.13	0.005	0.06	0.06	0.001	0	0.03	0	0.015	0	0.002	0.007		1.0000
8	0.509	0.035	0	0.035	0.10	0.13	0.005	0.09	0.06	0.001	0	0	0.03	0	0.003	0.002	0		1.0000
9	0.535	0.013	0.015	0	0.10	0.13	0.005	0.09	0.09	0.001	0	0	0	0.015	0	0.006	0		1.0000
10	0.588	0.035	0	0.035	0.01	0.13	0.005	0.09	0.09	0.005	0	0	0	0	0.003	0.002	0.007		1.0000
11	0.627	0.035	0.015	0	0.10	0.02	0.005	0.09	0.09	0.005	0.007	0	0	0	0	0.006	0		1.0000
12	0.566	0.013	0.015	0.035	0.01	0.13	0	0.09	0.09	0.005	0.007	0.03	0	0	0	0.002	0.007		1.0000
13	0.603	0.013	0	0.035	0.10	0.02	0.005	0.06	0.09	0.005	0.007	0.03	0.03	0	0	0.002	0		1.0000
14	0.496	0.035	0	0	0.10	0.13	0	0.09	0.06	0.005	0.007	0.03	0.03	0.015	0	0.002	0		1.0000
15	0.567	0.035	0.015	0	0.01	0.13	0.005	0.06	0.09	0.001	0.007	0.03	0.03	0.015	0.003	0.002	0		1.0000
16	0.663	0.013	0.015	0.035	0.01	0.02	0.005	0.09	0.06	0.005	0	0.03	0.03	0.015	0.003	0.006	0		1.0000
17	0.583	0.013	0	0.035	0.10	0.02	0	0.09	0.09	0.001	0.007	0	0.03	0.015	0.003	0.006	0.007		1.0000
18	0.519	0.035	0	0	0.10	0.13	0	0.06	0.09	0.005	0	0.03	0	0.015	0.003	0.006	0.007		1.0000
19	0.649	0.013	0.015	0	0.01	0.13	0.005	0.06	0.06	0.005	0.007	0	0.03	0	0.003	0.006	0.007		1.0000
20	0.679	0.035	0	0.035	0.01	0.02	0.005	0.09	0.06	0.001	0.007	0.03	0	0.015	0	0.006	0.007		1.0000
21	0.599	0.013	0.015	0	0.10	0.02	0	0.09	0.09	0.001	0	0.03	0.03	0	0.003	0.002	0.007		1.0000
22	0.606	0.013	0	0.035	0.01	0.13	0	0.06	0.09	0.005	0	0	0.03	0.015	0	0.006	0		1.0000
23	0.703	0.013	0	0	0.10	0.02	0.005	0.06	0.06	0.005	0.007	0	0	0.015	0.003	0.002	0.007		1.0000
24	0.834	0.013	0	0	0.01	0.02	0	0.06	0.06	0.001	0	0	0	0	0	0.002	0		1.0000

Table 6e - Theoretical TV Panel-type Glass Compositions – TV-pb1724

Theoretical Glass Compositions

Oksoy ID	SiO_2	B_2O_3	Al_2O_3	MgO	CaO	Na_2O	K_2O	Fe_2O_3	F	SO_3	Total
1	0.780	0.03	0	0.01	0.05	0.13	0	0	0	0	1.0000
2	0.712	0.03	0	0.05	0.05	0.13	0.02	0	0.006	0.002	1.0000
3	0.628	0.03	0	0.05	0.11	0.17	0	0.006	0.006	0	1.0000
4	0.666	0.03	0.06	0.01	0.05	0.17	0	0.006	0.006	0.002	1.0000
5	0.600	0.03	0.06	0.01	0.11	0.17	0.02	0	0	0	1.0000
6	0.592	0.03	0.06	0.05	0.11	0.13	0.02	0.006	0	0.002	1.0000
7	0.652	0.09	0	0.01	0.05	0.17	0.02	0.006	0	0.002	1.0000
8	0.628	0.09	0	0.01	0.11	0.13	0.02	0.006	0.006	0	1.0000
9	0.578	0.09	0	0.05	0.11	0.17	0	0	0	0.002	1.0000
10	0.592	0.09	0.06	0.01	0.11	0.13	0	0	0.006	0.002	1.0000
11	0.554	0.09	0.06	0.05	0.05	0.17	0.02	0	0.006	0	1.0000
12	0.614	0.09	0.06	0.05	0.05	0.13	0	0.006	0	0	1.0000
13	0.652	0.03	0	0.01	0.11	0.17	0.02	0	0.006	0.002	1.0000
14	0.712	0.03	0	0.01	0.11	0.13	0	0.006	0	0.002	1.0000
15	0.674	0.03	0	0.05	0.05	0.17	0.02	0.006	0	0	1.0000
16	0.688	0.03	0.06	0.01	0.05	0.13	0.02	0.006	0.006	0	1.0000
17	0.638	0.03	0.06	0.05	0.05	0.17	0	0	0	0.002	1.0000
18	0.614	0.03	0.06	0.05	0.11	0.13	0	0	0.006	0	1.0000
19	0.674	0.09	0	0.01	0.05	0.17	0	0	0.006	0	1.0000
20	0.666	0.09	0	0.05	0.05	0.13	0	0.006	0.006	0.002	1.0000
21	0.600	0.09	0	0.05	0.11	0.13	0.02	0	0	0	1.0000
22	0.638	0.09	0.06	0.01	0.05	0.13	0.02	0	0	0.002	1.0000
23	0.554	0.09	0.06	0.01	0.11	0.17	0	0.006	0	0	1.0000
24	0.486	0.09	0.06	0.05	0.11	0.17	0.02	0.006	0.006	0.002	1.0000

Table 6f - Theoretical Wool-type Fiberglass Compositions
WO-pb1024

Experimental Glass Compositions (as analyzed)

Oksoy ID	SiO_2	Al_2O_3	MgO	CaO	Li_2O	Na_2O	K_2O	Fe_2O_3	Cr_2O_3	TiO_2	SO_3	Total
1	0.8111	0.0114	0.0006	0.0694		0.1063	0.0025	0.0003	0	0.0001	0.0001	
2	0.7388	0.0101	0.0010	0.1177		0.1005	0.0208	0.0003	0.0026	0.0047	0.0024	0.9989
3	0.6902	0.0116	0.0010	0.1234	0.0093	0.1531	0.0002	0.0046	0.0031	0.0001	0.0029	0.9995
4	0.7340	0.0109	0.0295	0.0681		0.1462	0.0002	0.0043	0.0029	0.0050	0.0002	1.0013
5	0.7097	0.0112	0.0308	0.0677	0.0091	0.1471	0.0197	0.0004	0	0.0001	0.0029	0.9987
6	0.6903	0.0113	0.0324	0.1164	0.0089	0.1072	0.0209	0.0046	0	0.0051	0.0002	0.9973
7	0.7206	0.0312	0.0006	0.0677		0.1466	0.0204	0.0046	0	0.0051	0.0028	0.9996
8	0.7505	0.0324	0.0006	0.0680	0.0092	0.1085	0.0208	0.0046	0.0030	0.0001	0.0002	0.9979
9	0.6821	0.0319	0.0011	0.1214	0.0091	0.1472	0.0001	0.0003	0	0.0052	0.0002	0.9986
10	0.7397	0.0318	0.0314	0.0696	0.0091	0.1068	0.0003	0.0005	0.0030	0.0051	0.0011	0.9984
11	0.6488	0.0312	0.0315	0.1157		0.1472	0.0212	0.0005	0.0029	0.0001	0.0002	0.9993
12	0.7059	0.0305	0.0284	0.1213		0.1034	0.0002	0.0039	0	0.0001	0.0026	0.9963
13	0.7450	0.0114	0.0001	0.0716	0.0056	0.1366	0.0213	0.0002	0.0028	0.0054	0.0001	1.0001
14	0.7953	0.0109	0.0006	0.0679	0.0092	0.1051	0.0006	0.0043	0	0.0050	0.0014	1.0003
15	0.7002	0.0105	0.0010	0.1203		0.1446	0.0209	0.0379	0	0.0001	0.0003	1.0358
16	0.7513	0.0102	0.0280	0.0695		0.1096	0.0206	0.0004	0.0030	0.0001	0.0023	0.9950
17	0.6873	0.0111	0.0345	0.1149		0.1525	0.0002	0.0003	0	0.0050	0.0024	1.0082
18	0.7105	0.0115	0.0335	0.1205	0.0092	0.1091	0.0003	0.0006	0.0028	0.0001	0.0002	0.9982
19	0.7375	0.0320	0.0006	0.0699		0.1479	0.0002	0.0004	0.0032	0.0001	0.0025	0.9943
20	0.7298	0.0311	0.0010	0.1219		0.1015	0.0003	0.0038	0.0028	0.0050	0.0004	0.9976
21	0.7110	0.0325	0.0008	0.1186	0.0099	0.0998	0.0211	0.0004	0	0.0001	0.0029	0.9971
22	0.7312	0.0291	0.0279	0.0689		0.1087	0.0207	0.0003	0	0.0052	0.0003	0.9923
23	0.7123	0.0321	0.0279	0.0745	0.0107	0.1379	0.0001	0.0044	0	0.0001	0.0001	1.0001
24	0.6294	0.0313	0.0315	0.1140	0.0096	0.1474	0.0202	0.0044	0.0030	0.0050	0.0027	0.9985

Table 7a - Analyzed Container-type Glass Compositions – CO-pb1124

Experimental Glass Compositions (as analyzed)

Oksoy ID	SiO_2	B_2O_3	Al_2O_3	MgO	CaO	Na_2O	K_2O	Fe_2O_3	TiO_2	F	Total
1	0.6920	0.0000	0.1220	0.0054	0.1570	0.0000	0.0000	0.0000	0.0000	0.0000	0.9764
2	0.6570	0.0000	0.1500	0.0153	0.1580	0.0000	0.0052	0.0059	0.0100	0.0017	1.0031
3	0.5570	0.0000	0.1120	0.0503	0.2470	0.0205	0.0000	0.0080	0.0100	0.0000	1.0048
4	0.6250	0.0000	0.1500	0.0056	0.1700	0.0205	0.0000	0.0081	0.0101	0.0052	0.9945
5	0.5760	0.0000	0.1530	0.0058	0.2540	0.0204	0.0056	0.0000	0.0000	0.0000	1.0148
6	0.5290	0.0000	0.1470	0.0588	0.2530	0.0000	0.0053	0.0084	0.0000	0.0051	1.0066
7	0.5960	0.0868	0.1120	0.0053	0.1680	0.0204	0.0054	0.0079	0.0000	0.0052	1.0070
8	0.5300	0.0849	0.1120	0.0053	0.2460	0.0000	0.0050	0.0084	0.0098	0.0000	1.0014
9	0.4980	0.0863	0.1200	0.0393	0.2260	0.0205	0.0000	0.0000	0.0000	0.0039	0.9940
10	0.4800	0.0859	0.1530	0.0046	0.2220	0.0000	0.0000	0.0000	0.0094	0.0031	0.9580
11	0.5000	0.0898	0.1500	0.0468	0.1680	0.0203	0.0053	0.0000	0.0101	0.0000	0.9903
12	0.5380	0.0883	0.1490	0.0464	0.1680	0.0000	0.0000	0.0080	0.0000	0.0000	0.9977
13	0.5890	0.0000	0.1120	0.0055	0.2500	0.0201	0.0054	0.0000	0.0099	0.0052	0.9971
14	0.6170	0.0000	0.1110	0.0067	0.2510	0.0000	0.0000	0.0081	0.0000	0.0054	0.9992
15	0.6320	0.0000	0.1220	0.0420	0.1600	0.0213	0.0051	0.0081	0.0000	0.0000	0.9905
16	0.6570	0.0000	0.1480	0.0199	0.1490	0.0000	0.0051	0.0050	0.0100	0.0026	0.9966
17	0.6040	0.0000	0.1480	0.0455	0.1690	0.0209	0.0000	0.0000	0.0000	0.0049	0.9923
18	0.5390	0.0000	0.1460	0.0518	0.2460	0.0000	0.0000	0.0000	0.0098	0.0000	0.9926
19	0.6460	0.0883	0.0933	0.0044	0.1350	0.0195	0.0000	0.0000	0.0080	0.0000	0.9945
20	0.5530	0.0881	0.1140	0.0474	0.1730	0.0000	0.0000	0.0082	0.0105	0.0047	0.9989
21	0.5280	0.0855	0.1110	0.0418	0.2270	0.0000	0.0049	0.0000	0.0000	0.0000	0.9982
22	0.5710	0.0891	0.1530	0.0058	0.1710	0.0000	0.0053	0.0000	0.0000	0.0047	0.9999
23	0.4740	0.0889	0.1540	0.0049	0.2200	0.0213	0.0000	0.0077	0.0000	0.0000	0.9708
24	0.4130	0.0926	0.1600	0.0438	0.2460	0.0213	0.0046	0.0083	0.0101	0.0059	1.0056

Table 7b - Analyzed E-type Fiberglass Compositions – E-pb1024

Experimental Glass Compositions (as analyzed)

Oksoy ID	SiO_2	Al_2O_3	MgO	CaO	MnO_2	Na_2O	K_2O	Fe_2O_3	Cr_2O_3	$Co3O_4$	TiO_2	SO_3	Se	Total
1														
2	0.7219	0.0022	0.0261	0.0709		0.1423	0.0055	0.0146			0.0106	0.0003	0.0001	0.9944
3														
4														
5														
6	0.6704	0.0210	0.0367	0.0940		0.1512	0.0218	0.0012	0.0039		0.0006	0.0003		1.0011
7	0.6901	0.0196	0.0362	0.0904		0.1189	0.0207	0.0141			0.0006	0.0004	0.0001	0.9910
8														
9	0.6980	0.0198	0.0367	0.0730	0.0027	0.1175	0.0209	0.0142			0.0104	0.0003		0.9935
10														
11														
12														
13	0.7049	0.0022	0.0377	0.0974		0.1228	0.0059	0.0148	0.0001	0.0020	0.0109	0.0004	0.0001	0.9971
14														
15	0.7006	0.0184	0.0244	0.0647		0.1334	0.0202	0.0127	0.0038		0.0094	0.0003	0.0001	0.9879
16														
17														
18														
19														
20	0.6901	0.0023	0.0278	0.0983	0.0023	0.1440	0.0056	0.0148	0.0040		0.0006	0.0004	0.0001	0.9902
21	0.7321	0.0022	0.0378	0.0725	0.0027	0.1210	0.0214	0.0013			0.0107	0.0003	0.0002	1.0020
22	0.7149	0.0212	0.0280	0.0913		0.1213	0.0059	0.0012		0.0020	0.0104	0.0003		0.9945
23														
24														

Table 7c - Analyzed Float-type Glass Compositions – FL-pb1224

Experimental Glass Compositions (as analyzed)

Oksoy ID	SiO_2	B_2O_3	Al_2O_3	CaO	Na_2O	K_2O	BaO	Total
1	0.8390	0.0990	0.0221	0.0000	0.0374	0.0000	0.0000	0.9975
2	0.7880	0.1030	0.0218	0.0191	0.0385	0.0000	0.0195	0.9899
3	0.7460	0.1000	0.0226	0.0194	0.0799	0.0290	0.0000	0.9969
4	0.7610	0.1040	0.0687	0.0000	0.0389	0.0300	0.0000	1.0026
5	0.6940	0.1020	0.0714	0.0000	0.0864	0.0321	0.0205	1.0064
6	0.7070	0.1030	0.0713	0.0201	0.0868	0.0000	0.0207	1.0089
7	0.7370	0.1490	0.0218	0.0000	0.0411	0.0296	0.0205	0.9990
8	0.7330	0.1490	0.0221	0.0000	0.0821	0.0000	0.0208	1.0070
9	0.7130	0.1500	0.0225	0.0194	0.0795	0.0291	0.0000	1.0135
10	0.7060	0.1540	0.0719	0.0000	0.0778	0.0000	0.0000	1.0097
11	0.6740	0.1500	0.0731	0.0203	0.0410	0.0302	0.0203	1.0089
12	0.7180	0.1510	0.0717	0.0201	0.0436	0.0000	0.0000	1.0044
13	0.7740	0.0899	0.0214	0.0000	0.0769	0.0272	0.0195	1.0089
14	0.8040	0.1020	0.0208	0.0000	0.0784	0.0000	0.0000	1.0052
15	0.7670	0.1050	0.0213	0.0190	0.0410	0.0300	0.0196	1.0029
16	0.7850	0.0986	0.0689	0.0000	0.0300	0.0000	0.0169	0.9994
17	0.7410	0.0998	0.0725	0.0196	0.0389	0.0290	0.0000	1.0008
18	0.7250	0.0998	0.0722	0.0205	0.0831	0.0000	0.0000	1.0006
19	0.7600	0.1520	0.0224	0.0000	0.0397	0.0303	0.0000	1.0044
20	0.7650	0.1500	0.0230	0.0175	0.0405	0.0000	0.0000	0.9960
21	0.7180	0.1550	0.0221	0.0198	0.0808	0.0000	0.0201	1.0158
22	0.7200	0.1530	0.0725	0.0000	0.0461	0.0000	0.0211	1.0127
23	0.6520	0.1490	0.0712	0.0000	0.0827	0.0289	0.0198	1.0036
24	0.6190	0.1540	0.0734	0.0210	0.0833	0.0305	0.0211	1.0023

Figure 7d - Analyzed Low-expansion Borosilicate-type Glass Compositions LO-pb724

Experimental Glass Compositions (as analyzed) [TV Panel]

Oksoy ID	SiO_2	Al_2O_3	MgO	CaO	SrO	BaO	Li_2O	Na_2O	K_2O	TiO_2	CeO_2	ZrO_2	PbO	ZnO	As_2O_3	Sb_2O_3	F	Fe_2O_3	Total
1	0.6475	0.0138	0.0001	0.0004	0.0093	0.1270		0.0911	0.0606	0.0010	0.0068	0.0297	0.0001	0.0000	0.0025	0.0071	0.0006		0.9976
2	0.6970	0.0345	0.0000	0.0000	0.0100	0.0201	0.0050	0.0603	0.0892	0.0008	0.0000	0.0286	0.0284	0.0000	0.0000	0.0055	0.0062	0.0004	0.9860
3	0.7127	0.0336	0.0146	0.0000	0.0106	0.0192	0.0000	0.0827	0.0608	0.0057	0.0000	0.0000	0.0296	0.0209	0.0000	0.0020	0.0061	0.0004	0.9989
4	0.7103	0.0360	0.0151	0.0311	0.0103	0.0193	0.0000	0.0560	0.0881	0.0008	0.0081	0.0000	0.0000	0.0197	0.0031	0.0018	0.0000	0.0004	1.0001
5	0.6365	0.0358	0.0143	0.0336	0.0967	0.0202		0.0586	0.0594	0.0050	0.0001	0.0294	0.0003	0.0000	0.0027	0.0067	0.0000		0.9993
6	0.5339	0.0363	0.0154	0.0326	0.1004	0.1321	0.0000	0.0670	0.0581	0.0008	0.0057	0.0000	0.0294	0.0000	0.0000	0.0054	0.0067	0.0002	1.0240
7	0.5396	0.0136	0.0140	0.0319	0.0976	0.1283	0.0050	0.0605	0.0608	0.0010	0.0008	0.0295	0.0002	0.0147	0.0004	0.0025	0.0076		1.0080
8	0.5258	0.0368	0.0000	0.0332	0.0992	0.1330	0.0054	0.0945	0.0580	0.0008	0.0000	0.0000	0.0291	0.0000	0.0020	0.0019	0.0000	0.0002	1.0199
9	0.5423	0.0138	0.0137	0.0006	0.0996	0.1300	0.0050	0.0893	0.0889	0.0010	0.0007	0.0002	0.0002	0.0150	0.0003	0.0069	0.0000		1.0075
10	0.5926	0.0351	0.0000	0.0333	0.0096	0.1298	0.0051	0.0918	0.0903	0.0052	0.0005	0.0000	0.0000	0.0000	0.0027	0.0026	0.0075		1.0061
11	0.6316	0.0366	0.0136	0.0007	0.0986	0.0206	0.0050	0.0890	0.0885	0.0051	0.0062	0.0000	0.0001	0.0000	0.0000	0.0070	0.0007		1.0033
12	0.5712	0.0135	0.0135	0.0316	0.0094	0.1284		0.0904	0.0896	0.0052	0.0068	0.0298	0.0000	0.0001	0.0000	0.0026	0.0084		1.0005
13	0.6061	0.0132	0.0007	0.0344	0.1020	0.0208	0.0051	0.0613	0.0907	0.0052	0.0065	0.0305	0.0312	0.0000	0.0003	0.0025	0.0007		1.0112
14	0.5068	0.0355	0.0000	0.0000	0.0969	0.1286	0.0000	0.0934	0.0588	0.0046	0.0059	0.0289	0.0279	0.0120	0.0000	0.0019	0.0000	0.0002	1.0014
15	0.5746	0.0352	0.0142	0.0005	0.0093	0.1280	0.0050	0.0612	0.0899	0.0010	0.0070	0.0297	0.0283	0.0147	0.0028	0.0025	0.0005		1.0044
16	0.6609	0.0135	0.0143	0.0321	0.0100	0.0201	0.0050	0.0925	0.0601	0.0051	0.0002	0.0298	0.0295	0.0147	0.0028	0.0069	0.0000		0.9975
17	0.5834	0.0134	0.0004	0.0346	0.1009	0.0207		0.0910	0.0894	0.0010	0.0066	0.0002	0.0311	0.0147	0.0030	0.0070	0.0078		1.0052
18	0.5331	0.0345	0.0000	0.0000	0.0965	0.1290	0.0000	0.0655	0.0882	0.0048	0.0000	0.0284	0.0000	0.0121	0.0021	0.0053	0.0063	0.0002	1.0060
19	0.6492	0.0134	0.0143	0.0008	0.0095	0.1288	0.0050	0.0614	0.0608	0.0051	0.0070	0.0000	0.0293	0.0001	0.0028	0.0071	0.0080		1.0026
20	0.6762	0.0345	0.0000	0.0333	0.0099	0.0198	0.0050	0.0924	0.0604	0.0009	0.0060	0.0288	0.0001	0.0143	0.0000	0.0068	0.0079		0.9963
21	0.6031	0.0135	0.0142	0.0005	0.1030	0.0209		0.0911	0.0901	0.0010	0.0003	0.0308	0.0321	0.0001	0.0031	0.0025	0.0074		1.0137
22	0.6072	0.0136	0.0004	0.0338	0.0095	0.1280		0.0619	0.0897	0.0052	0.0008	0.0000	0.0292	0.0148	0.0001	0.0071	0.0000		1.0013
23	0.7101	0.0141	0.0000	0.0000	0.1026	0.0198	0.0052	0.0574	0.0598	0.0056	0.0077	0.0000	0.0000	0.0206	0.0035	0.0020	0.0069	0.0004	1.0157
24	0.8062	0.0120	0.0000	0.0000	0.0102	0.0189	0.0000	0.0590	0.0636	0.0009	0.0000	0.0000	0.0000	0.0000	0.0000	0.0019	0.0000	0.0004	0.9731

Table 7e - Analyzed TV Panel-type Glass Compositions – TV-pb1724

Experimental Glass Compositions (as analyzed)

Oksoy ID	SiO_2	B_2O_3	Al_2O_3	MgO	CaO	Na_2O	K_2O	Fe_2O_3	F	SO_3	Total
1											
2											
3											
4											
5	0.5780	0.0298	0.0586	0.0098	0.1100	0.1710	0.0201				0.9773
6	0.5540	0.0340	0.0644	0.0496	0.1270	0.1440	0.0221	0.0069	0.0001		1.0021
7	0.6280	0.0885		0.0092	0.0480	0.1730	0.0201	0.0062		0.0017	0.9747
8	0.6050	0.0888		0.0098	0.1130	0.1320	0.0201	0.0065	0.0053		0.9805
9											
10	0.5290	0.0931	0.0621	0.0111	0.1350	0.1370			0.0078	0.0028	0.9779
11											
12											
13	0.6620	0.0313		0.0099	0.0536	0.1830	0.0211		0.0047	0.0022	0.9678
14											
15											
16											
17	0.6200	0.0300	0.0635	0.0454	0.0528	0.1780				0.0021	0.9918
18	0.6110	0.0306	0.0589	0.0443	0.1160	0.1340		0.0004			0.9952
19											
20											
21	0.6130	0.0889		0.0096	0.0500	0.1330	0.0197				0.9142
22											
23											
24											

Table 7f - Analyzed Wool-type Fiberglass Compositions
WO-pb1024

CO glass			
sample no.	10^{13} Poise	10^{12} Poise	10^{11} Poise
	T (°C)	T (°C)	T (°C)
base	564	588	611
1			
2	589	608	630
3			
4			
5			
6			
7			
8			
9	538	558	580
10			
11			
12	604	626	649
13	524	547	572
14			
15	557	577	597
16	560	583	608
17	559	579	599
18			
19	559	582	607
20	611	631	661
21	548	569	592
22	569	589	622
23	523	541	586
24			

Table 8a - Beam-bending Viscosity Isokom Temperatures
Container-type Glass Compositions

E Glass

Sample no.	10^{13} Poise T (°C)	10^{12} Poise T (°C)	10^{11} Poise T (°C)
base	663	690	717
1			
2	742	766	790
3	698	720	745
4	709	734	762
5	699	722	745
6	705	731	753
7	645	666	693
8			
9	632	653	675
10	665	685	706
11	654	677	701
12	677	702	728
13	699	724	748
14	725	750	777
15	705	730	755
16	740	769	794
17	707	724	750
18	737	761	786
19	658	681	706
20	656	680	705
21	661	683	708
22	681	708	736
23	652	673	695
24	630	650	671

Table 8b - Beam-bending Viscosity Isokom Temperatures
E-type Fiberglass Compositions

FL glass

Sample no.	10^{13} Poise T (°C)	10^{12} Poise T (°C)	10^{11} Poise T (°C)
base	551	576	602
1			
2	520	541	563
3			
4			
5			
6	542	565	588
7	555	579	604
8			
9	559	581	605
10			
11			
12			
13	562	587	612
14			
15	552	575	601
16			
17			
18			
19			
20	551	573	596
21	550	575	601
22	571	596	621
23			
24			

Table 8c - Beam-bending Viscosity Isokom Temperatures
Float-type Glass Compositions

LO Glass

Sample no.	10^{13} Poise T (°C)	10^{12} Poise T (°C)	10^{11} Poise T (°C)
base	554	592	634
1	594	625	660
2	627	663	
3	591	613	638
4	579	612	649
5	587	609	636
6	595	619	644
7	566	593	623
8	581	604	627
9	576	600	625
10	558	585	615
11	570	600	629
12	583	616	651
13	594	616	643
14	600	624	653
15	600	627	656
16	591	622	656
17	591	622	656
18	592	615	639
19	553	584	615
20	597	632	666
21	582	606	631
22	560	594	632
23	566	588	612
24	571	593	616

Table 8d - Beam-bending Viscosity Isokom Temperatures
Low Expansion Borosilicate-type Glass Compositions

TV panel glass

Sample no.	10^{13} Poise T (°C)	10^{12} Poise T (°C)	10^{11} Poise T (°C)
base	521	544	570
1	507	530	554
2	483	512	543
3	487	513	540
4	558	585	612
5	591	616	644
6	532	556	580
7	520	542	567
8	529	551	576
9	474	495	515
10	474	496	519
11	496	519	542
12	498	522	547
13	538	558	579
14	496	518	540
15	507	530	554
16	515	537	560
17	489	510	533
18	532	556	581
19	473	494	518
20	506	528	550
21	491	509	529
22	522	540	559
23	502	527	554
24	520	550	583

Table 8e - Beam-bending Viscosity Isokom Temperatures
TV Panel-type Glass Compositions

WO glass

Sample no.	10^{13} Poise T (°C)	10^{12} Poise T (°C)	10^{11} Poise T (°C)
base	543	562	582
1	556	574	601
2			
3	540	558	578
4			
5	548	564	582
6	555	574	593
7	549	566	586
8	556	574	593
9	558	574	593
10	558	574	593
11			
12	563	584	606
13	522	540	563
14	566	587	609
15	518	538	559
16			
17	551	571	592
18	564	585	607
19	548	566	585
20			
21	569	589	610
22	564	583	603
23			
24			

Table 8f - Beam-bending Viscosity Isokom Temperatures
Wool-type Fiberglass Compositions

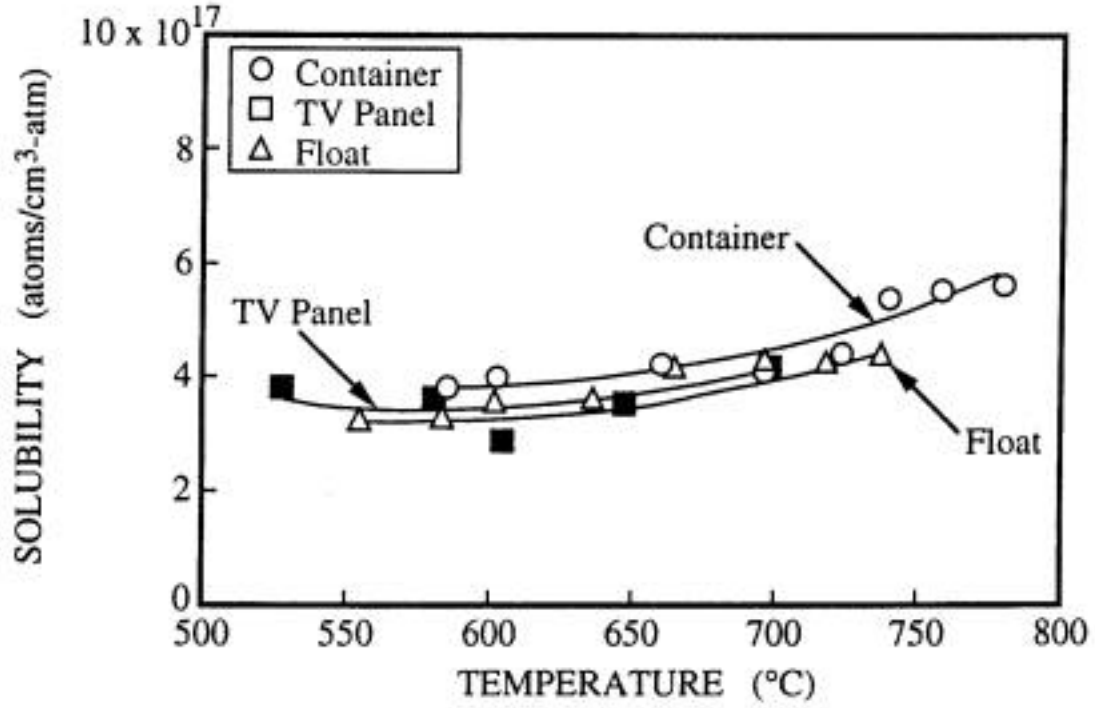

Figure 1 – Helium Solubility in Container, Float, and TV Panel Glasses in the Region Near the Glass Transformation Temperature

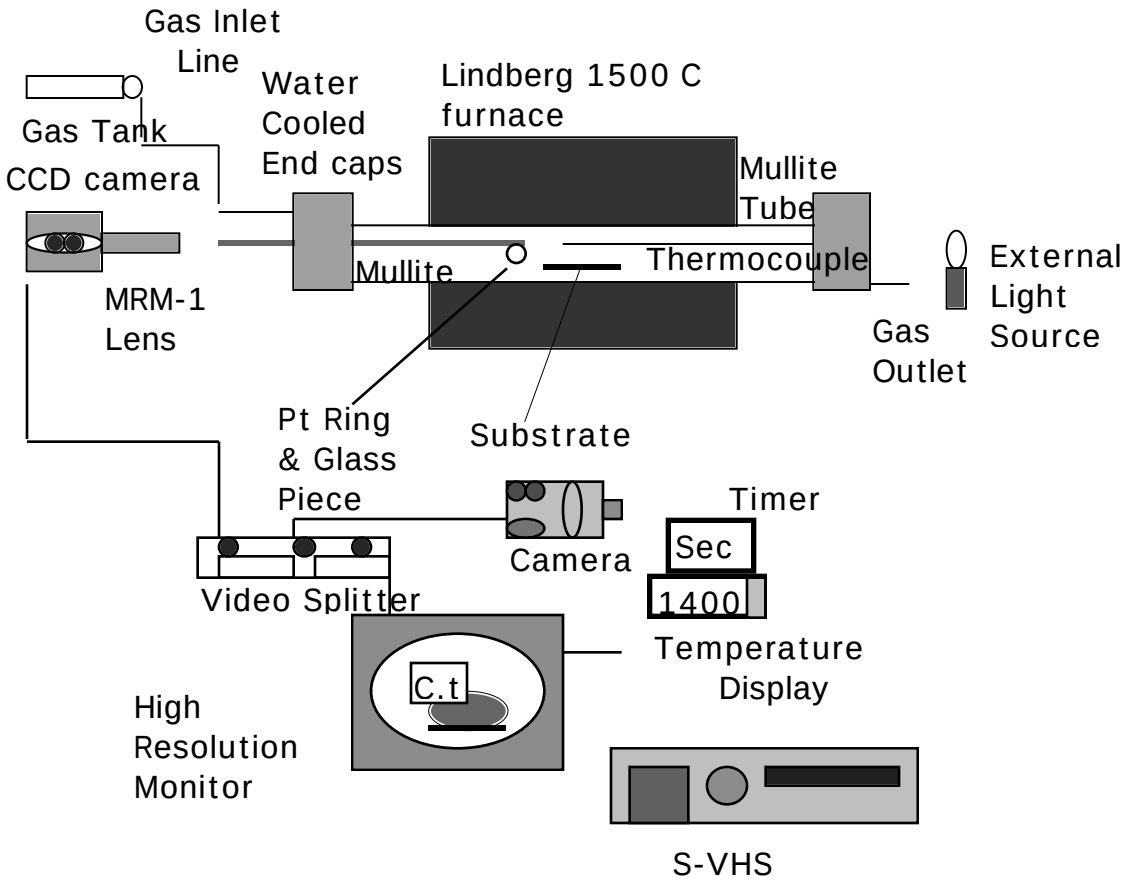

Figure 2a. Experimental Setup – Density and Surface Tension Measurements

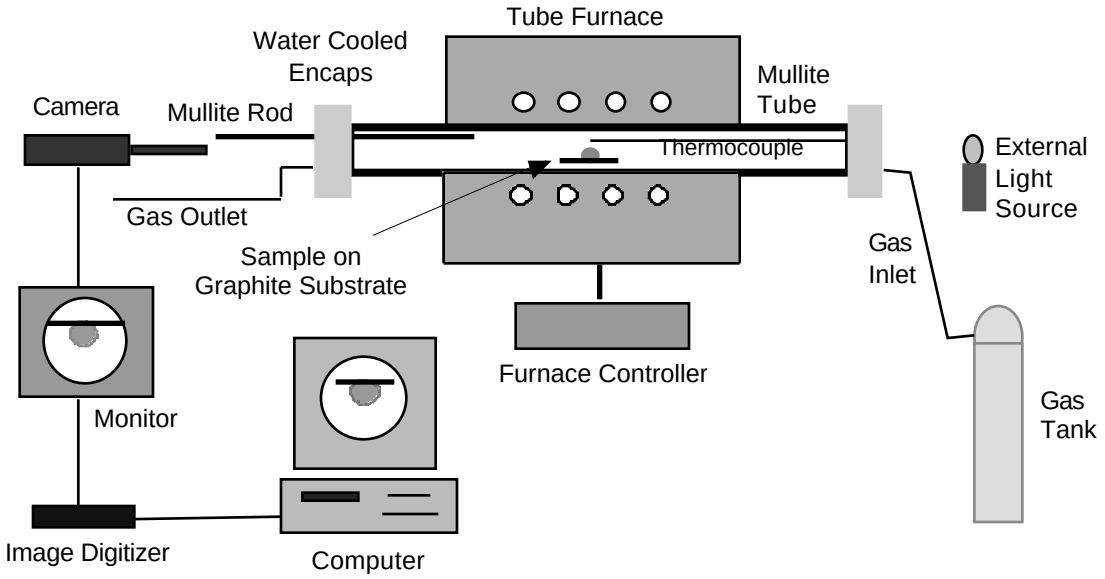

Figure 2b – Updated Density and Surface Tension Measurement Apparatus

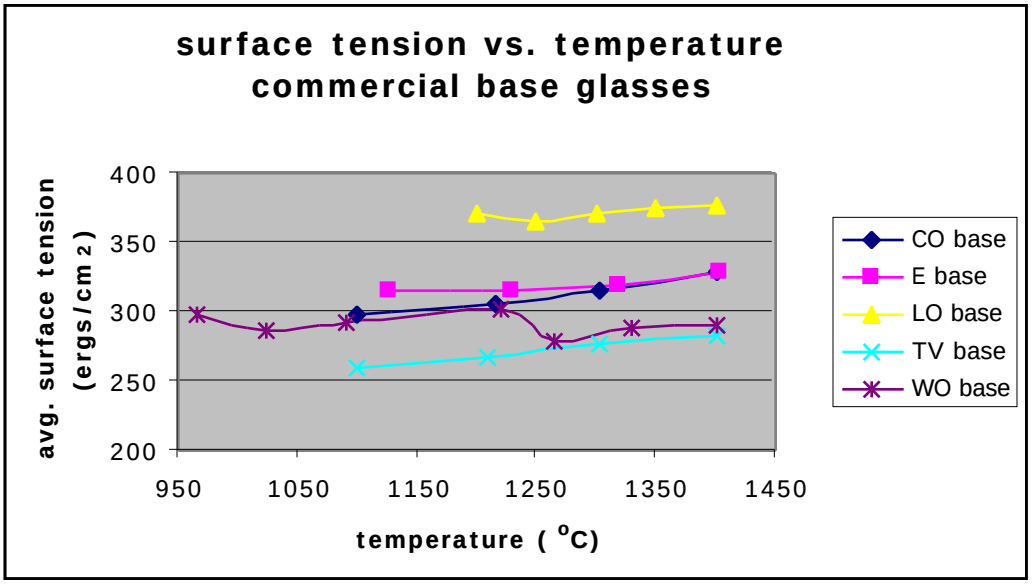

Figure 3a - Surface Tension versus Temperature (Commercial Base Glasses)

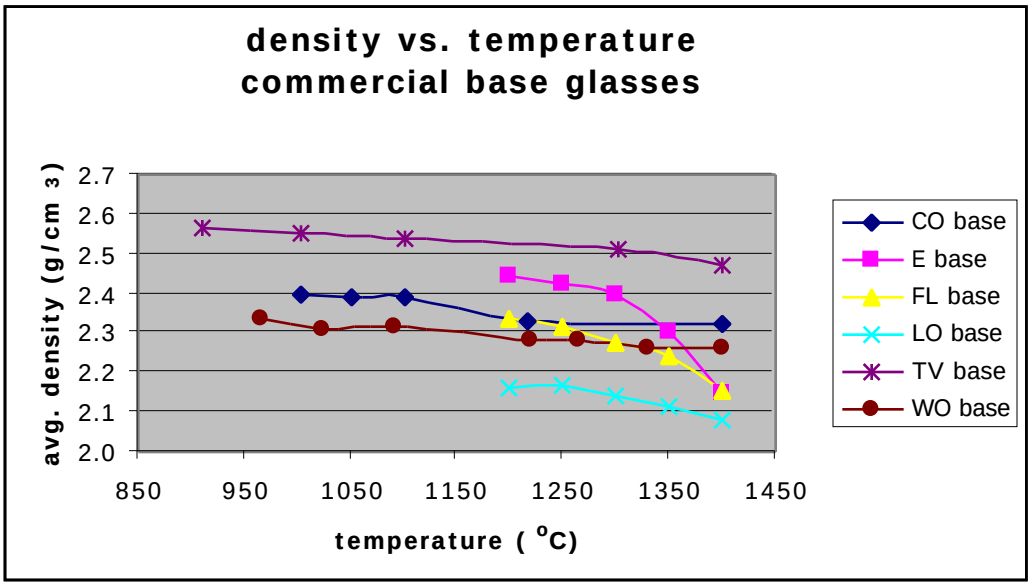

Figure 3b – Density versus Temperature (Commercial Base Glasses)

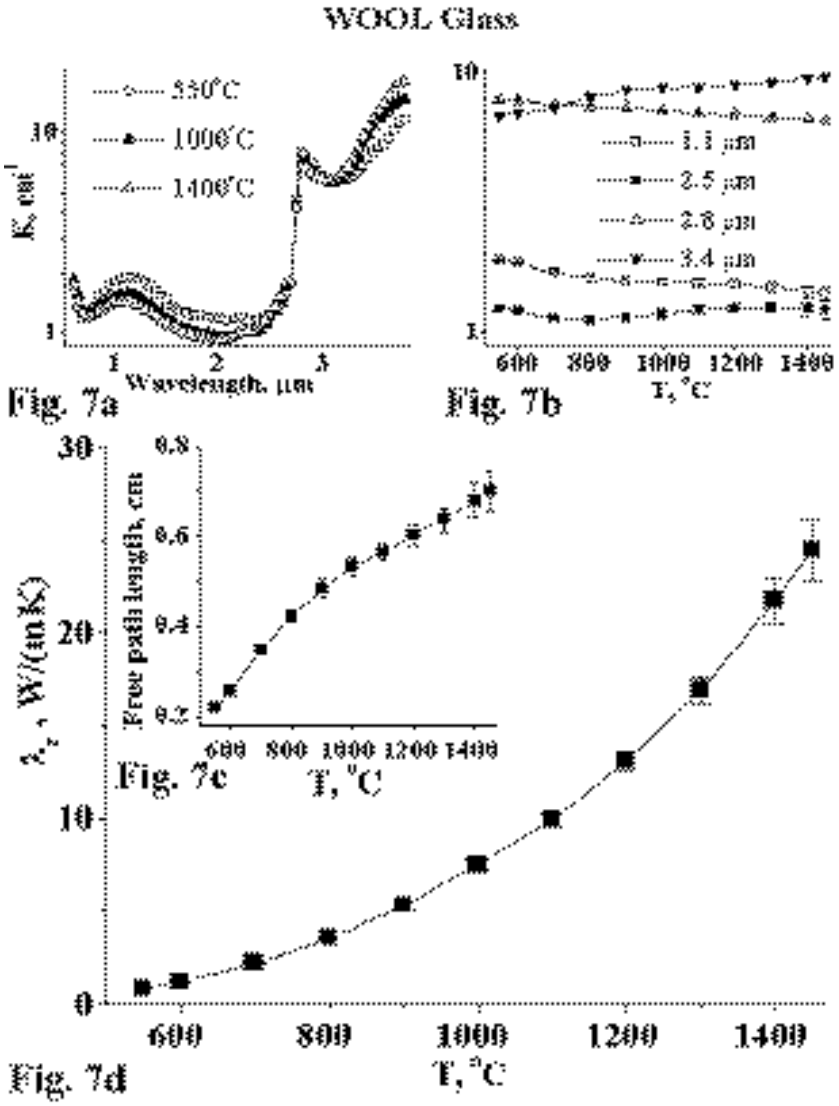

Figure 4a (Prokhorenko, Fig. 7) - Absorption spectra at temperatures 550, 1000 and 1400°C (a), and temperature dependences of absorption coefficients at 1.1, 2.2, 2.8 and 3.4 μm (b) measured for wool glass. Temperature dependences of free path length (c) and radiative conductivity (d) calculated for wool glass by using Rosseland formulas.

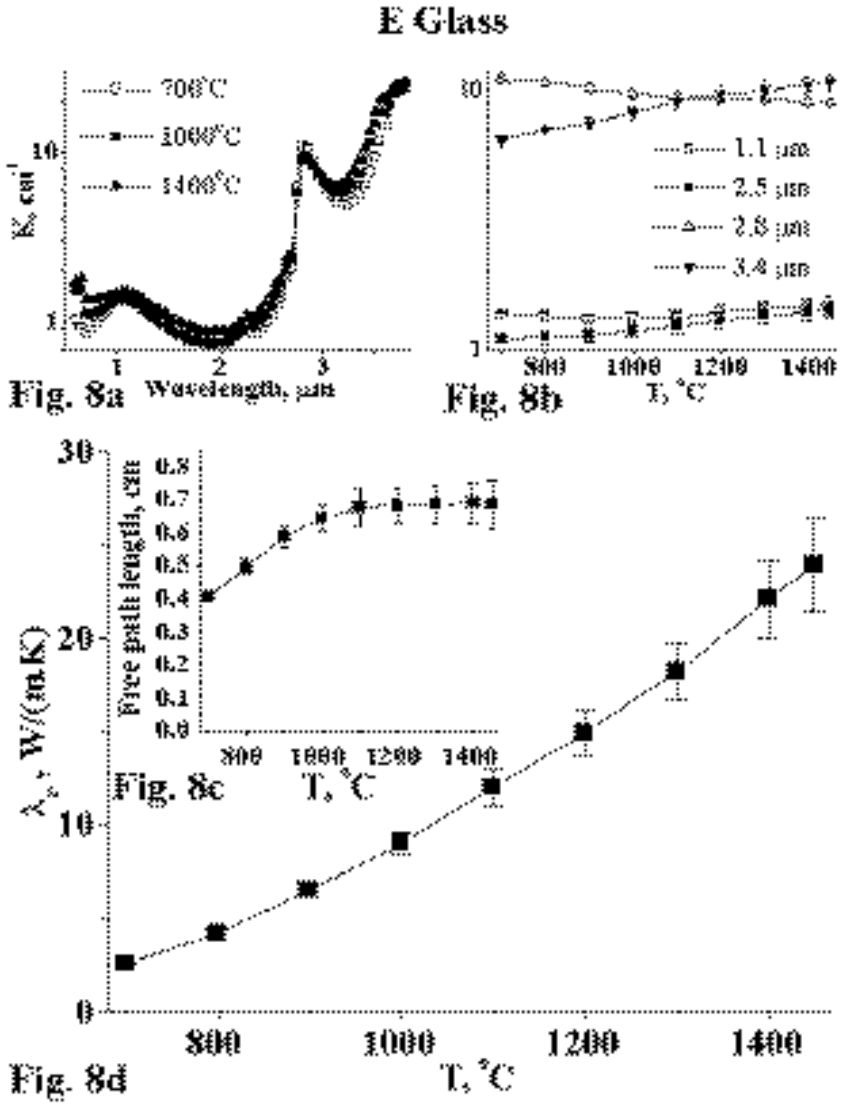

Figure 4b (Prokhorenko, Fig.8) - Absorption spectra at temperatures 700, 1000 and 1400°C (a), and temperature dependences of absorption coefficients at 1.1, 2.2, 2.8 and 3.4 μm (b) measured for E-glass. Temperature dependences of free path length (c) and radiative conductivity (d) calculated for E-glass by using Rosseland formulas.

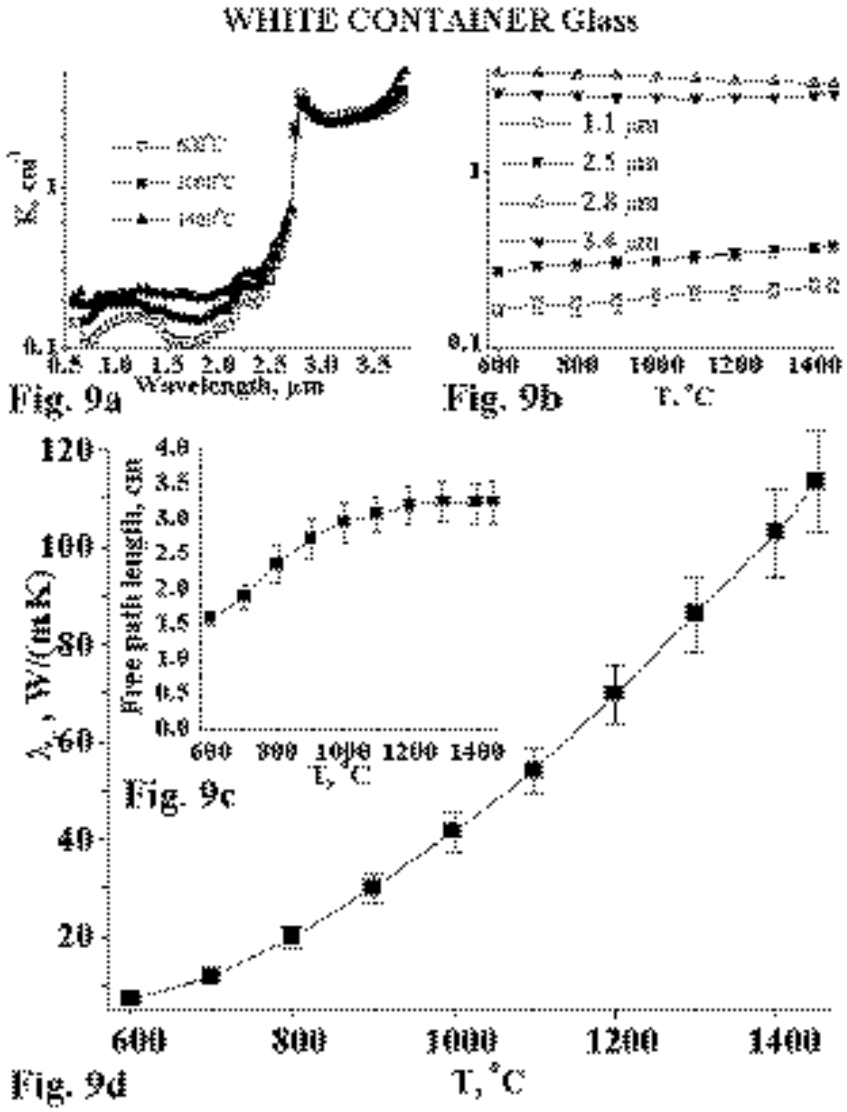

Figure 4c (Prokhorenko, Fig. 9) - Absorption spectra at temperatures 600, 1000 and 1400°C (a), and temperature dependences of absorption coefficients at 1.1, 2.2, 2.8 and 3.4 μm (b) measured for white container glass. Temperature dependences of free path length (c) and radiative conductivity (d) calculated for white container glass by using Rosseland formulas

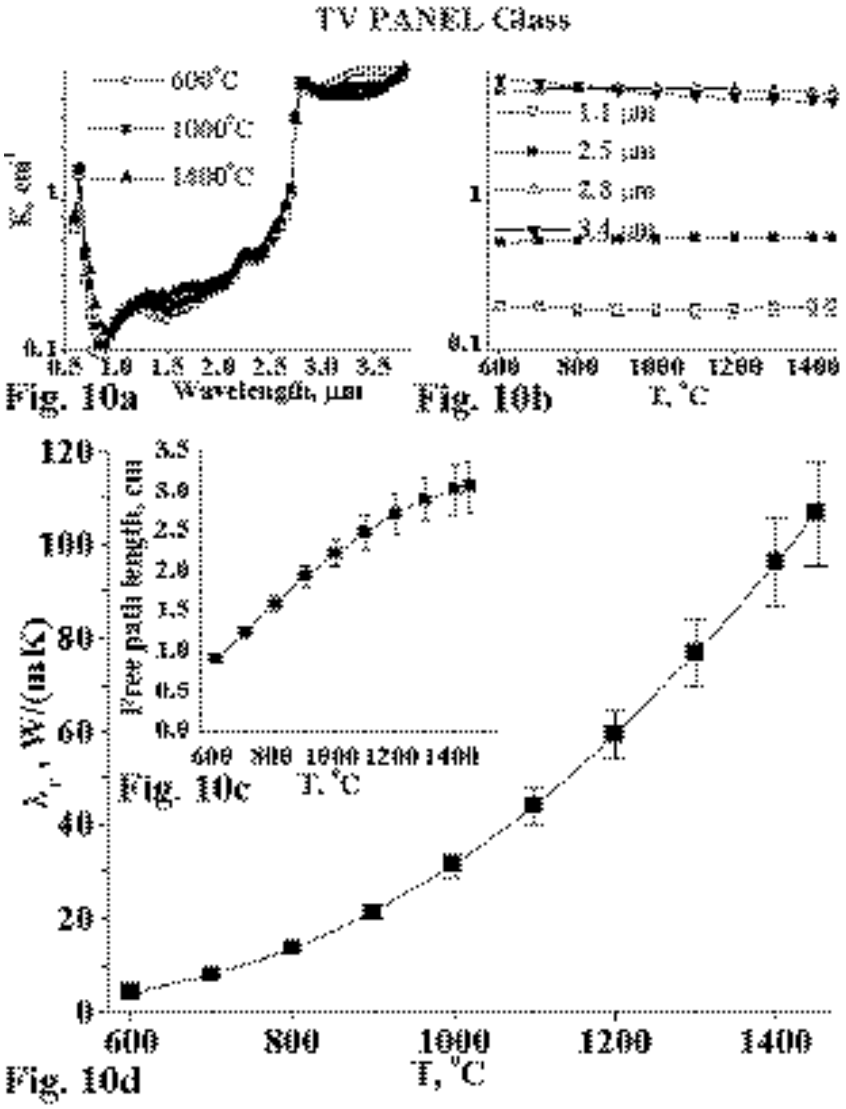

Figure 4d (Prokhorenko, Fig. 10) - Absorption spectra at temperatures 600, 1000 and 1400°C (a), and temperature dependences of absorption coefficients at 1.1, 2.2, 2.8 and 3.4 μm (b) measured for TV-panel glass. Temperature dependences of free path length (c) and radiative conductivity (d) calculated for TV-panel glass by using Rosseland formulas.

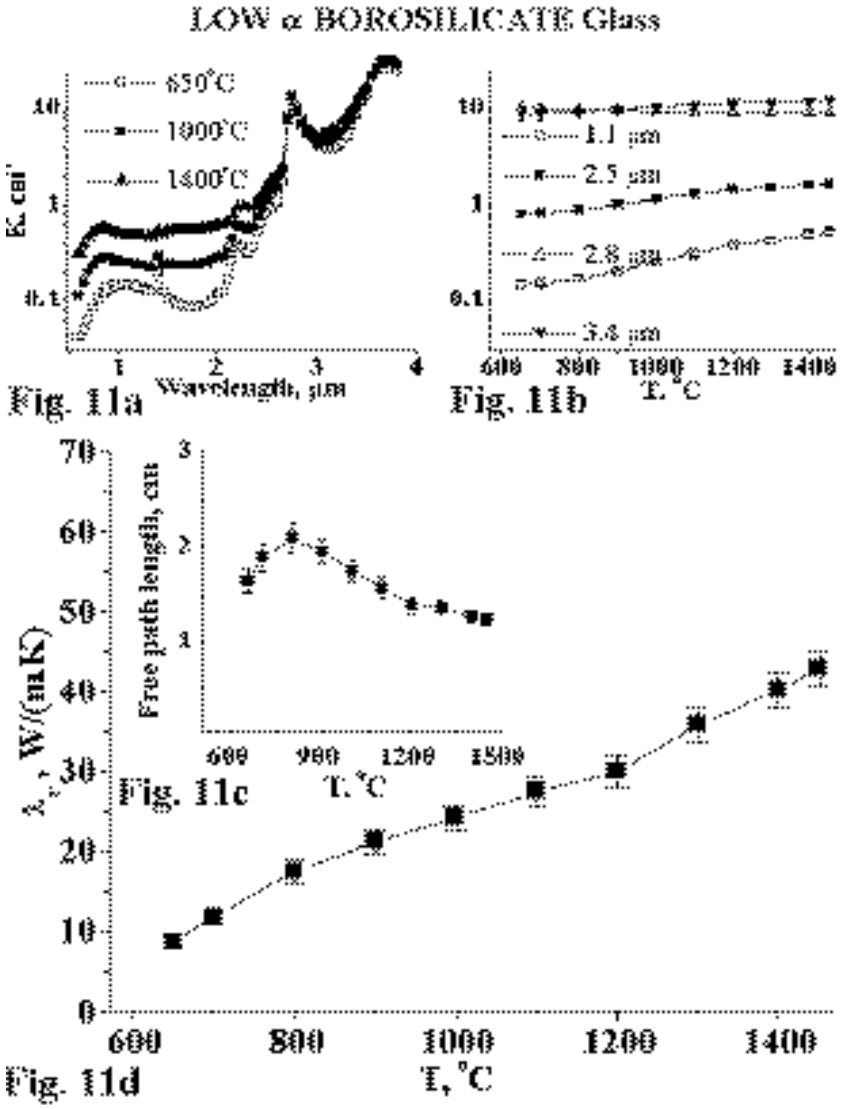

Figure 4e (Prokhorenko, Fig. 11) - Absorption spectra at temperatures 650, 1000 and 1400°C (a), and temperature dependences of absorption coefficients at 1.1, 2.2, 2.8 and 3.4 μm (b) measured for low α (hard) borosilicate glass. Temperature dependences of free path length (c) and radiative conductivity (d) calculated for low α (hard) borosilicate glass by using Rosseland formulas.

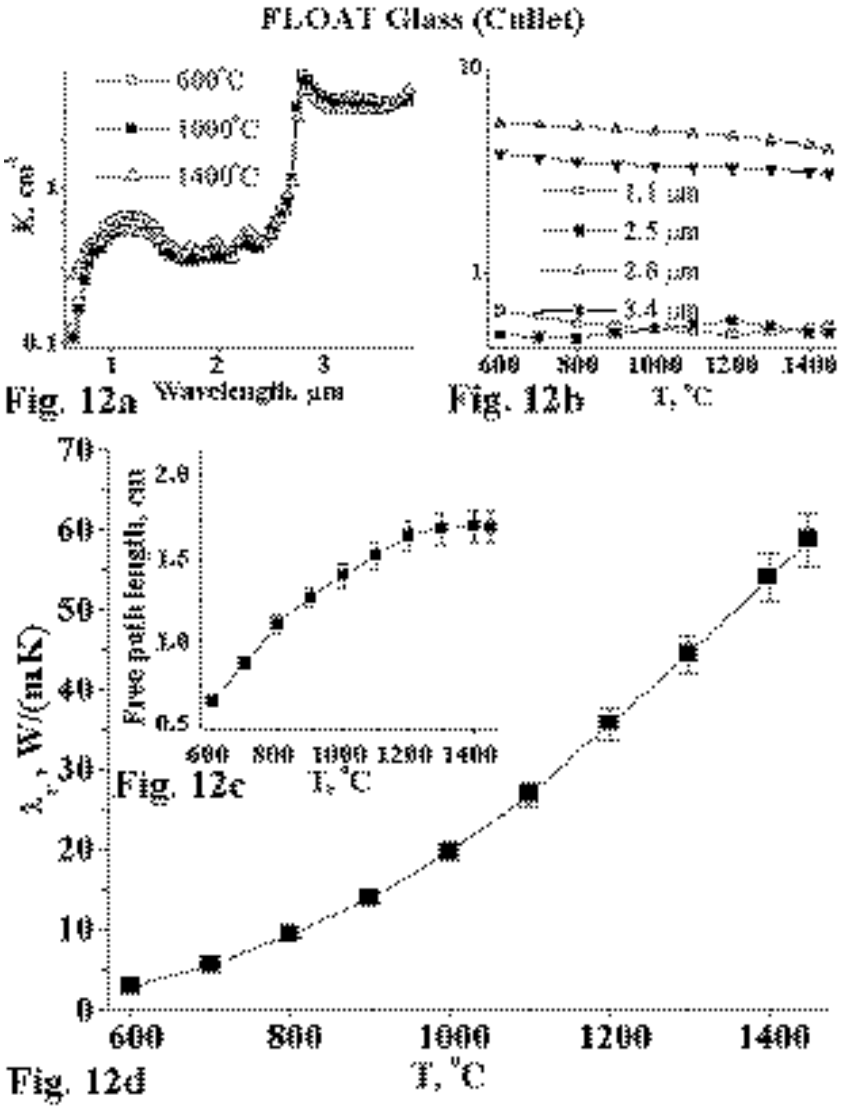

Figure 4f (Prokhorenko, Fig. 12) - Absorption spectra at temperatures 600, 1000 and 1400°C (a), and temperature dependences of absorption coefficients at 1.1, 2.2, 2.8 and 3.4 μm (b) measured for float glass. Temperature dependences of free path length (c) and radiative conductivity (d) calculated for float glass by using Rosseland formulas.

Actuator Speed (mm/min)	E-Glass	Soft Boro (wool)	Container	Color TV Panel	Float Glass
0.25	9.98300	9.99067	10.07333	10.14067	10.02500
0.75	9.89467	9.98033	9.98733	10.01467	10.01233
2	9.75167	9.65433	9.70033	9.72367	9.65633
3	9.53900	9.46900	9.45567	9.47133	9.53633
4	9.38433	9.32067	9.36467	9.27400	9.30400
5	9.28000	9.22767	9.20533	9.20133	9.22933
8	8.94767	8.94733	8.84850	8.76000	8.83500

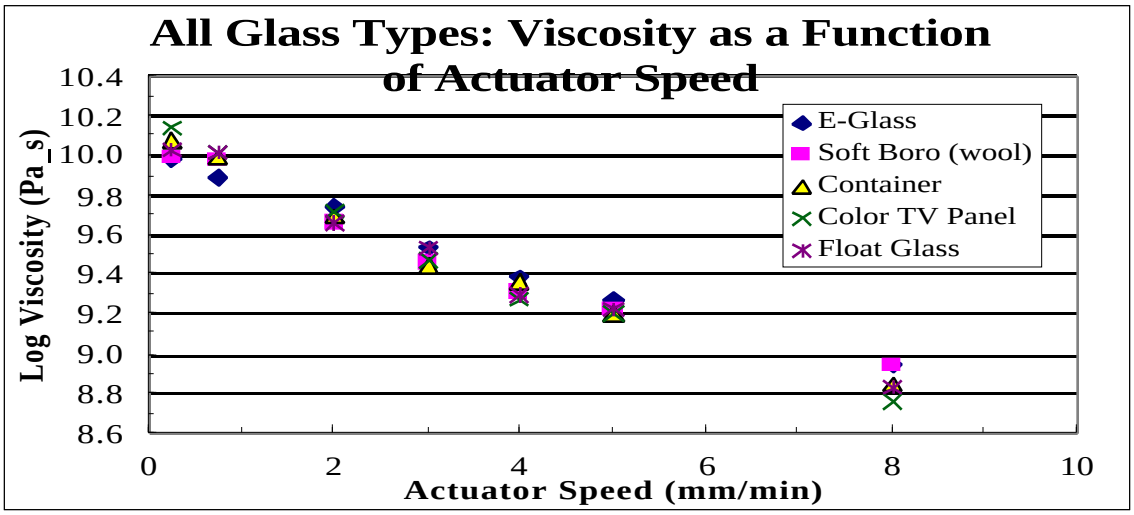

Figure 5 - Non-Newtonian Viscosity Behavior

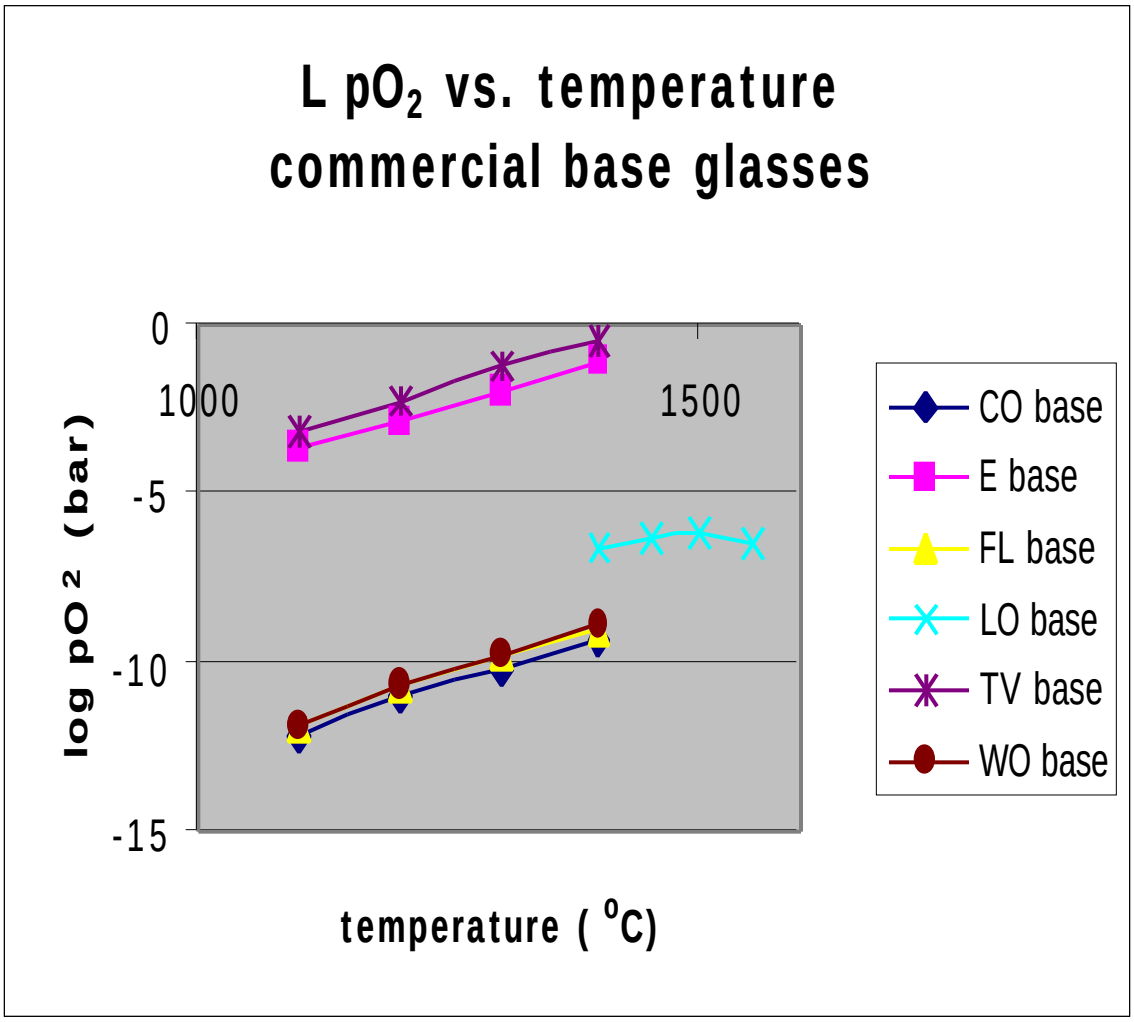

Figure 6 - Oxygen Partial Pressure versus Temperature

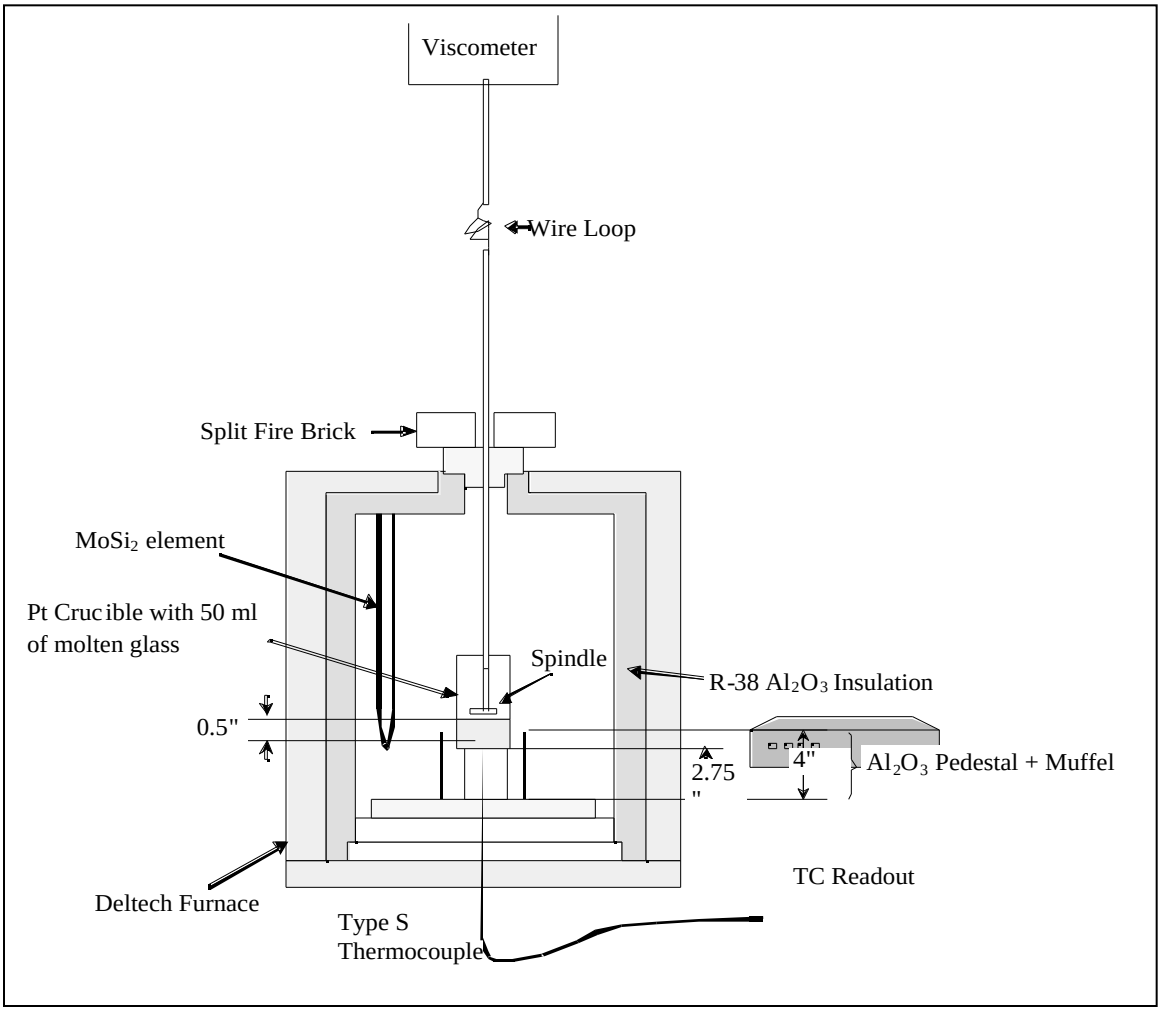

Figure 7 – PNNL Viscosity Measurement Apparatus

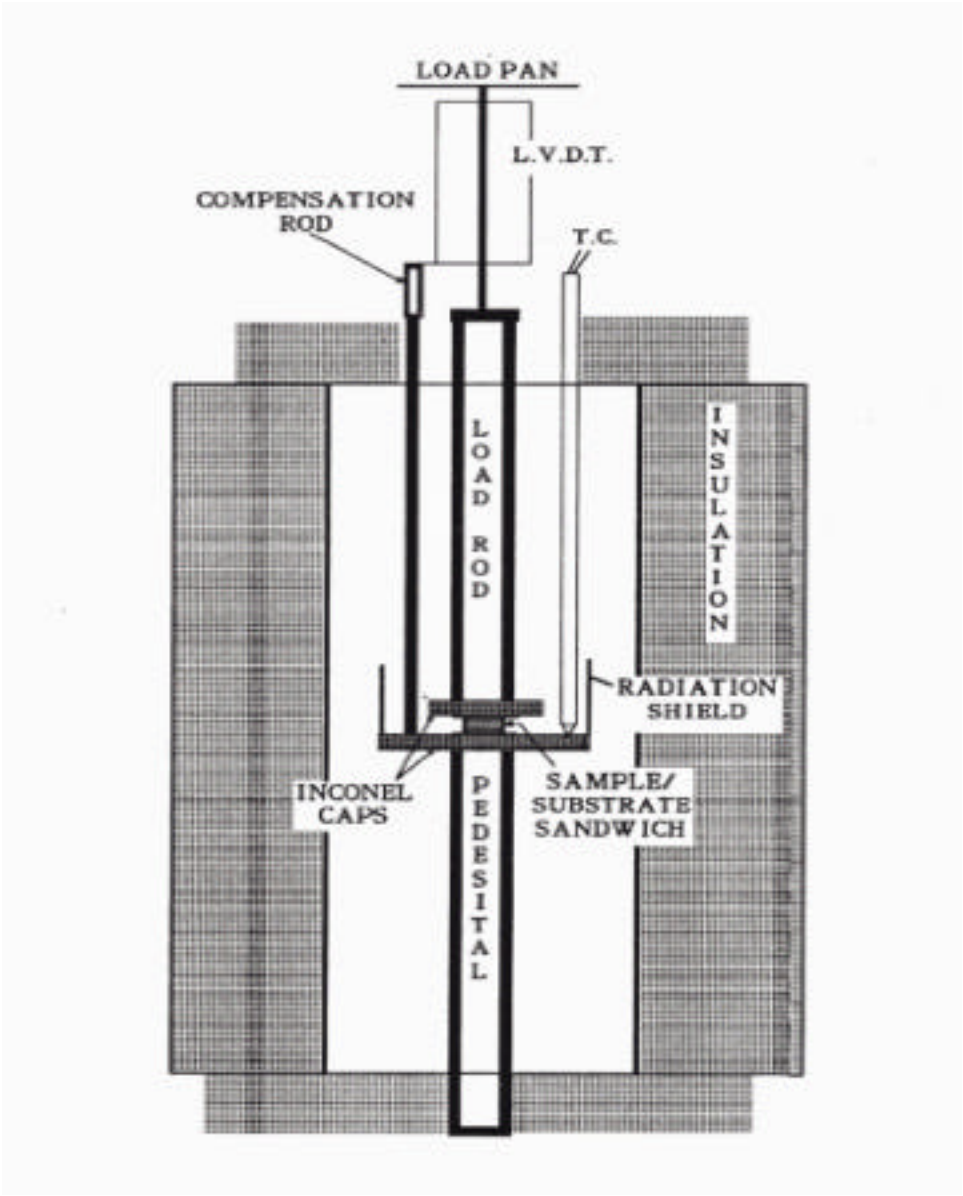

Figure 8 – Parallel-plate Viscosity Measurement Apparatus

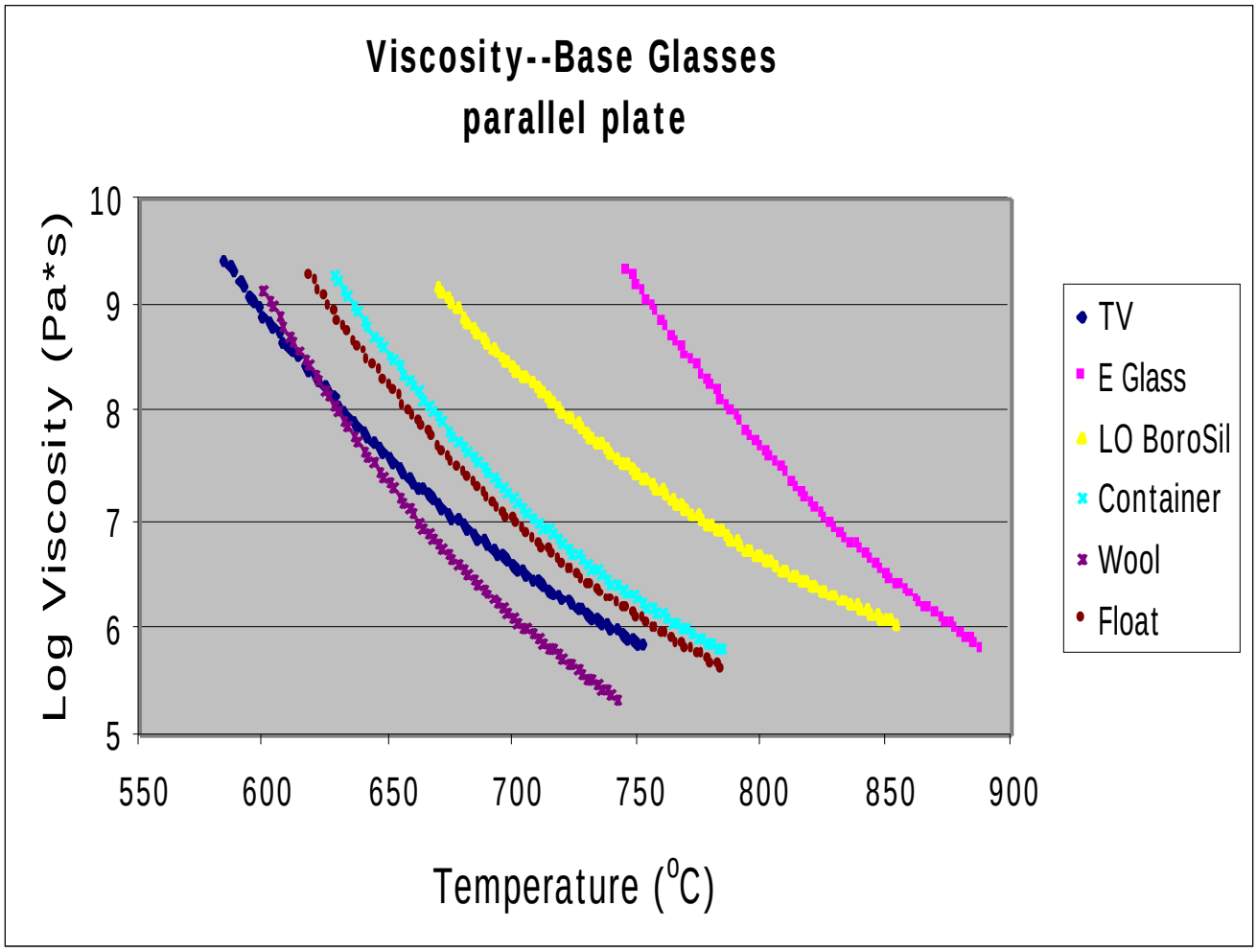

Figure 9 – Log Viscosity versus Temperature (Parallel-plate, six base glasses)

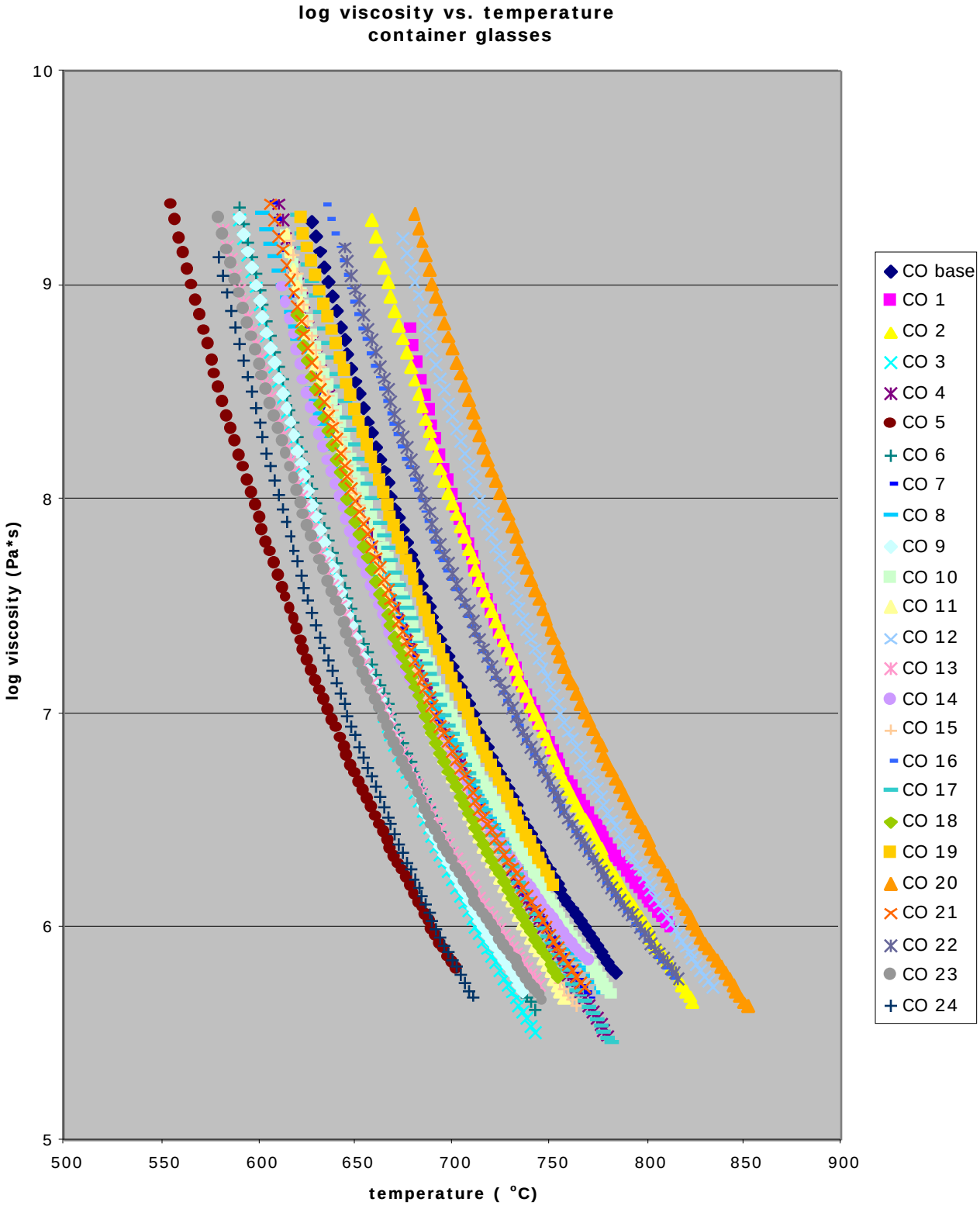

Figure 10a – Log Viscosity versus Temperature – Container Glass

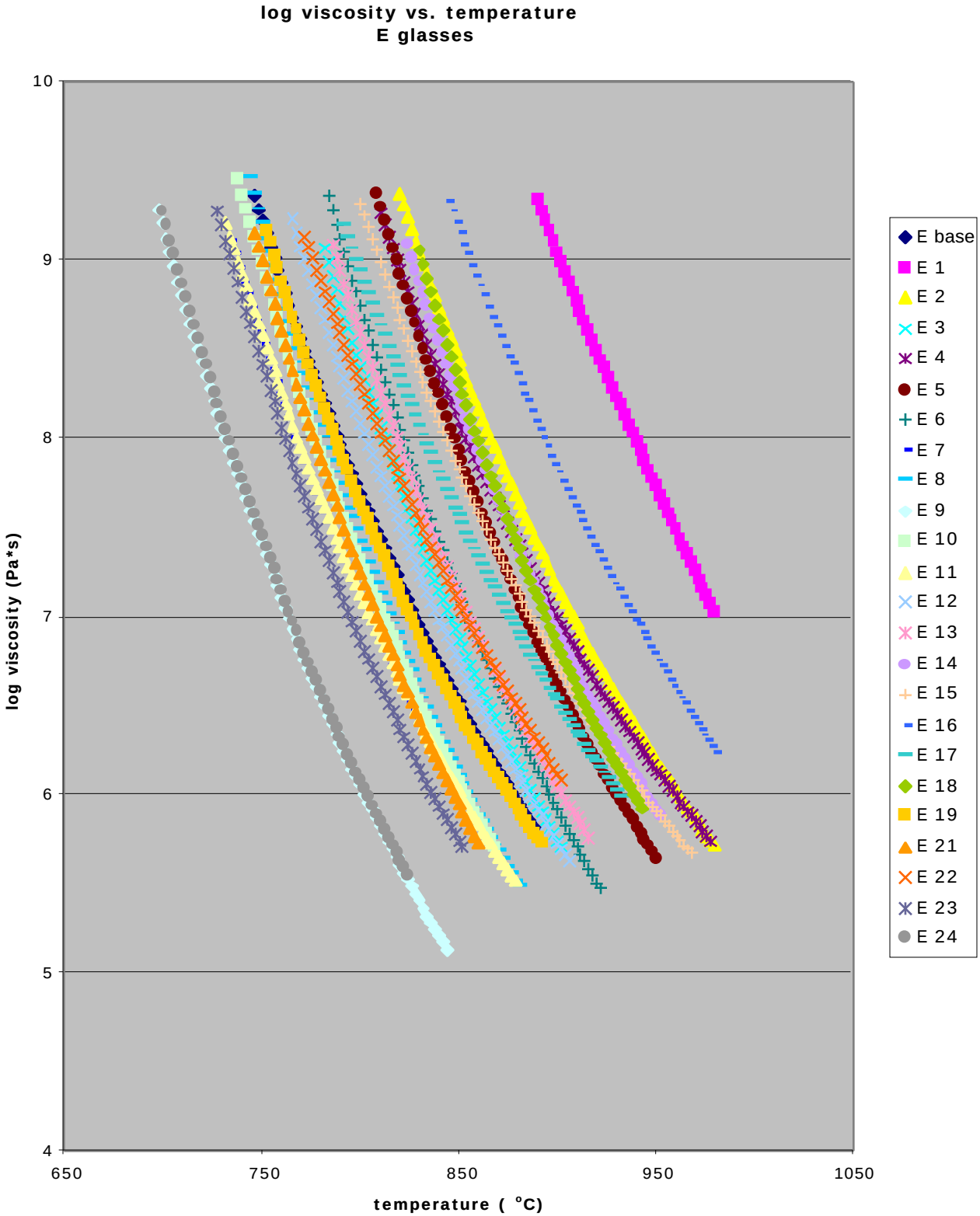

Figure 10b – Log Viscosity versus Temperature – E-type Fiberglass

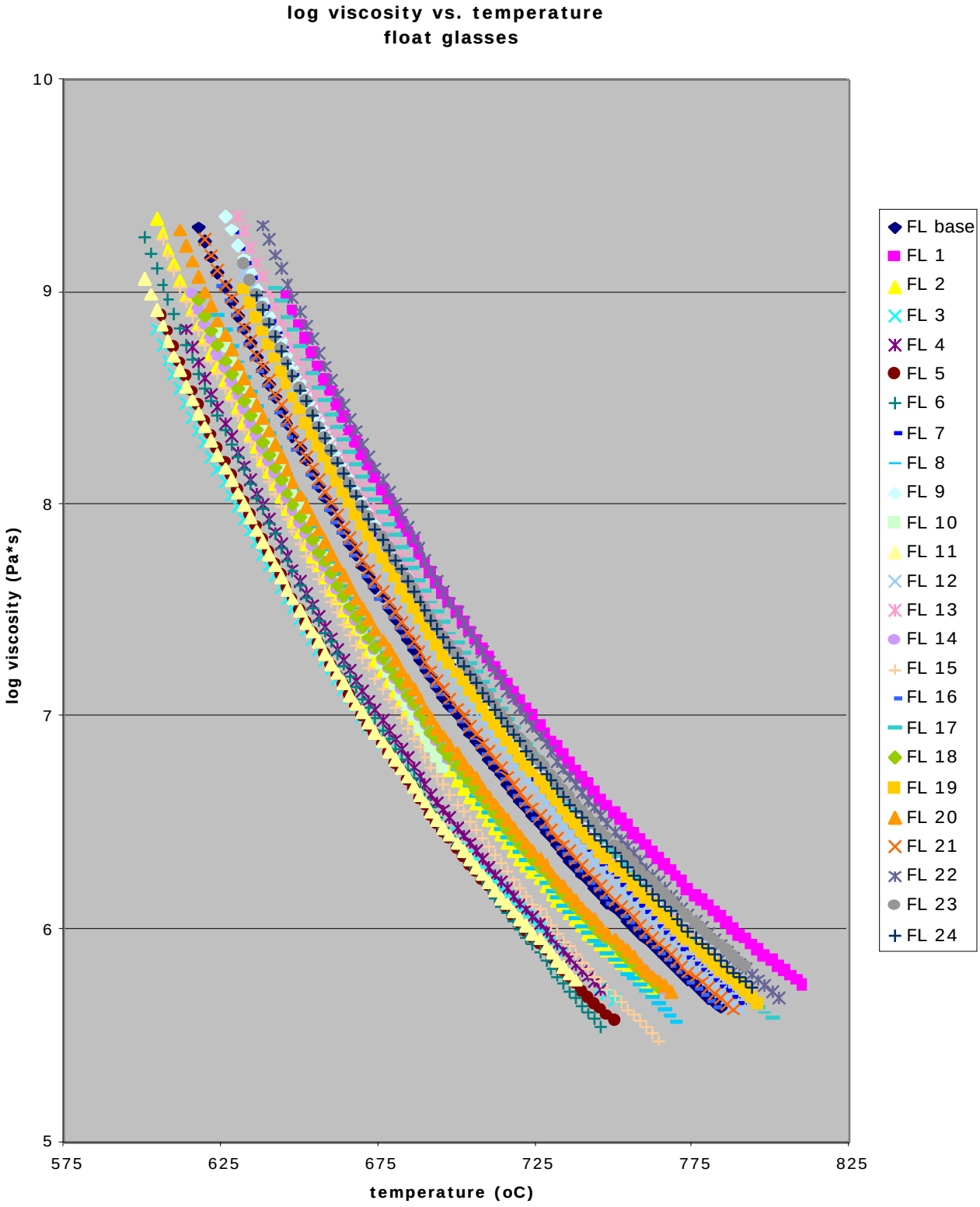

Figure 10c – Log Viscosity versus Temperature – Float Glass

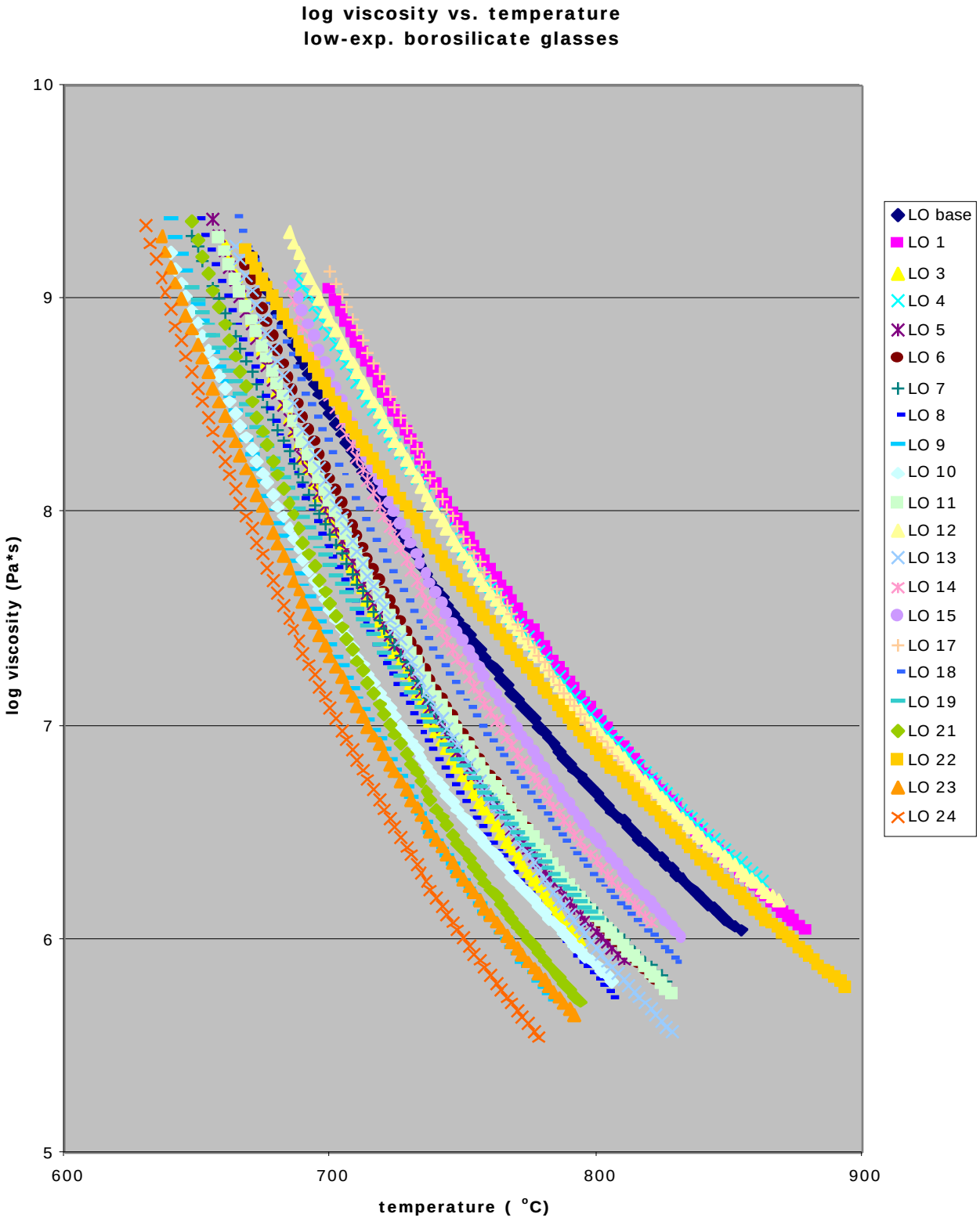

Figure 10d – Log Viscosity vs. Temperature – Low-α Borosilicate Glass

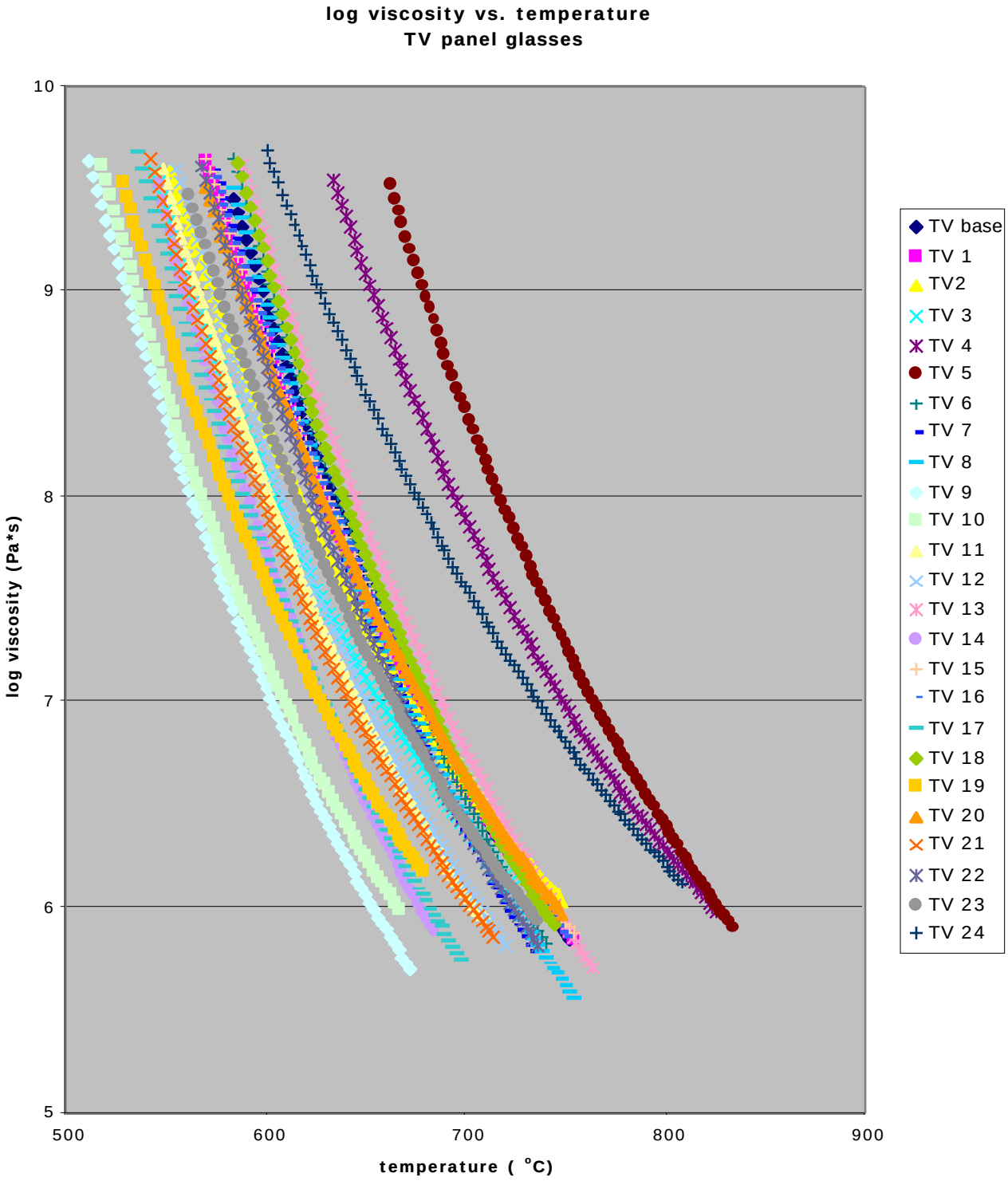

Figure 10e – Log Viscosity versus Temperature – TV Panel Glass

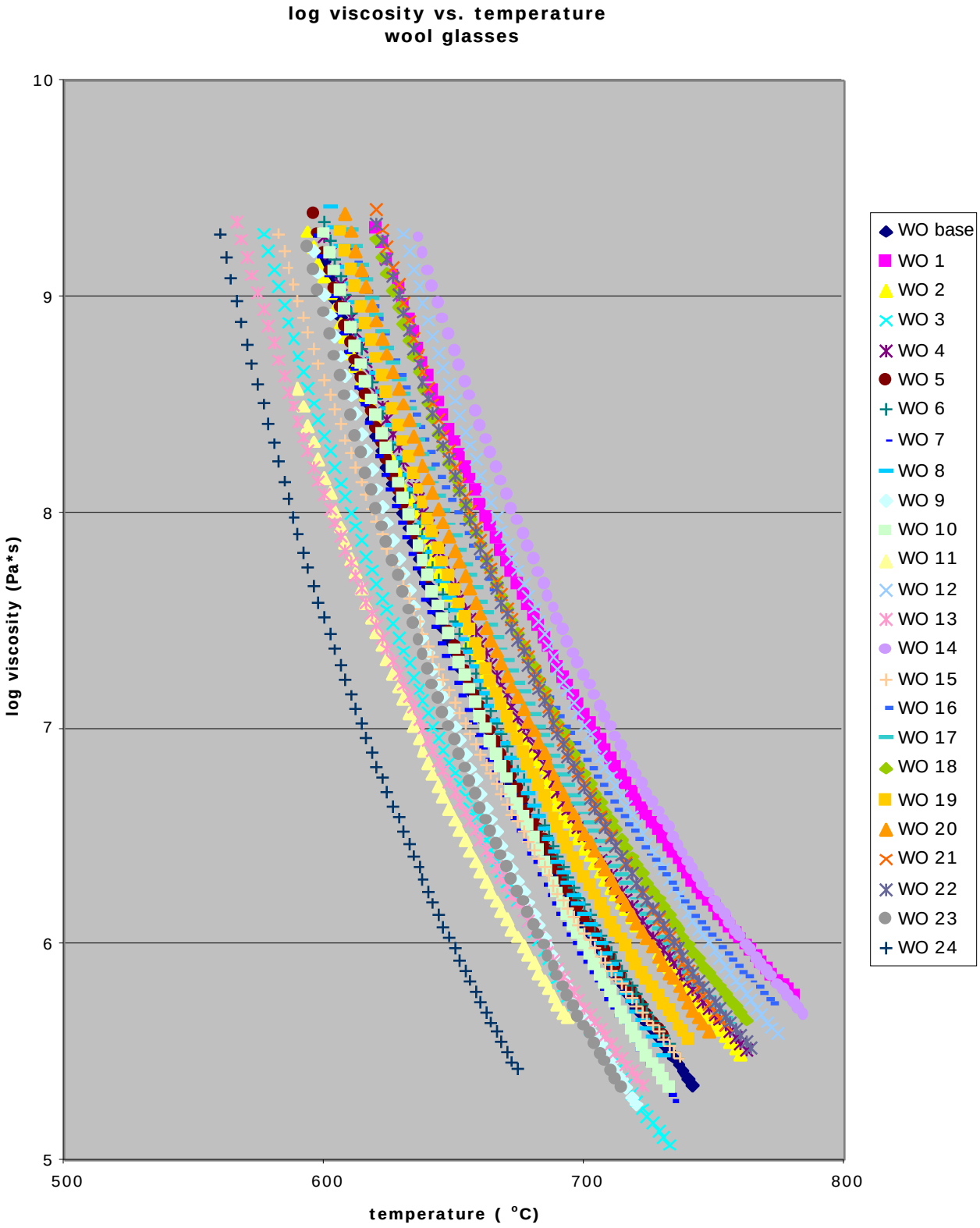

Figure 10f – Log Viscosity versus Temperature – Wool-type Fiberglass

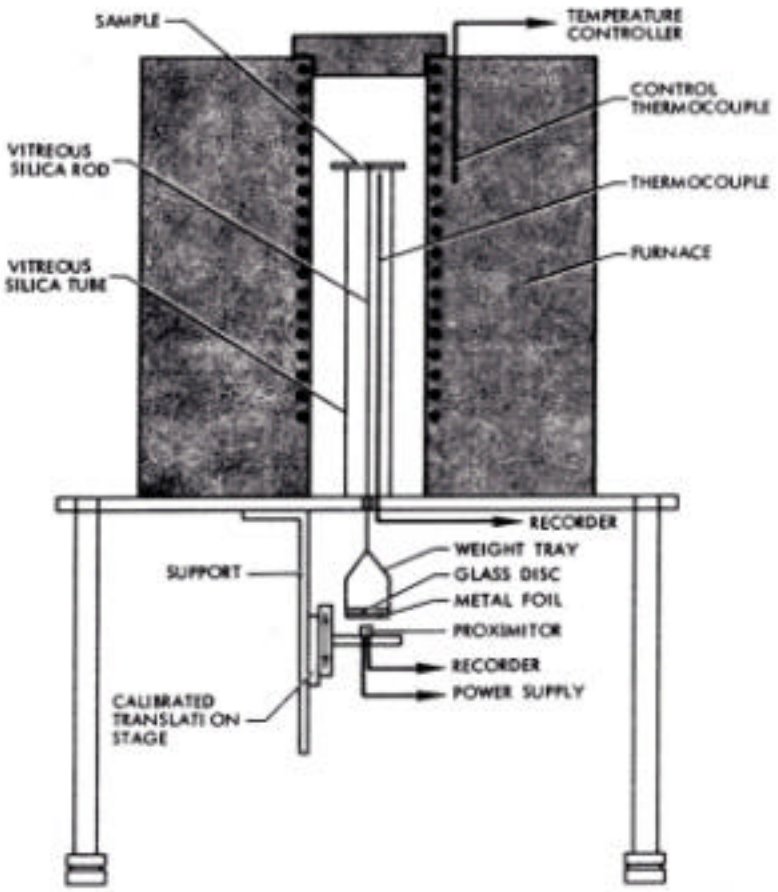

Figure 11 – Beam-bending Viscosity Measurement Apparatus

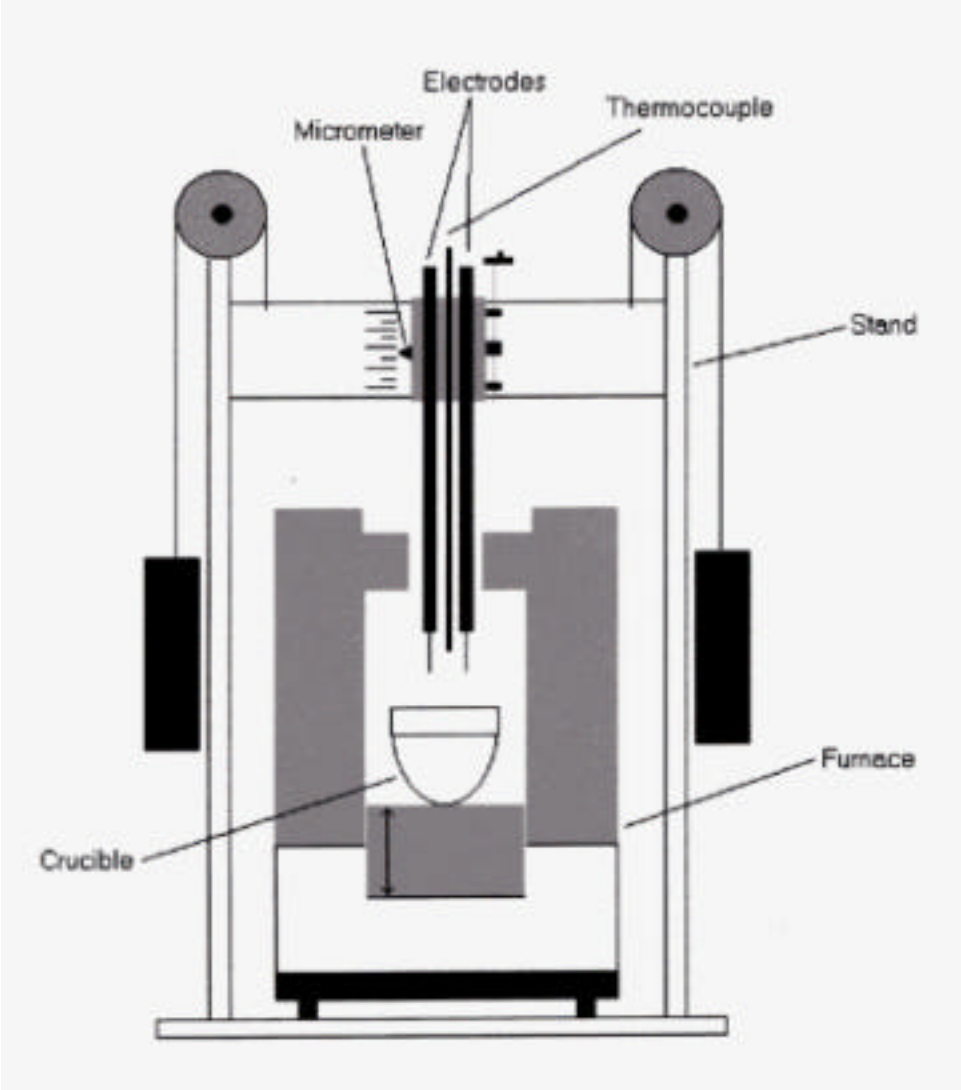

Figure 12 – Electrical Resistivity Measurement Apparatus

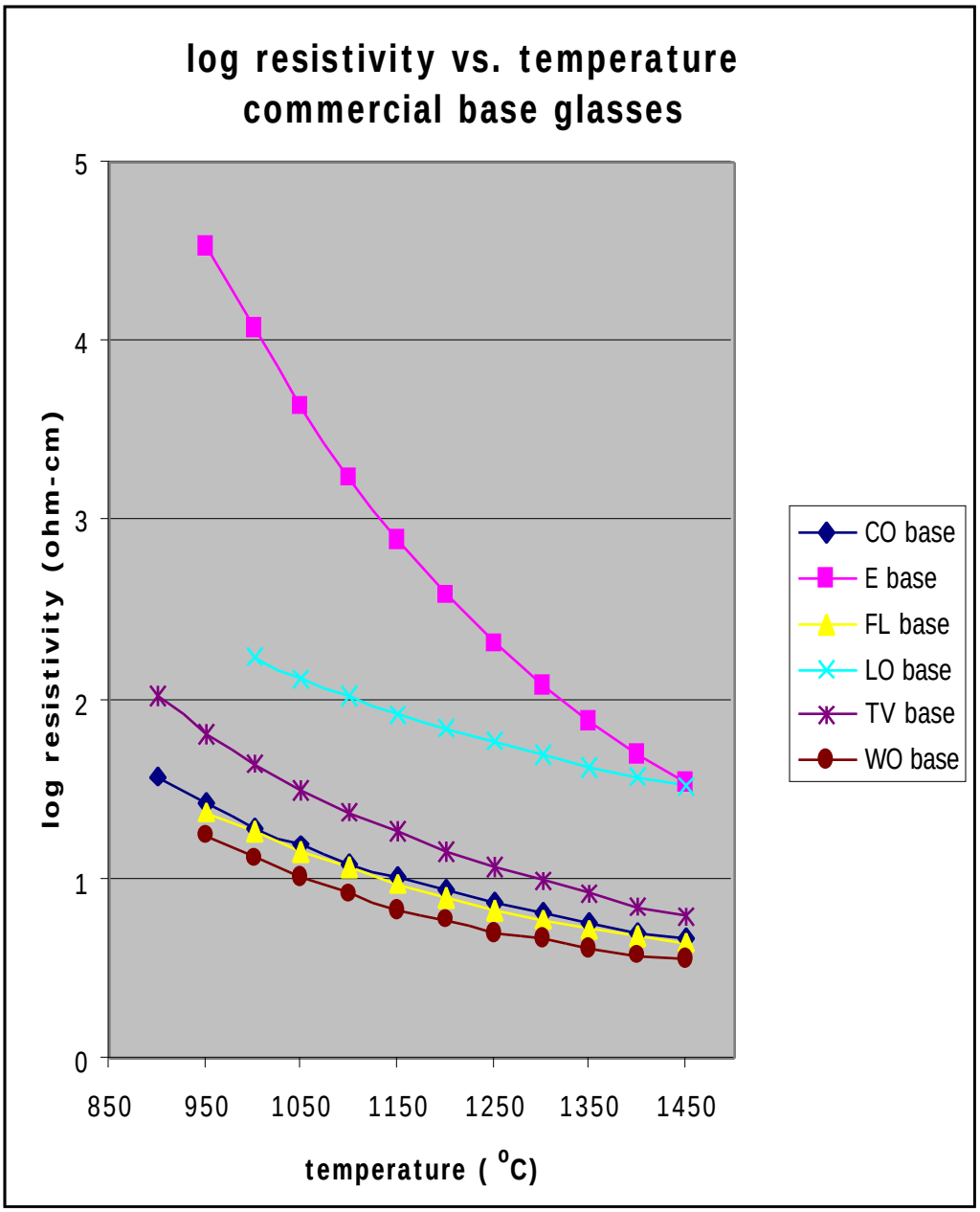

Figure 13 - Log Resistivity versus Temperature

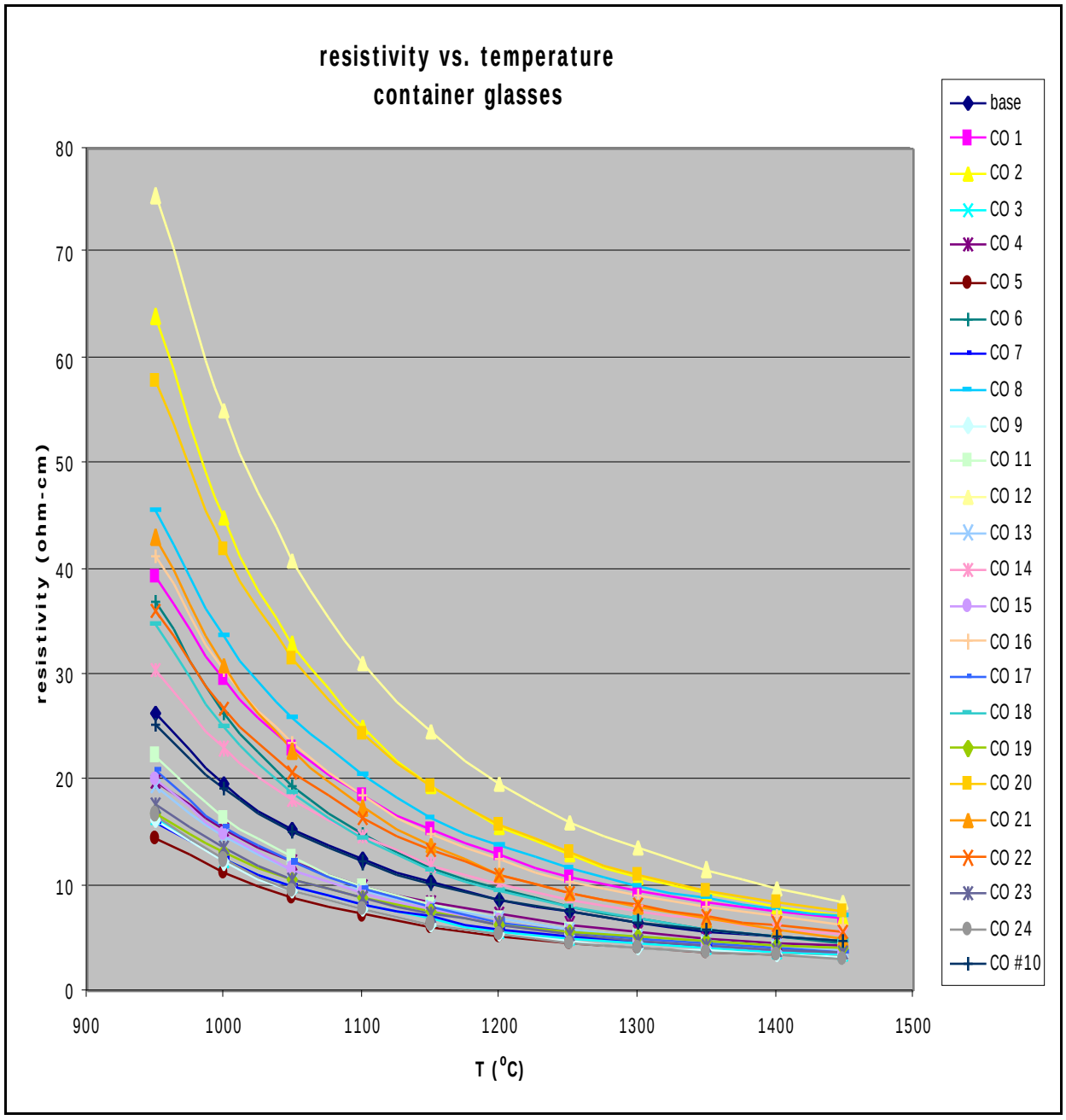

Figure 14a - Log Resistivity versus Temperature – Container Glasses

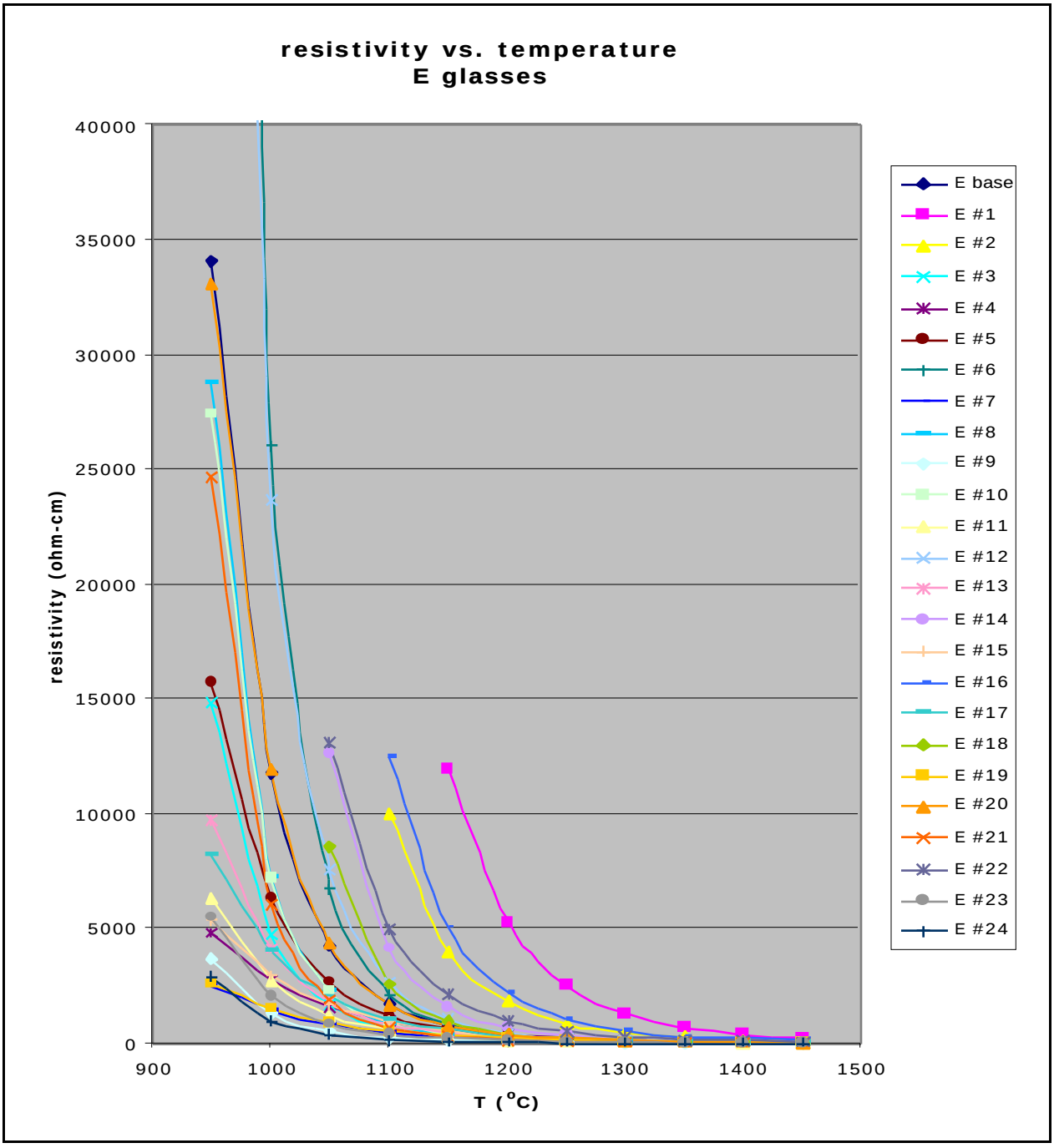

Figure 14b - Log Resistivity versus Temperature – E-Glasses

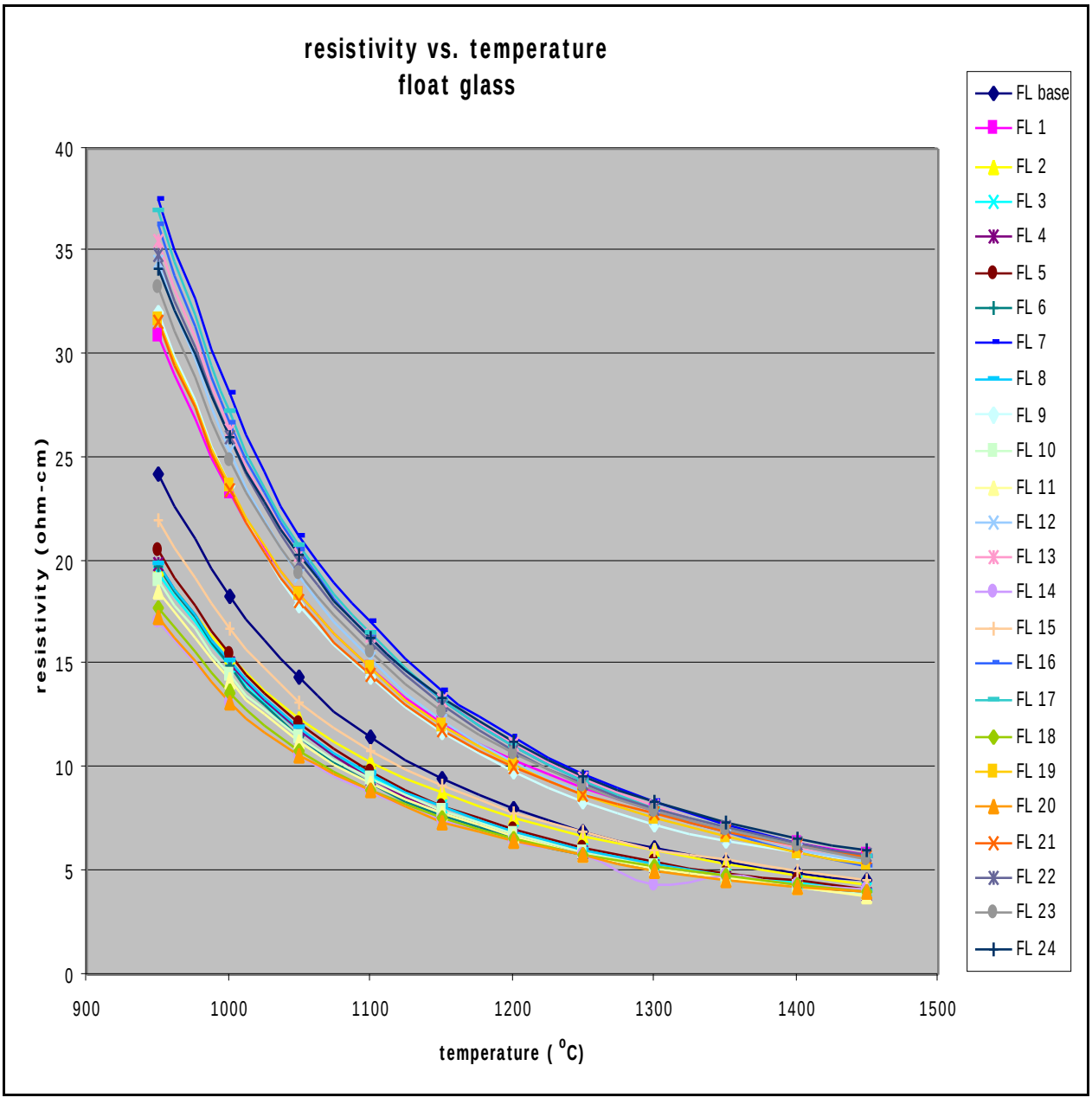

Figure 14c - Log Resistivity versus Temperature – Float Glasses

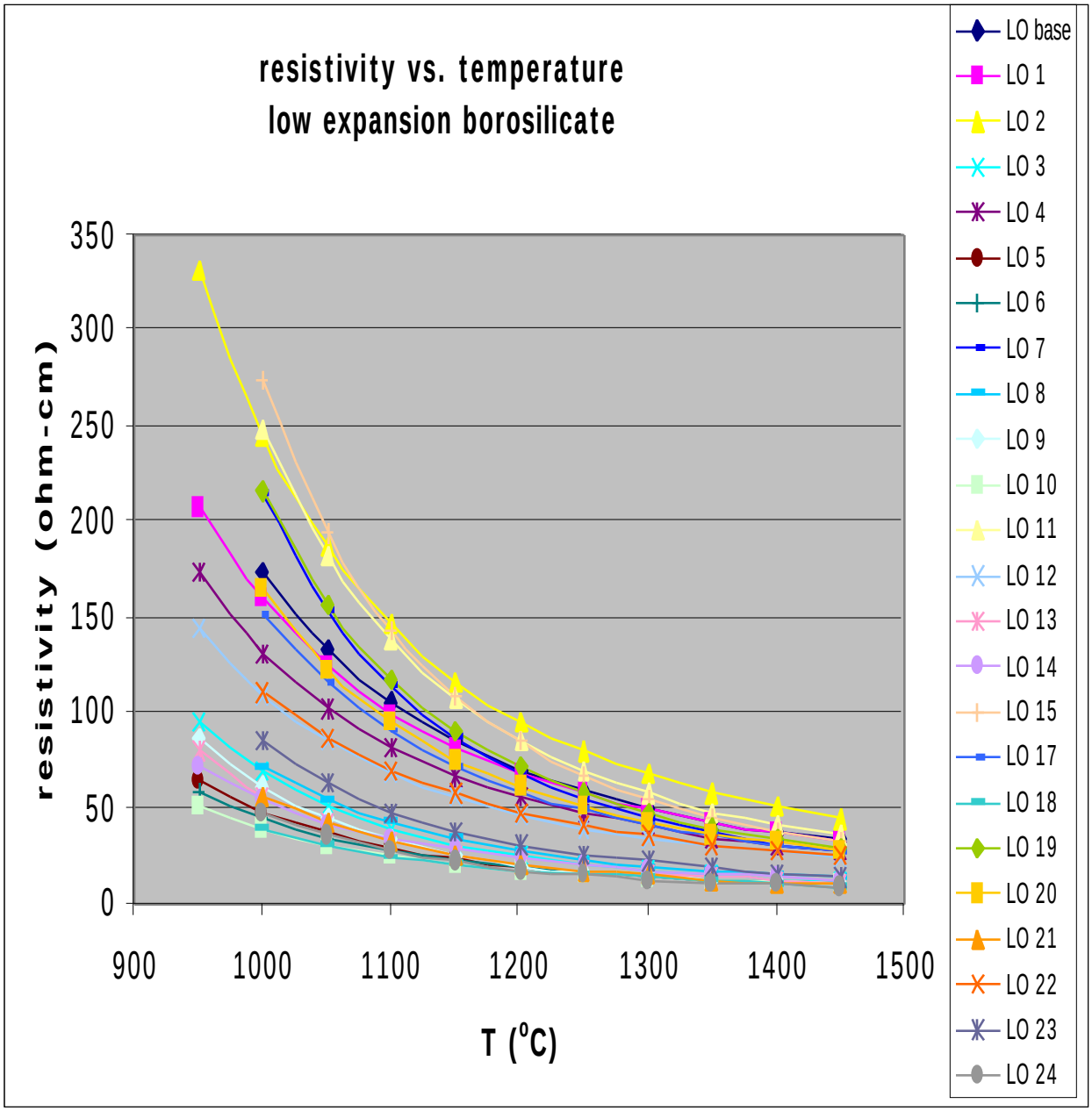

Figure 14d - Log Resistivity versus Temperature – Low-expansion Borosilicate Glasses

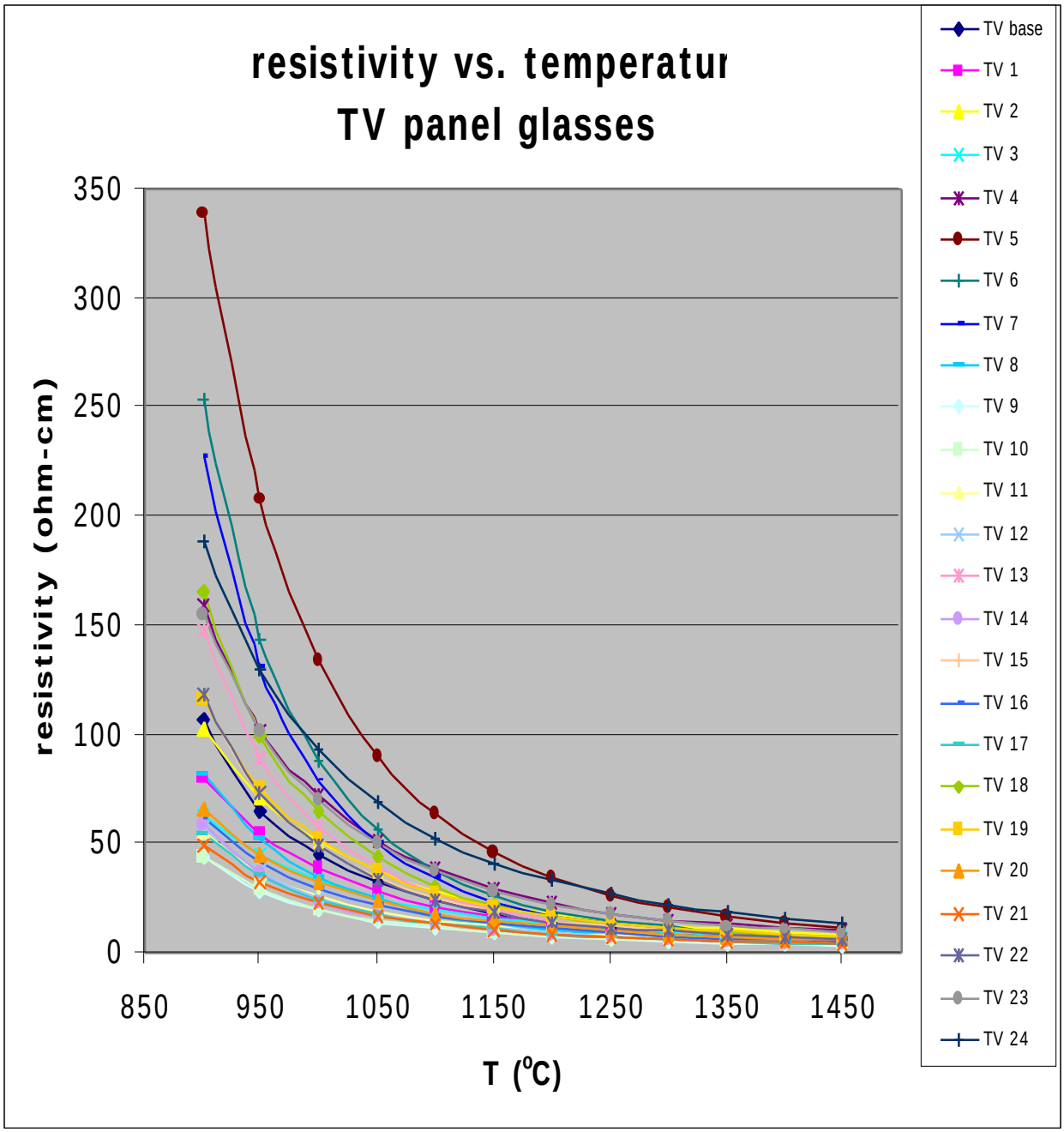

Figure 14e - Log Resistivity versus Temperature – TV Panel Glasses

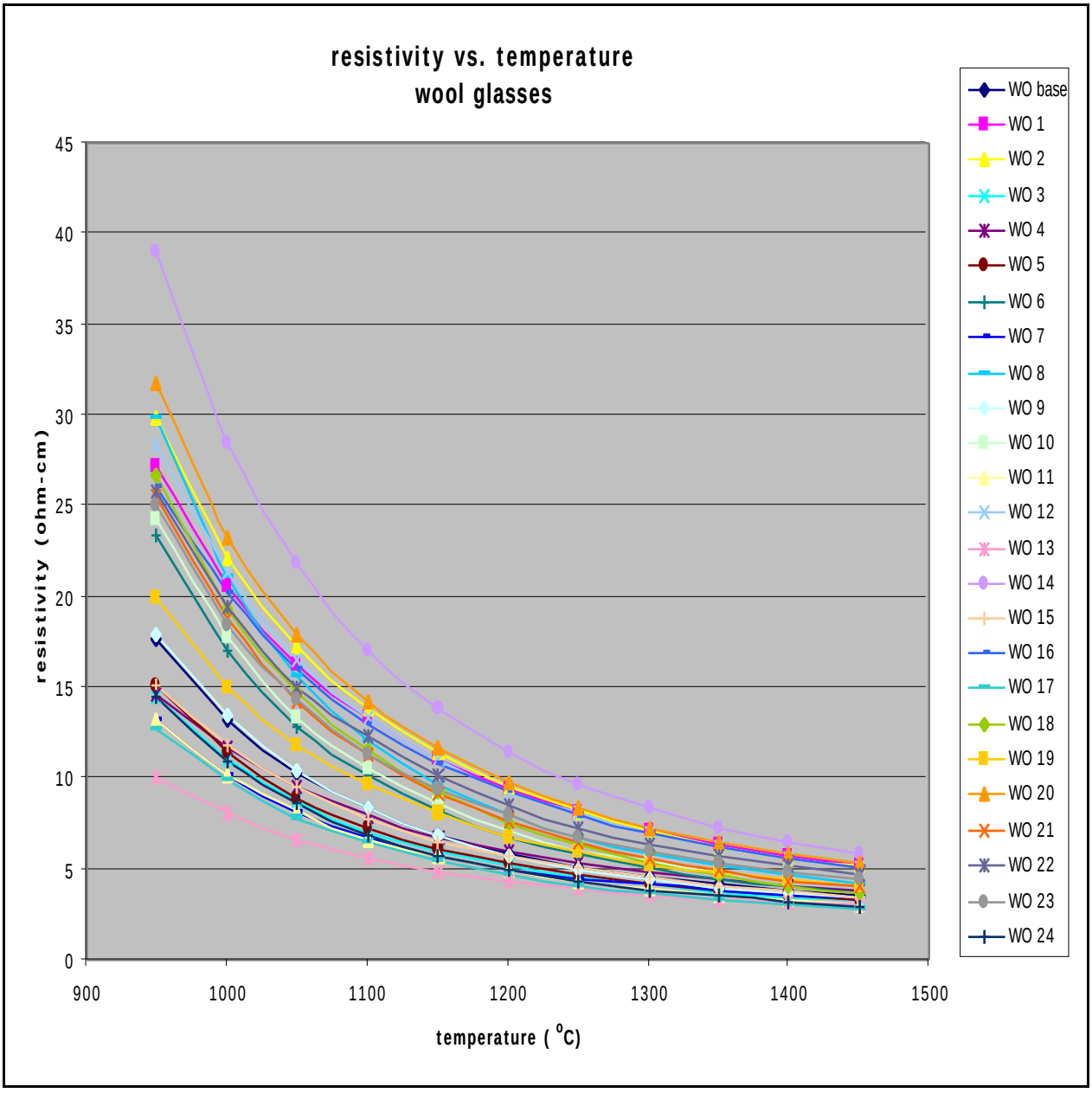

Figure 14f - Log Resistivity versus Temperature – Wool Glasses